COO-3244-83

MASTER

ANNUAL PROGRESS REPORT

DOE/ER/03244-71

Experimental Medium-Energy Physics

Carnegie-Mellon University

Pittsburgh, PA 15213

October 1980 - June 1981

DOE Contract: DE-AC02-76ERO 3244.A007

EXPERIMENTAL NUCLEAR PHYSICS

DOE Contract EY-76-S-02-3244

Carnegie-Mellon University

Pittsburgh, Pennsylvania 15213

Annual Progress Report October 1980 - June 1981

I. Introduction

This past year has been very productive for the CMU group. Our research program at the kaon beam line at the AGS has generated new and interesting data while analysis of data taken at LAMPF has produced new and stimulating results. Analysis of data on the hypernuclei ^{13}C, ^{14}N, ^{18}O is now complete. In particular a detailed interpretation of the level structure of ^{13}C is surprisingly simple and successful. Detailed momentum space calculations of our kaon-nucleus elastic scattering data are now complete. These and interpretation of the inelastic scattering data lead to some interesting and surprising conclusions about the suitability of a kaon as a nuclear probe. In studies of the (K^-,π^+) reaction on ^6Li and ^{16}O targets we see evidence for the formation of narrow states in Σ hypernuclei in agreement with related measurements reported by CERN.

In our studies of pion annihilation, an investigation of the $^7Li(\pi,pd)^4He^*$ reaction leads to statements about three body absorption mechanisms. We are now preparing for a major run at LAMPF for August, 1981.

A major new project has been initiated in the area of hypernuclear decay studies. In March the BNL program committee approved a CMU proposal to investigate the weak decay of a Λ imbedded in nuclear matter. Design and construction of detectors for this experiment is now in progress. In connection with this we report CMU beam line design studies that may facilitate the improvement of the Kaon flux at BNL.

A detailed discussion of the above mentioned work is presented below in section III. Associated work on hardware and software development as well as studies of kaon beam line design are presented in section IV. We review Professional Activities and Publications in sections V and VI.

Annual Progress Report

- Contents -

II. Group Personnel

During the post year Professor Fujio Takeutchi has returned to his faculty position at the University of Kyota, Kyota, Japan. In the meantime Dr. Gregory Franklin of the MIT-Bates lab has accepted a position at CMU to begin August, 1981. Our senior graduate student, Dan Marlow has completed his thesis work and received his degree of Doctor of Philosophy in the Department of Physics, Carnegie-Mellon University in May, 1981. Our personnel roster for the year was as follows:

a) Peter D. Barnes, Professor of Physics and Co-Principal Investigator

b) Robert A. Eisenstein, Associate Professor of Physics and Co-Principal Investigator

c) William R. Wharton, Associate Professor of Physics

d) Bernd Bassalleck, Research Associate

e) Philip Pile, Research Associate

f) Nick Colella, Graduate Student

g) Richard Grace, Graduate Student

h) Christopher Maher, Graduate Student

i) Dan Marlow, Graduate Student

j) Ron Rieder, Graduate Student

III. Research Program

The research activities for the past year were chiefly related to experiments with the Moby Dick Magnetic Spectrometer on the kaon beam line at the AGS and with our Ge crystal spectrometer on the LEP beam line at LAMPF. Additional work includes development of fast scintillator timing techniques and design studies connected with the development of a higher flux modified version of our current BNL kaon beam line. All these activities are described below.

III.A. Hypernuclear and Kaon Scattering Studies at the AGS

The following sections describe a series of experiments conducted in collaboration with BNL and the University of Houston and M.I.T. in which we have built up and instrumented a moderately high resolution beam line and spectrometer system at the AGS which allows us to study a variety of kaon induced reactions.

III. A. 1 Formation of Λ Hypernuclei in the $(K^- \pi^-)$ Reaction on $^{12,13}C$, ^{14}N, ^{18}O

Data taking on experiment 746 at BNL, a study of hypernuclear states in $^{13}_{\Lambda}C$, $^{14}_{\Lambda}N$ and $^{18}_{\Lambda}O$, was finished this past year. The hypernuclei were formed using the (K^-,π^-) strangeness exchange reaction. The experiment was performed on the hypernuclear spectrometer at the BNL AGS Low Energy Separated Beam, with a typical resolution of 2.5 MeV FWHM in the binding energy of the Λ.

An extensive off-line analysis of all the data was done on the CMU VAX computer using our program 'EVAL' that was described in last year's progress report.

The observed hypernuclear spectra proved to be very rich in structure. This is particularly true for ^{13}C where the momentum transfer was varied from ∿ 50 MeV/c to ∿ 330 MeV/c. Figures 1 and 2 show representative although not final results. As the momentum transfer is varied states of different configurations are preferentially excited. The observed excitation spectra could be interpreted in a simple consistent model involving substitutional states. In this model a Λ in either the 1s or the 1p shell is coupled to those core nucleus states that have the strongest one neutron hole strength. The location and strength of these core states is taken from cfp calculations and from single neutron pick-up reactions. The $^{13}_{\Lambda}C$ results are consistent with a very small Λ-nucleus spin-orbit interaction, as deduced from upper limits on level shifts.

A careful analysis of the absolute cross sections was also undertaken. By looking at new data for $^{12}_{\Lambda}C$, taken prior to the $^{13}_{\Lambda}C$ data, we found that the previously obtained cross section had to be renormalized by a factor of ∿ 2. The new numbers are now in good agreement with theoretical calculations as well as with the CERN results on $^{12}_{\Lambda}C$. For this determination of the absolute cross sections extensive use was made of a Monte Carlo code. This program had been written at CMU in order to establish the effective solid angle of the hypernuclear spectrometer.

A first draft of a publication has been written and the final version should be submitted soon.

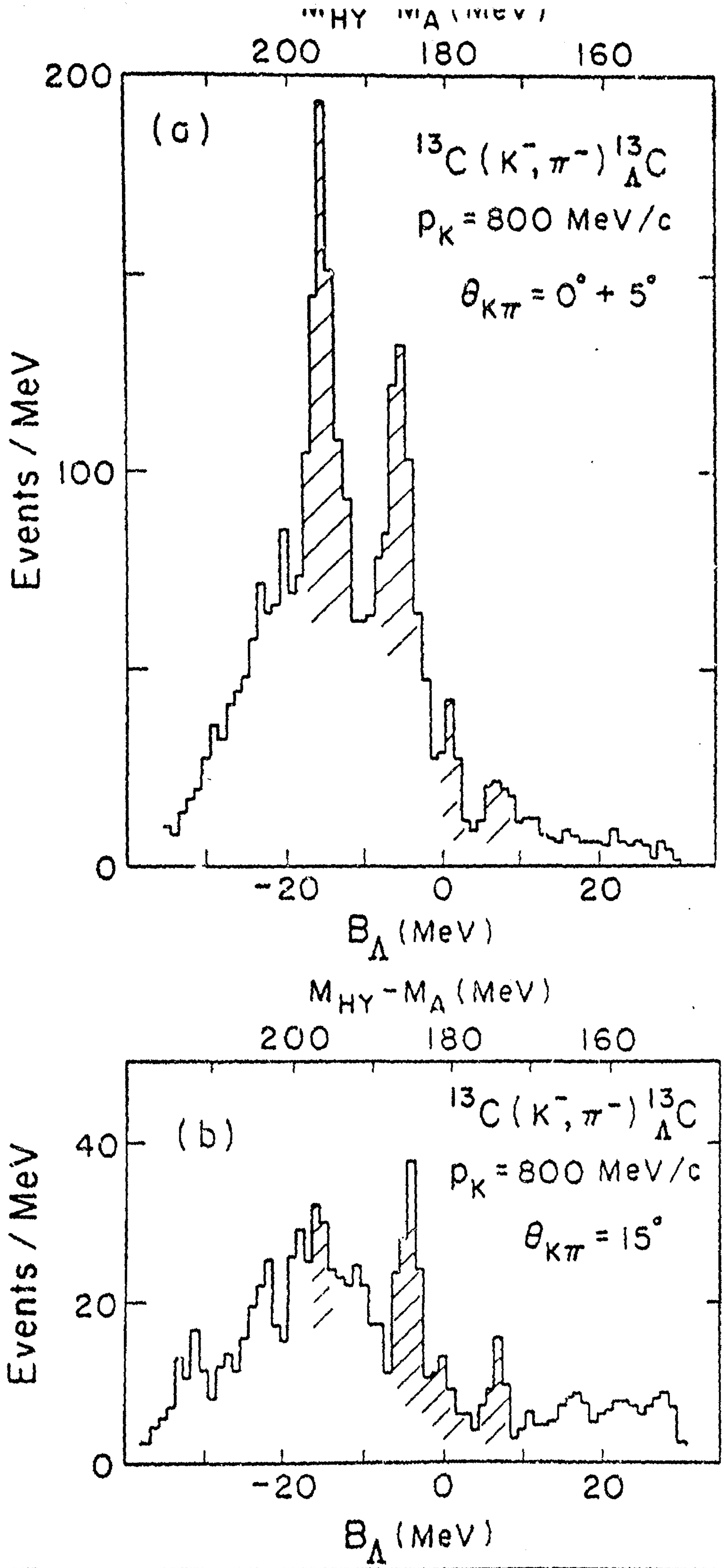

M_HY − M_Λ (MeV)
200
180
160
200
100
0
(a)
$^{13}C(K^-,\pi^-)^{13}_{\Lambda}C$
p_K = 800 MeV/c
$\theta_{K\pi}$ = 0° + 5°
Events / MeV
−20
0
20
B_Λ (MeV)
$M_{HY} - M_\Lambda$ (MeV)
200
180
160
40
20
0
(b)
$^{13}C(K^-,\pi^-)^{13}_{\Lambda}C$
p_K = 800 MeV/c
$\theta_{K\pi}$ = 15°
Events / MeV
−20
0
20
B_Λ (MeV)

Fig. 1

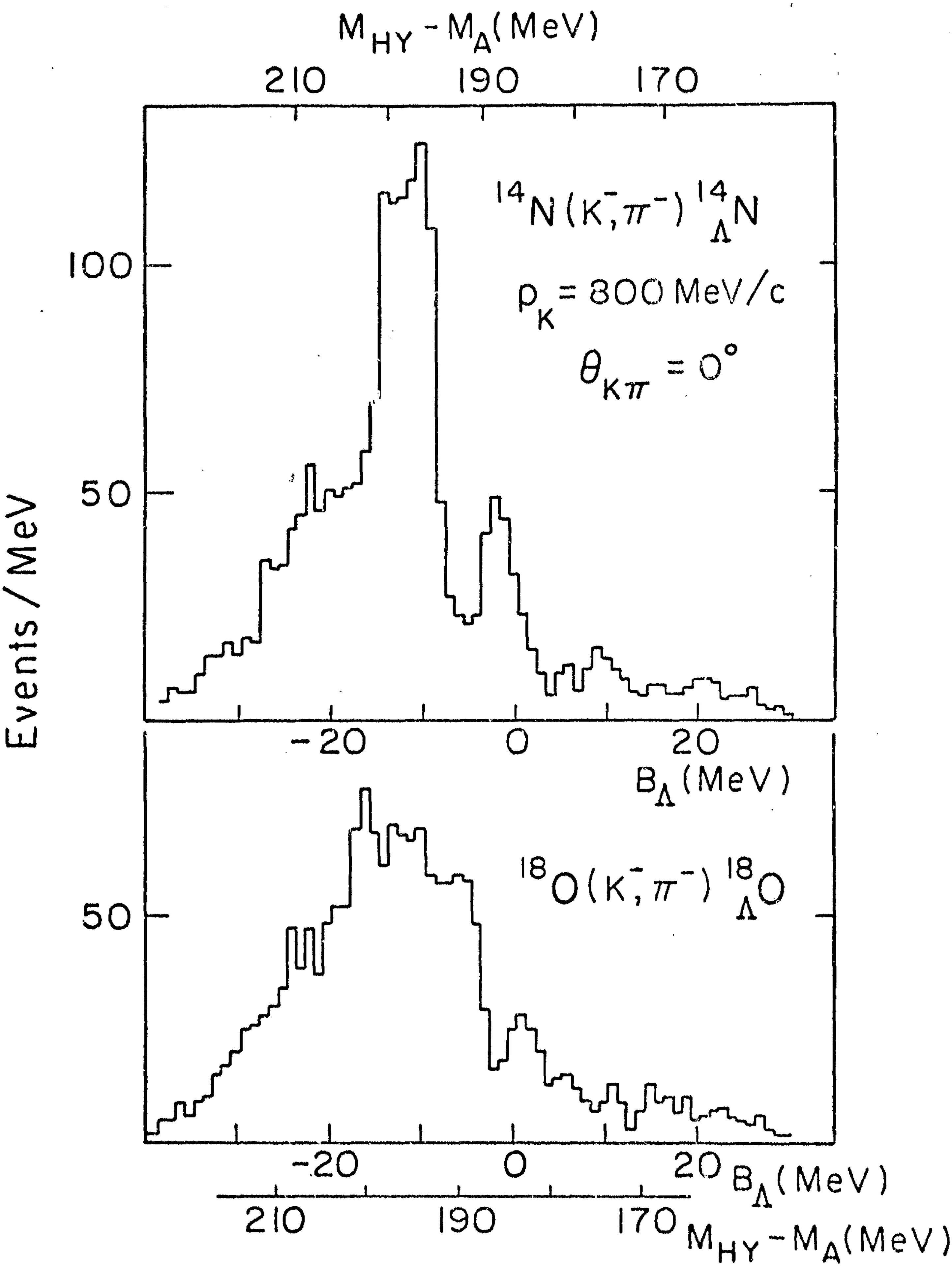

M_HY - M_A (MeV)
210
190
170
100
50
Events / MeV
14N(K-, π-) 14ΛN
pK = 800 MeV/c
θKπ = 0°
-20
0
20
BΛ (MeV)
18O(K-, π-) 18ΛO
50
-20
0
20 BΛ (MeV)
210
190
170 M_HY - M_A (MeV)

Fig. 2

III. A. 2 Formation of Σ Hypernuclei in (K^-,π^+) Reaction on ^{6}Li and ^{16}O

Data taking on experiment 752 at BNL, a search for narrow Σ^- hypernuclear states in ^{6}Li and ^{16}O was finished in May 1981. The primary interest in these narrow Σ states stems from the fact that the strong $\Sigma N \rightarrow \Lambda N$ conversion in nuclear matter should result in the nonexistence of narrow states, at least in a first approximation.

The (K^-,π^+) reaction at P_K = 720 MeV/c was chosen. Only isospin 3/2 levels in the residual Σ^--core hypernucleus are populated in this reaction. The experiment was performed on the same beam line and spectrometer at BNL as the previously mentioned Λ-hypernuclear studies. Due to the different polarities in the K and π spectrometers the excitation spectra were very clean and essentially free of background from kaon decays.

^{6}Li data were taken at spectrometer settings of 0°, 9°, 13°. ^{16}O was studied at 0° first with a water target, then with a liquid oxygen target in order to avoid the strong peak due to the free $K^-p \rightarrow \Sigma^-\pi^+$ reaction. Figure 3 shows some of the results.

In ^{6}Li at 0° we observed a clear indication of a narrow peak and a somewhat broader structure at lower excitation energies. Because of the relatively high momentum transfer there is a strong contribution from the quasifree continuum. The structures in ^{6}Li are interpreted as primarily substitutional states in the 1s and the 1p shell, respectively. This interpretation is based on a comparison with the $^6_\Lambda$Li and $^9_\Sigma$Be spectra measured at CERN. At the large angles the spectrum appears much more featureless.

A main motivation behind the ^{16}O target was the hope to learn something about the Σ-nucleus spin-orbit interaction by studying the splitting of the $P_{3/2}$ and $P_{1/2}$ substitutional states, if they could be clearly identified. Indeed, the spectrum taken with the water target (see Fig. 3) shows traces of two narrow peaks at rather high excitation energies. Another run with a liquid oxygen target resulted in a distribution without clear indications of any structure. This could be due to the very thick target resulting in a worsening of the resolution. The final interpretation of the ^{16}O results and conclusions on the question of the Σ-nucleus spin-orbit interaction are being worked on.

A first draft of a letter with the ^{6}Li results has been circulated among the collaborators.

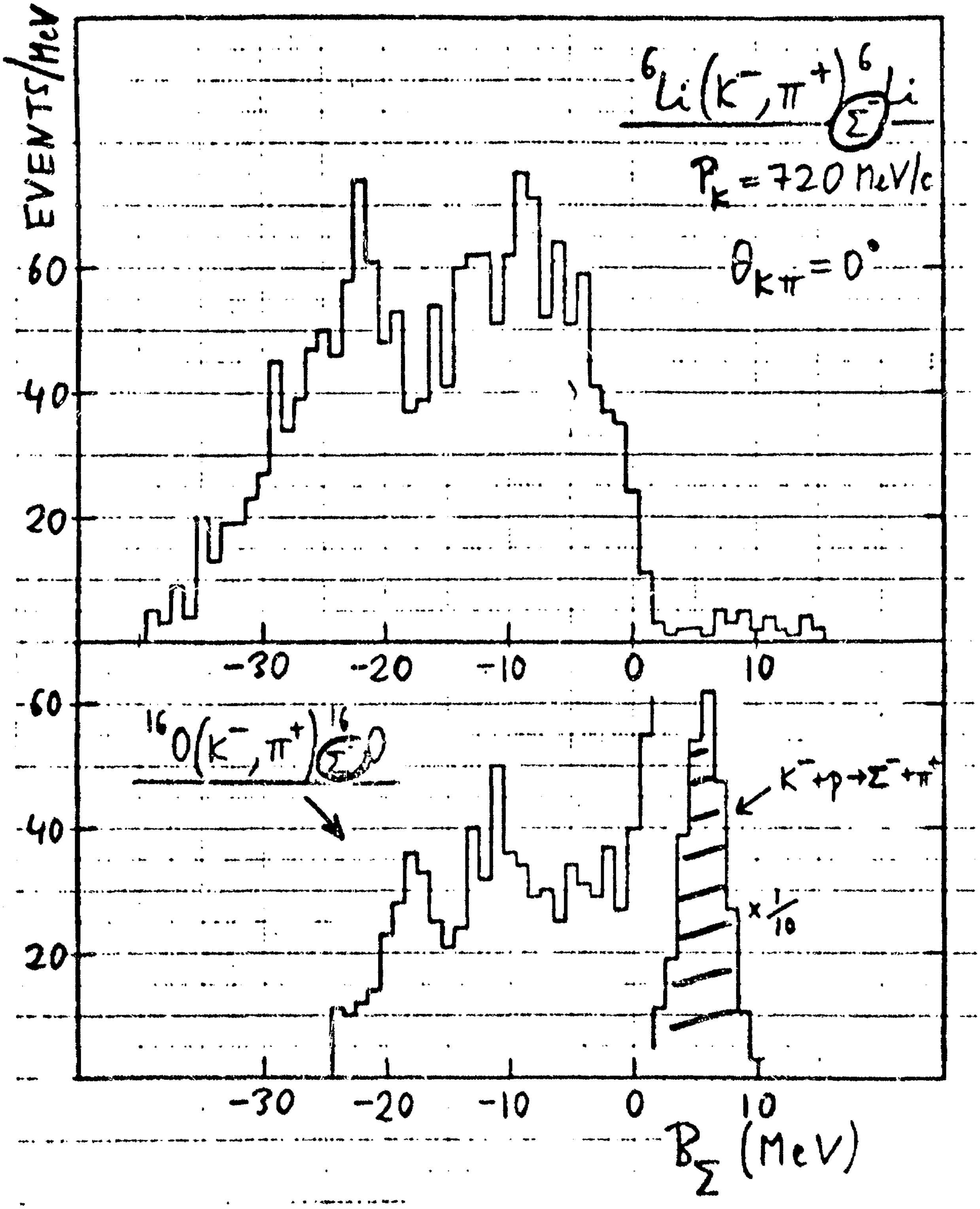
EVENTS/MeV
$^6Li(K^-,\pi^+)^6_{\Sigma}Li$
$P_K = 720$ MeV/c
$\theta_{K\pi} = 0°$
60
40
20
-30
-20
-10
0
10
$^{16}O(K^-,\pi^+)^{16}_{\Sigma}O$
$K^- + p \to \Sigma^- + \pi^+$
×1/10
60
40
20
-30
-20
-10
0
10
B_Σ (MeV)

Fig. 3

III. A. 3 Elastic and Inelastic Kaon Scattering on ^{12}C and ^{40}Ca

We have recently completed analysis of BNL experiment 692 which was a study of $K^{\pm}$ elastic and inelastic scattering from ^{12}C and ^{40}Ca at 800 MeV/c. There were two principal aims of the experiment: (1) to investigate whether or not the fundamental differences in $K^{+}N$ and $K^{-}N$ amplitudes would lead to widely disparate interactions with nuclei, and whether such differences could be understood theoretically; and (2) to provide phenomenological distorted wave information for use in the studies of the (K^{-},π^{-}) reactions. An interesting sidelight of the experiment was the simultaneous accumulation of rather high quality $\pi^{\pm}$ elastic and inelastic data in an energy region where no previous data exist (see below).

All data were accumulated at the Moby Dick spectrometer installation at BNL. A schematic diagram of the apparatus is shown in fig. 4. The device is in reality two spectrometers symmetrically placed about the target location. Each arm is about 8 m long, and together with the LESB I channel (not shown in the figure), make up a flight path of roughly 24 m. At the momentum of our experiment only 10% of the kaons survive to form good event triggers. The π/K ratio at the entrance to the spectrometer was about 12/1, so that pion counting statistics were quite high. The kaon rates at the target for 4×10^{12} protons on the production target were 20,000 and 60,000 for K^{-} and K^{+} respectively. The larger elementary cross sections for $K^{-}N$ over $K^{+}N$ nearly equalized the number of scattered particles from for each sign of kaon. Kaons were well identified using a combination of time-of-flight measurement and Fitch Ĉerenkov counter techniques. Pions were not so well identified and that part of the experiment suffers uncertainties due to muon contamination. A typical spectrum for kaons is shown in fig. 5; the resolution is about 2 MeV.

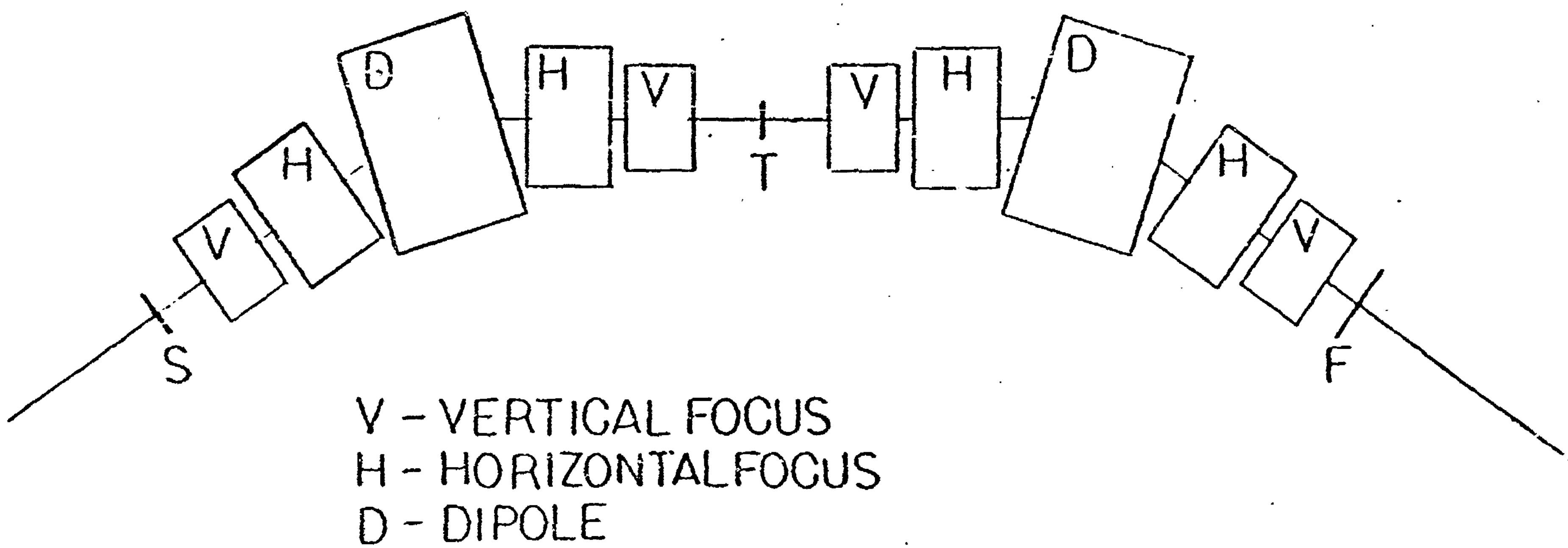

Figure 4 The Moby Dick magnets and their functions. Magnets marked D are horizontal bending magnets. V and H denote vertically and horizontally focusing quadrupole magnets.

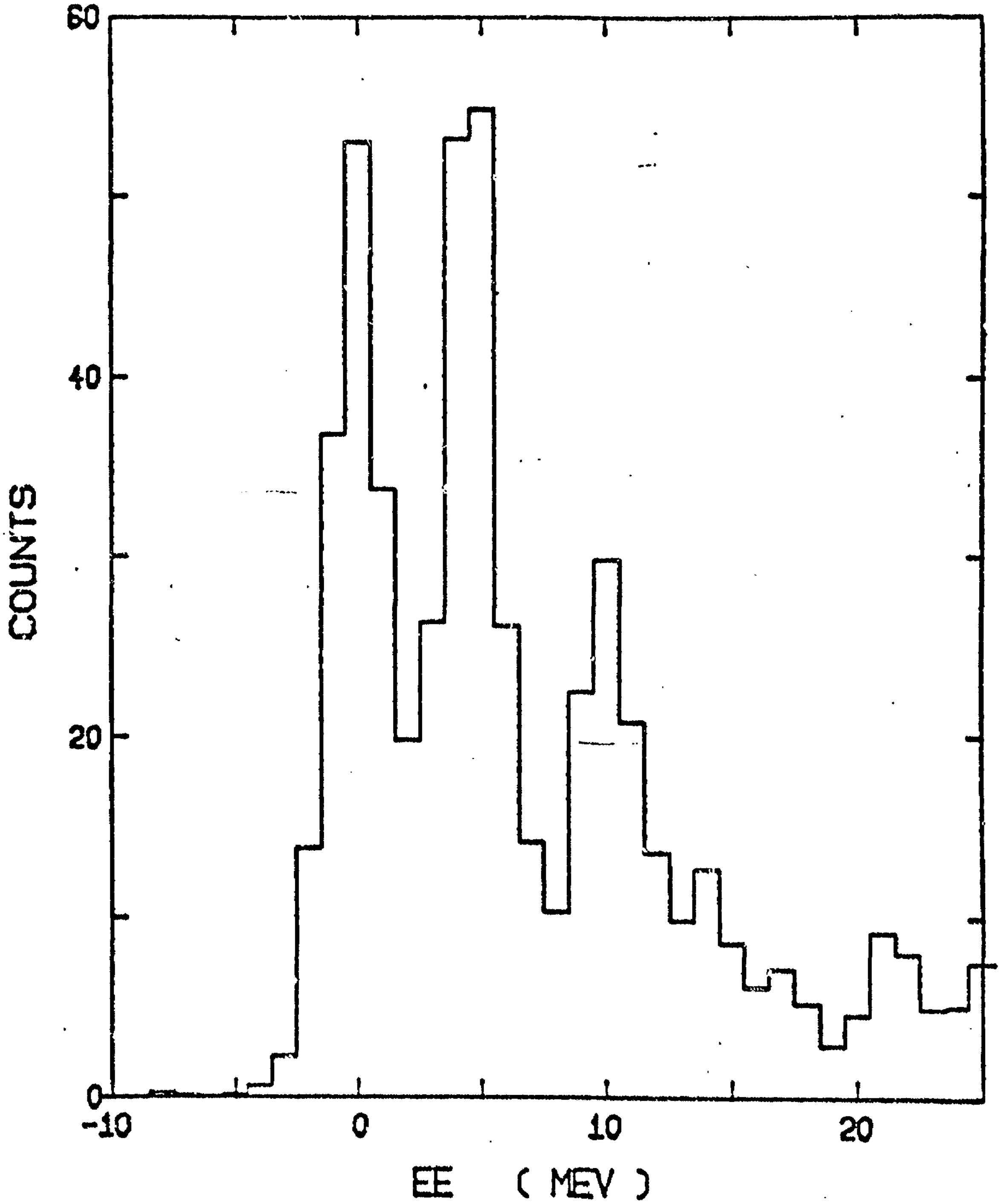

Figure 5 Excitation spectrum for the reaction $^{12}C(K^-,K^-)$. The events in the spectrum come from a one degree scattering angle bin centered at 18.5 degrees. These events were collected at a variety of different angle settings of the spectrometer.

All of the data were normalized by measuring the scattering from hydrogen in a CH_2 target. This was done at several angles for all projectiles; the results are shown in figure 6 for kaons. Running on the CH_2 target allowed a direct normalization of carbon scattering to hydrogen scattering. For the kaons, an additional check was possible by observing "straight-through" decays $K \to \mu\nu$. Results of this check compared to our Monte Carlo simulation of the spectrometer acceptance are shown in fig. 7.

Let us now turn to an examination of the data. Figure 8 shows all of the elastic $K^{\pm}$ data on ^{12}C and ^{40}Ca. The data extend roughly over the angular range from 3 to 38 degrees. (We were limited at the upper end of the range by physical constraints of the spectrometer and also by counting rate.) The data for both nuclei fall rather sharply with angle and display minima which are characteristic of the nuclear sizes involved. However, they are not sharply diffractive because the basic KN amplitudes are not resonance dominated or particularly absorptive. If one is so inclined, one might conclude that the K^- minima are sharper than those for K^+. For both nuclei, the K^+ minima are further out in angle (typically $\sim 3°$) than for K^-, indicating, if the language of diffraction theory is correct, that K^+ sees a smaller nucleus than K^-.

Shown also in fig. 5 are calculations using the coordinate space optical potential program NPIRK. The predictions shown were generated using a Kisslinger form of the optical potential, viz

$$2EV_K(r) = - Ab_0 k^2 \rho(r) + Ab_1 \vec{\nabla}\cdot\rho\vec{\nabla}$$

The complex parameters b_0 and b_1 were generated using the best available phase shift information, and correspond in the theory to KN s- and p-waves

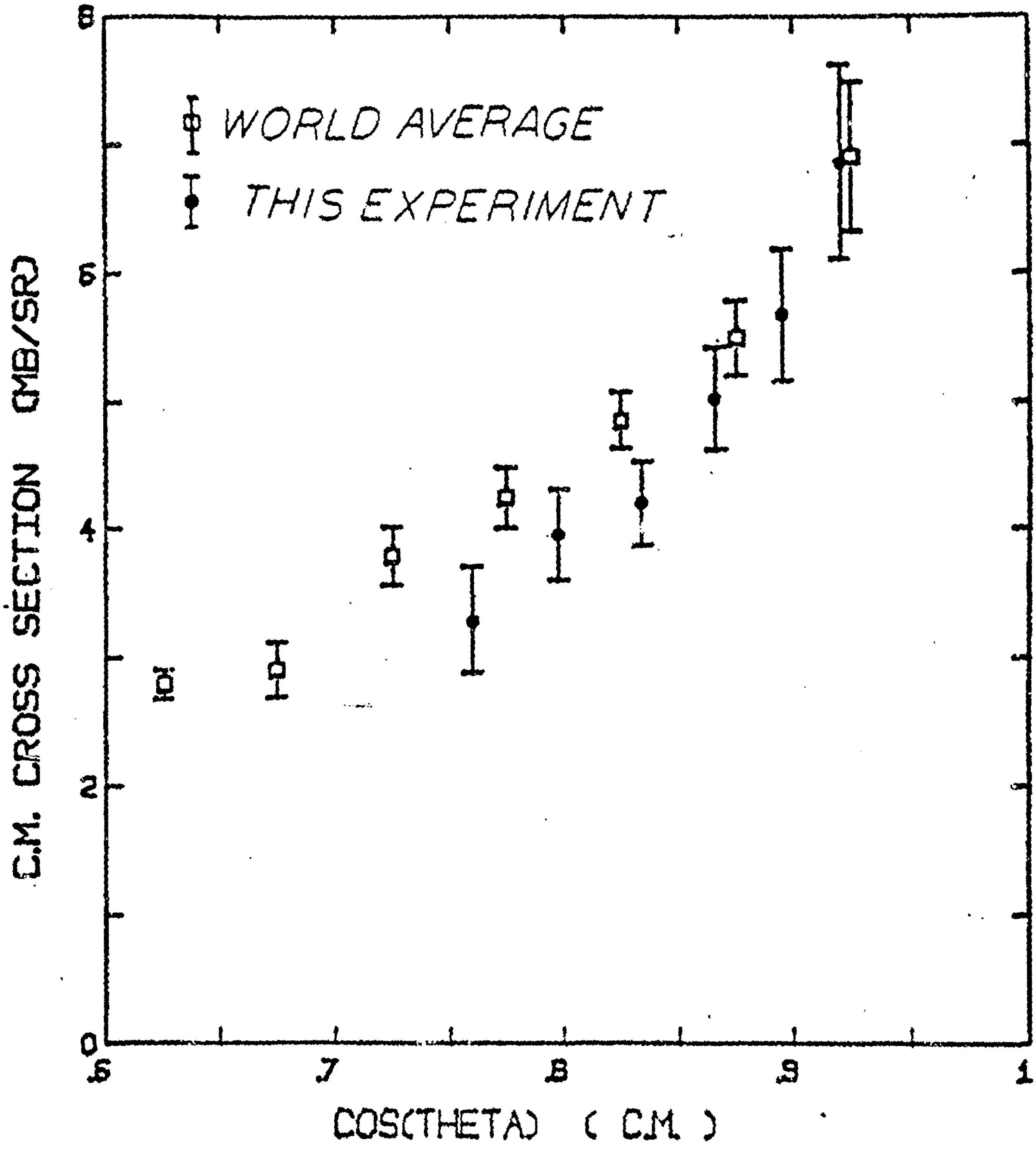

Figure 6a Center of mass cross sections for the reaction p(K^-,K^-)p at or near 800 MeV/c kaon lab momentum. The results of this experiment compared to the weighted average of the individual measurements.

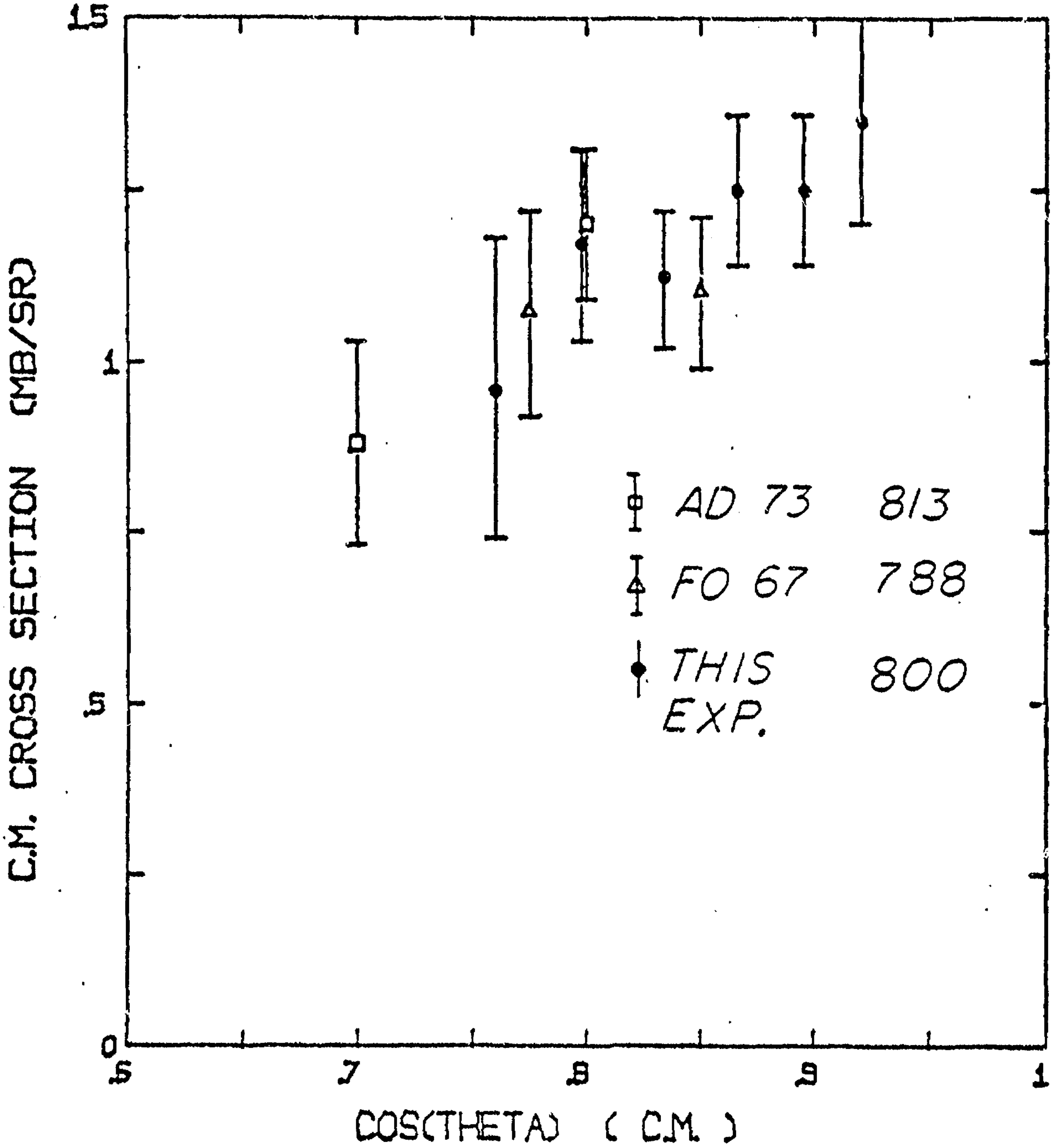

Figure 6b Center of mass cross sections for the reaction p(K^+,K^+)p at or near 800 MeV/c kaon lab momentum. The results of this experiment are compared to the results of previously published measurements: AD73, C. J. Adams, et al., Nucl. Phys. B66, 36 (1973); FO67, S. Focardi, et al., Phys. Letts. 24B, 314 (1967).

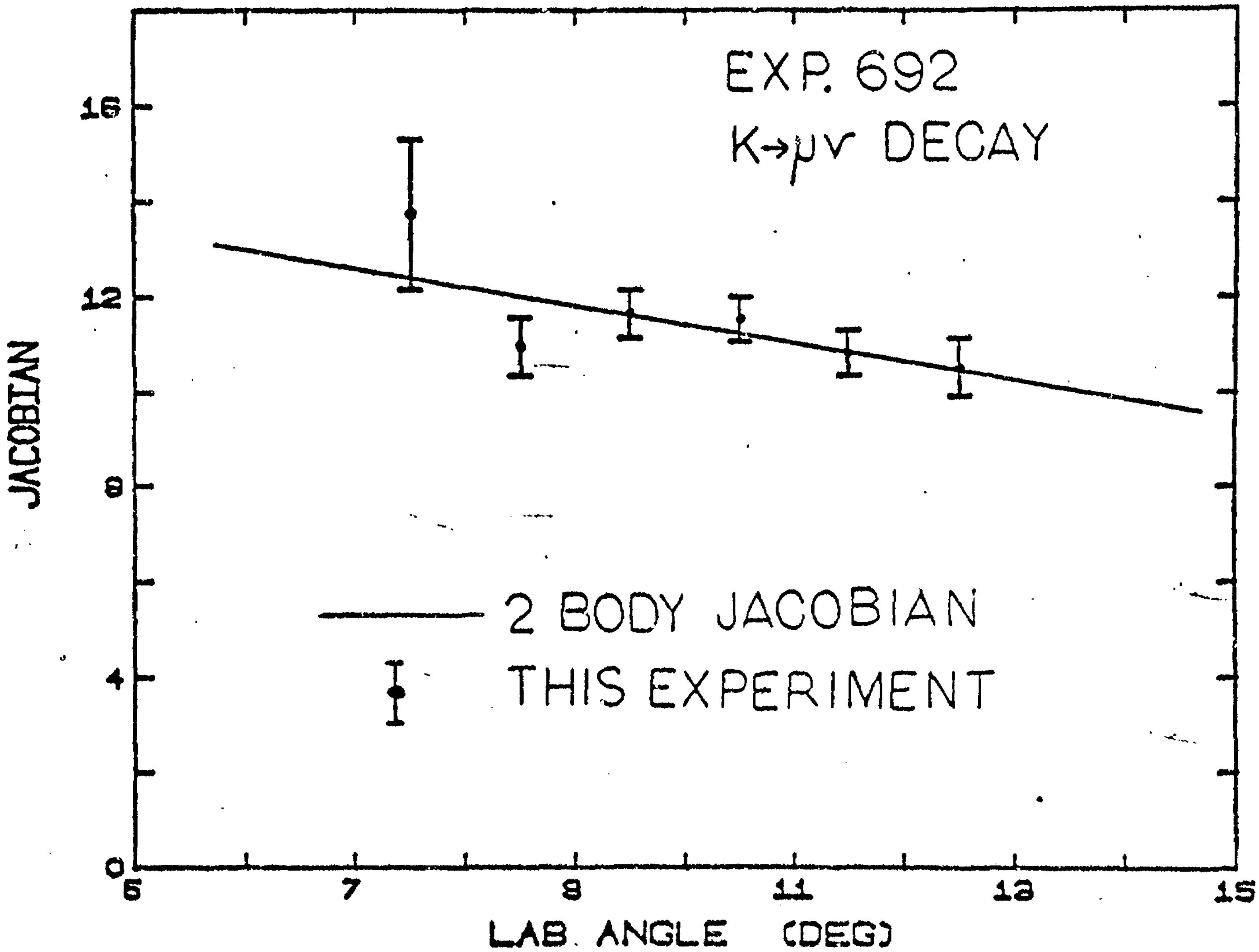

Figure 7 Calculated (solid line) and measured values (data points) of the Jacobian for the reaction

respectively. For K^+, our data show a clear preference for the results obtained by B. R. Martin over the earlier work of the BGRT collaboration. The parameters used for the K^+ calculations are given in Table I. In calculating the coefficients b_0 and b_1, K^+ partial waves s through f were used. Since there are ambiguities associated with the generation of optical potential terms in coordinate space corresponding to KN partial waves higher than the p-wave, all such higher waves were lumped together with the s-wave to yield an effective b_0. In fact the b_1 term includes only the contribution from P_{01}, since it is the largest contributing amplitude.

For the K^- calculations the amplitudes of Alston-Garnjost et al. and also of Gopal were used, but there was no discernible difference between them in predicting K^--nucleus scattering. In these calculations, all elementary partial waves were lumped together to give only an effective b_0 (see table I). No separate term in b_1 was included since the p-waves were all of equal size, or smaller, than the higher partial waves.

Several effects which could conceivably be important have been left out of these coordinate space calculations. The Kisslinger potential has several known deficiencies, including a zero-range fundamental KN amplitude with unphysical off-shell behavior. In addition, the nucleon finite size, which must be removed because it is already included in the elementary t-matrix, must be extracted simply by alteration of the parameters in the ground state nuclear density. For all of these effects, there are considerably more precise models available in momentum space; these are described below. The so-called "angle transformation" was omitted from consideration in the coordinate space calculations because there exists

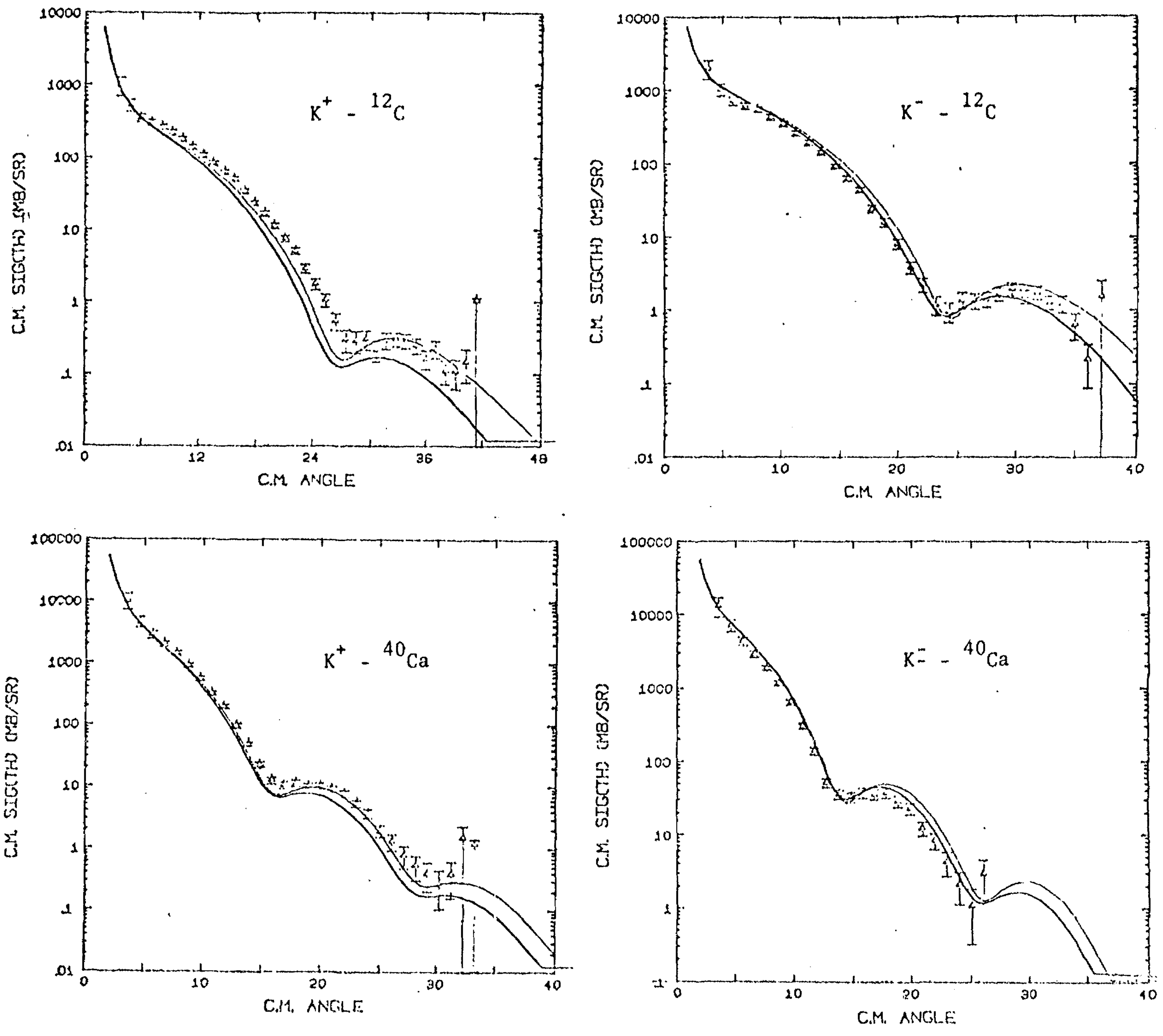

Fig. 8 Co-ordinate space calculations of kaon scattering. The upper curves use electron scattering densities corrected for finite nucleon size; the lower curves are uncorrected.

no accurate way to admix properly the d, f, g waves with the s and p waves. Therefore, this effect was also left to the momentum space treatment.

The curves shown for each case in fig. 8 correspond to different choices of the ground state density. The lower curves are obtained using unmodified electron scattering densities, while the upper ones are densities modified for finite size. For reasons not well understood, the K^+ data prefer the modified densities while the K^- prefer unmodified densities. The proper way of calculation using this particular coordinate space formulation is unclear, because while it is certainly true that the finite nucleon size is already included in the t-matrix and therefore should not be "double-counted" in the nuclear density, using an uncorrected density is a conceivable way of mocking up range effects not otherwise included in the model. In any case, it is clear that the calculations, which are unadjusted, reproduce the essential features of the data. If the parameters b_0 and b_1 are allowed to vary, excellent agreement can be achieved. This was done to describe the entrance channel as accurately as possible for the inelastic measurements described below.

More accurate momentum space calculations also were done for these nuclei. The results for $K^{\pm}$ scattering from ^{12}C are shown in figure 9. In these calculations, the questions raised above regarding KN range, nucleon size, and inclusion of higher partial waves in the elementary t-matrix are correctly resolved in the context of a first-order optical potential.

In fig. 10, calculations of K^- scattering from ^{12}C and ^{40}Ca using a coordinate space rendition of "doorway" theory are presented. This theory, which has been formulated for kaons by Kisslinger, seeks to describe the K^--nuclear interaction via the formation and decay of Λ and Σ resonances

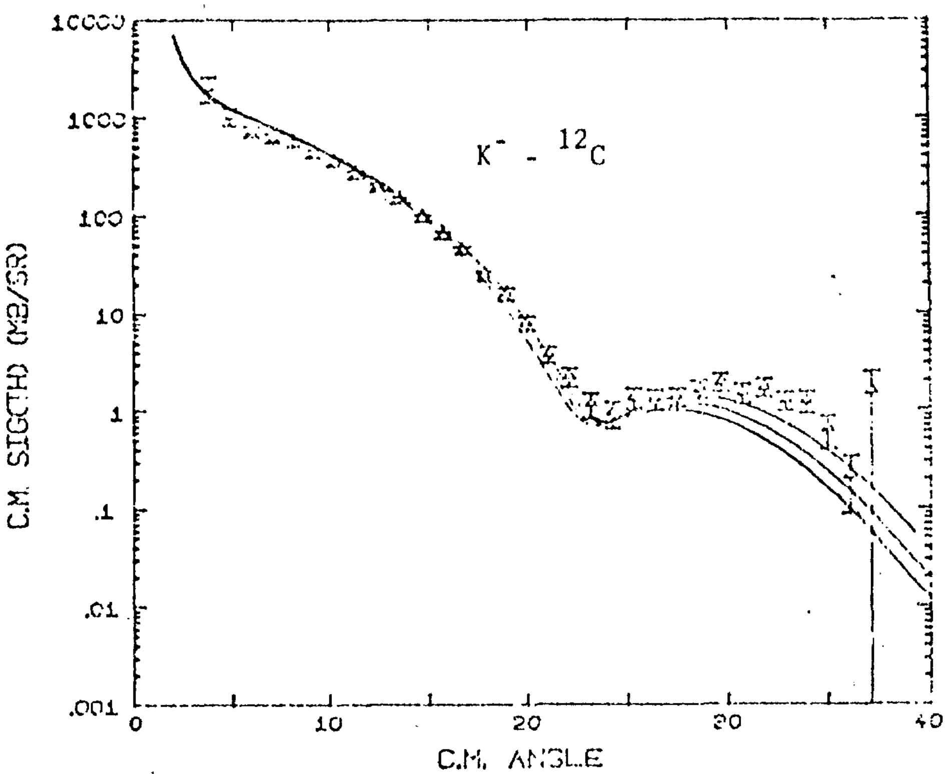

Upper curve: Gaussian finite size correction.
Middle curve: Dipole correction
Lower curve: Uncorrected

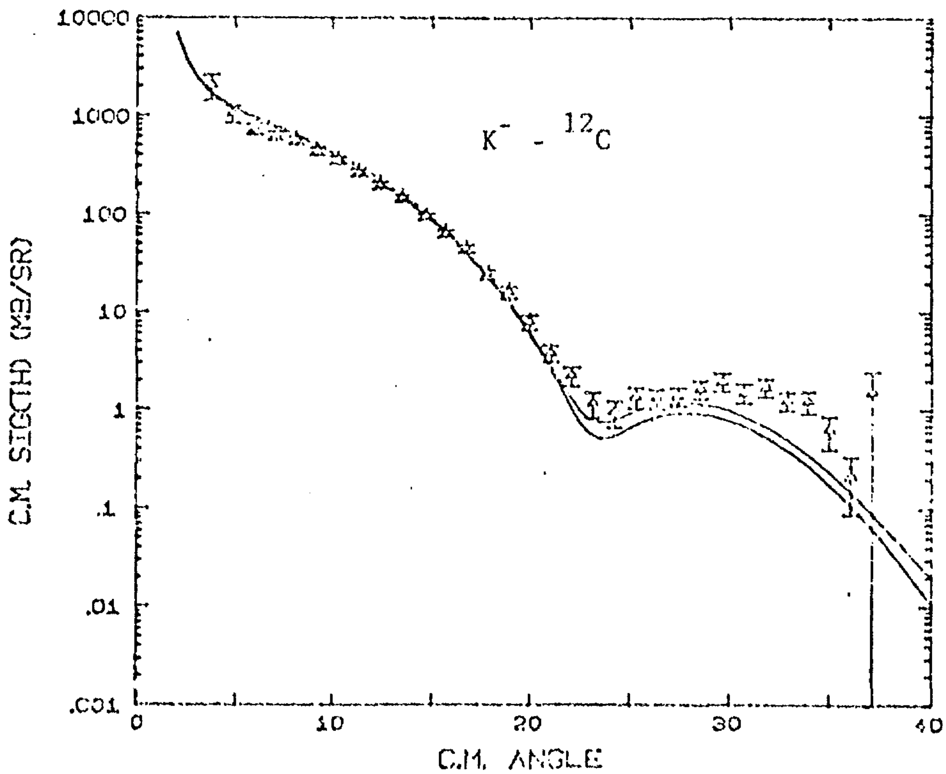

Upper curve: Yukawa off-shell form factor, 800 MeV/c.
Lower curve: Yukawa off-shell form factor, 300 MeV/c.

Fig. 9a Momentum space calculations of K^- scattering on ^{12}C.

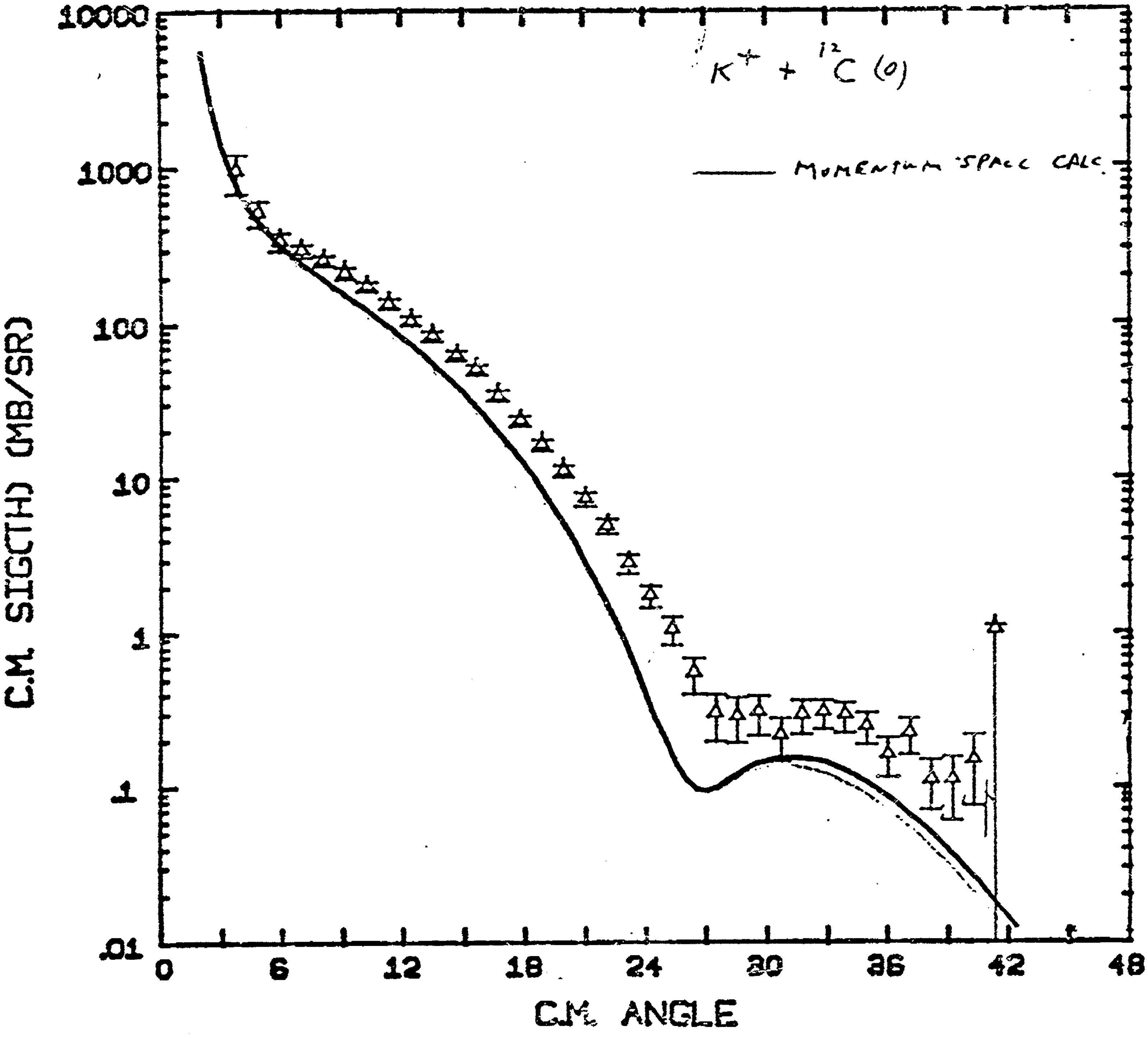

10000
1000
100
10
1
.1
.01
C.M. SIG(TH) (MB/SR)
0
6
12
18
24
30
36
42
48
C.M. ANGLE
$K^+ + {}^{12}C$ (0)
MOMENTUM SPACE CALC.

Fig 9b

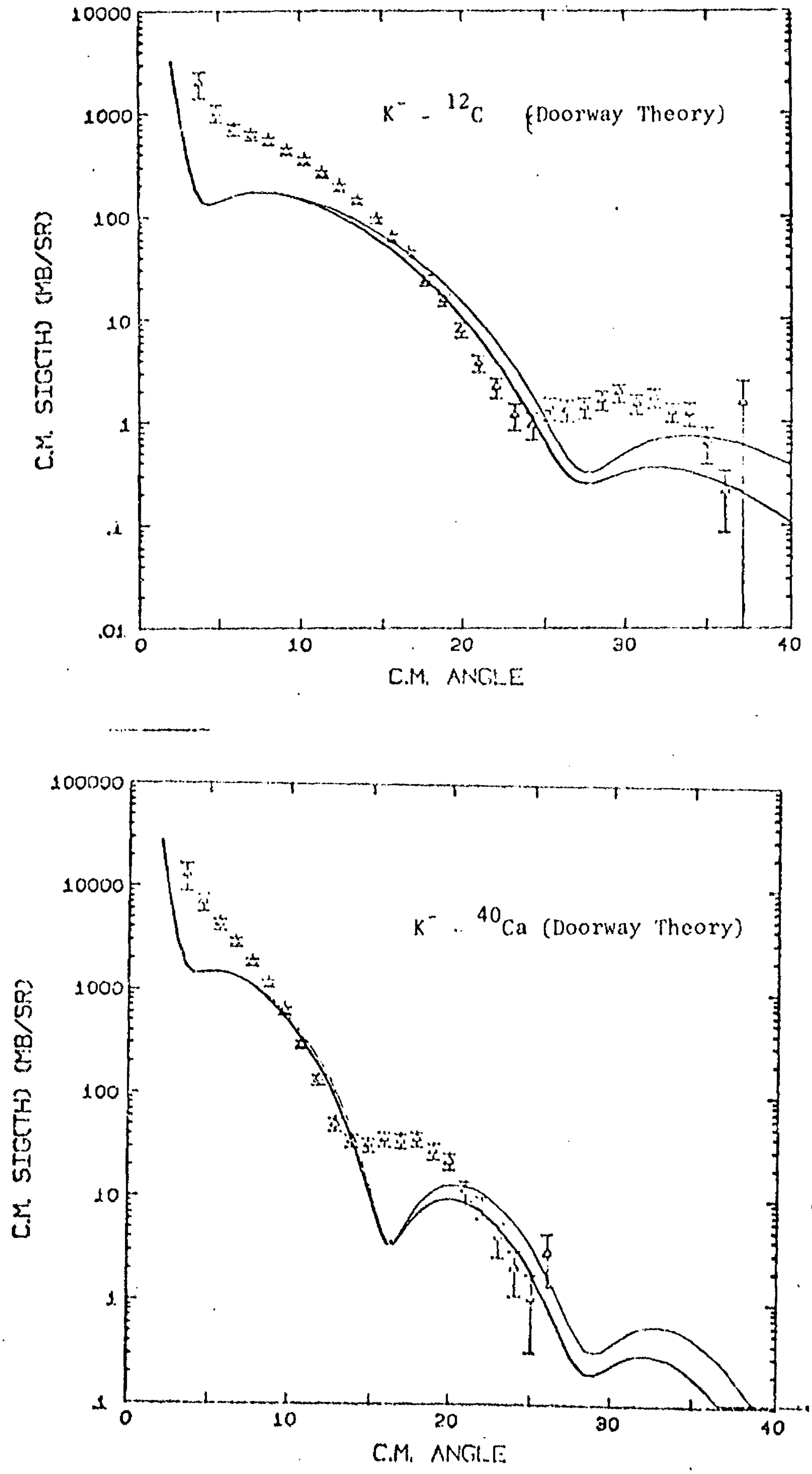

Fig. 10 Doorway theory calculations of K^- scattering on C and Ca.

as the K^- propagates through the nucleus. Kisslinger's paper provides a scheme for expressing these ideas in coordinate space using an optical potential of the form

$$2EV(r) = A[-b_0 k^2 \rho + b_1 \nabla \cdot \rho \nabla + b_2 \nabla^2 \rho + b_3 \nabla^4 \rho ,$$

where the coefficients b_0 through b_3 are generated from the elementary phase shift information. The very poor agreement of the theory with the data probably points more to the deficiencies of the coordinate space optical potential form given above than to problems with the basic doorway model. It is clear, however, that more work in this area remains to be done.

The last results from our kaon experiment to be discussed are the inelastic scattering data obtained for the 2^+ and 3^- states in ^{12}C at 4.4 MeV and 9.6 MeV, respectively. These are shown in figure 11 compared to calculations using the coordinate space distorted wave program NDWPI. As mentioned above, the elastic channel is described using a best-fit optical potential to the elastic data from NPIRK. The inelastic transitions are described using transition densities which are taken from electron scattering, as presented by Gustaffson and Lambert. These are of the form

$$\rho_{tr}(r) = r^L(a + b\ r^2 + c\ r^4)e^{-dr^2} ,$$

with the parameters a, b, c, d depending on the nuclear transition involved. Other values of these parameters can be found from a standard rotational model or from the particle-hole calculations of Gillet and Vinh Mau. The

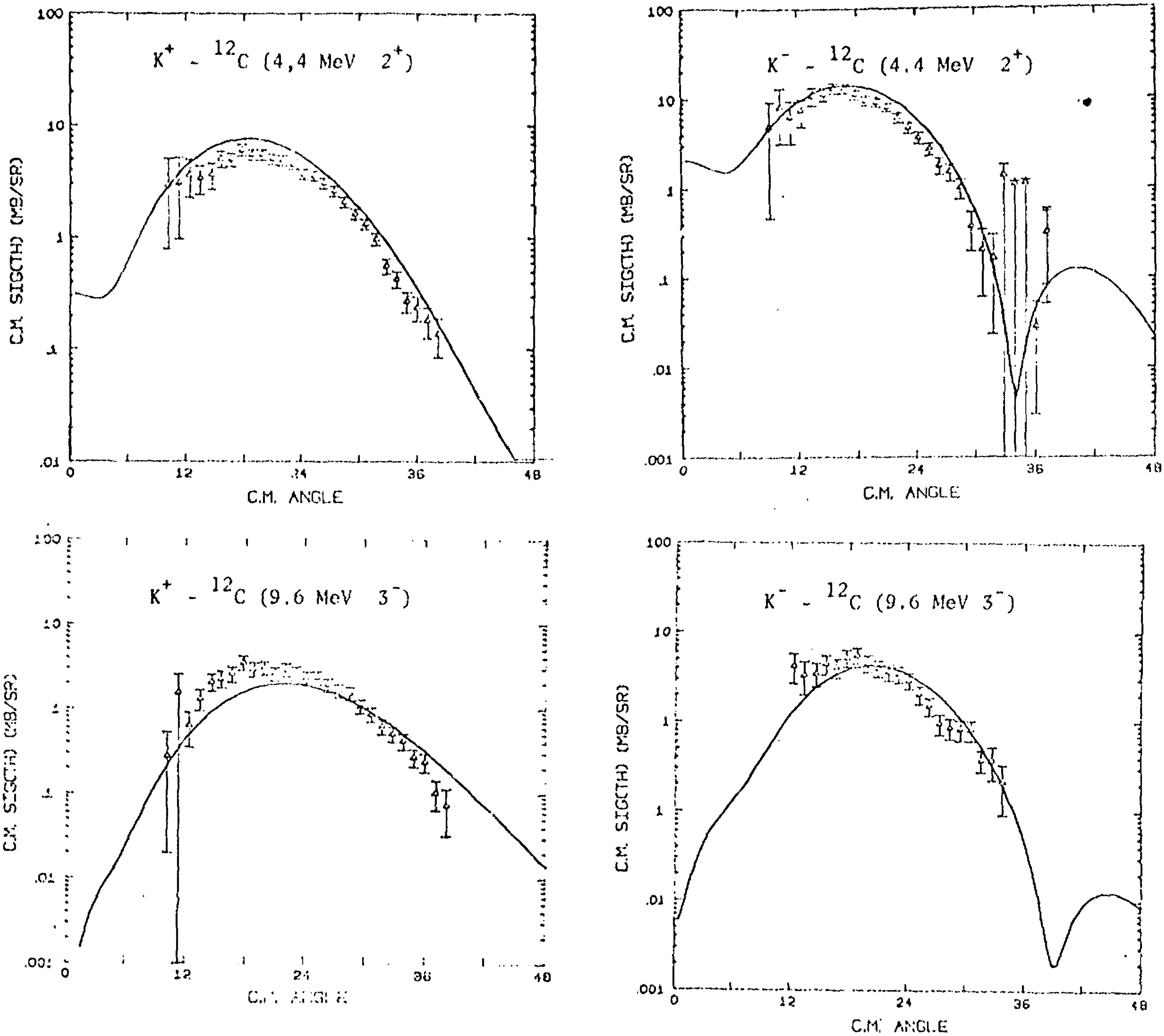

Fig. 11 Calculations of inelastic scattering for kaons on ^{12}C.

three densities so obtained are very different from each other, as shown in figure 12, and yield different predictions for the angular distributions. This is especially true for the K^+ study. Since the transition density for a given state is the same for K^- or K^+, the observed differences must be due to the distortions in the elastic channel. These clearly have a large effect on the inelastic scattering. It is both interesting and satisfying that each of these transitions can be so well described for different projectiles by a common transition density.

	$Re(b_0)$	$Im(b_0)$	$Re(b_1)$	$Im(b_1)$
K^-				
Gopal	.61	.84	-	-
K^+				
Martin	-.335	.241	.084	.161
BGRT D(i)	-.142	.209	.101	.198

Table 1: Table of the optical model parameters calculated by Rosenthal and Tabakin. The elementary kaon nucleon amplitudes have been taken from the analyses of Gopal et. al. , Martin , and the BGRT group. Note that for the K^-, all of the kaon nucleon partial waves have been combined into a single complex parameter, b_0.

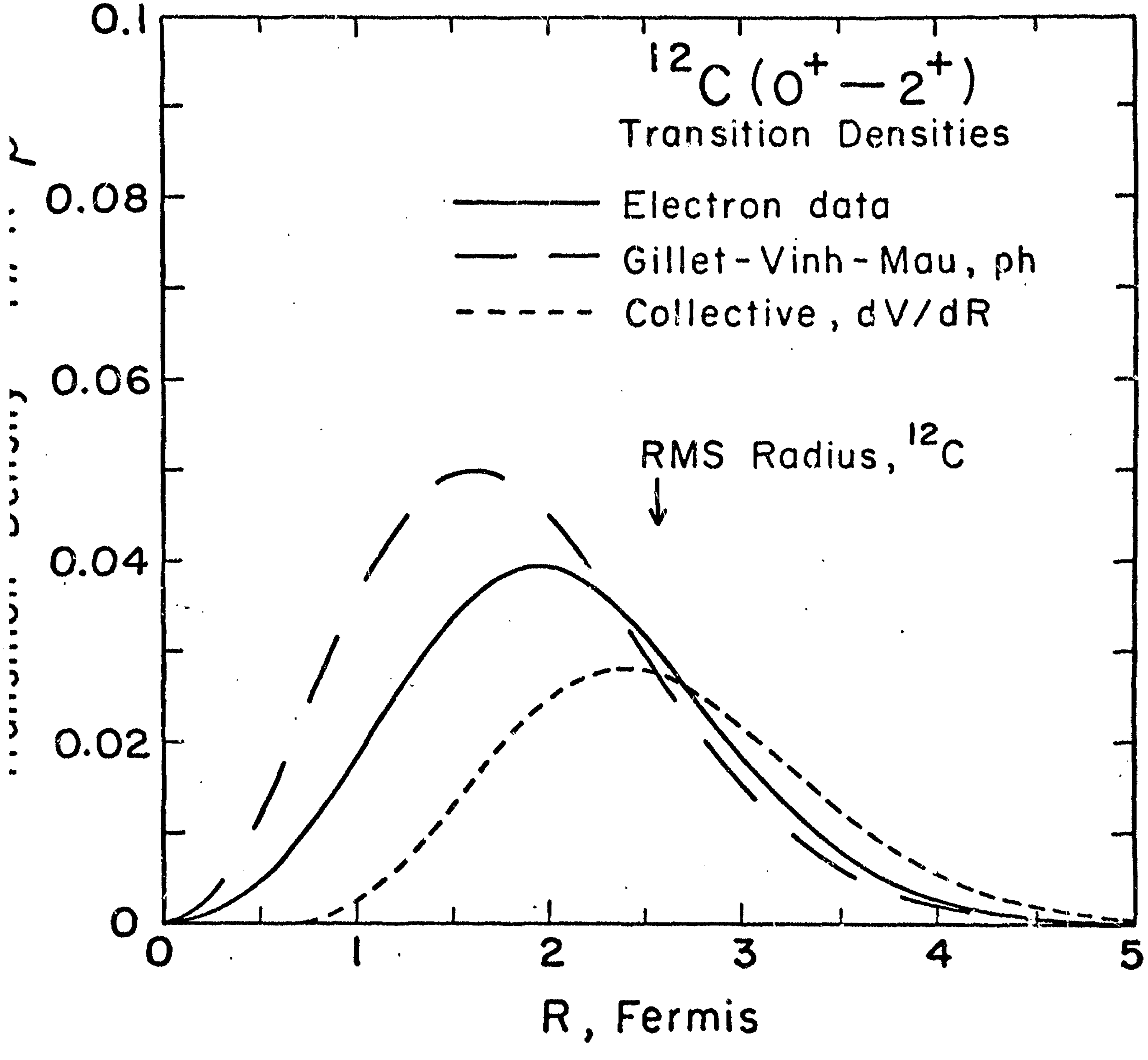

$^{12}C\,(0^+ - 2^+)$
Transition Densities
Electron data
Gillet-Vinh-Mau, ph
Collective, dV/dR
RMS Radius, ^{12}C
0.1
0.08
0.06
0.04
0.02
0
0
1
2
3
4
5
R, Fermis

Fig 12

III. A. 4 $\pi^{\pm}$ Scattering on Carbon and Calcium

During the winter and spring of 1979 differential cross sections were measured for the elastic and inelastic scattering of 800 MeV/c pions from carbon and calcium covering a 4 to 34 degree angular range. The measurements were made simultaneously with those of kaon scattering by using an additional trigger channel.

The data were accumulated using the hypernuclear spectrometer at the BNL AGS Low-Energy Separated Beam with an overall system resolution of about 2.5 MeV with a 2 gram/cm^2 target. The pion beam flux was 1-3 x 10^5 per sec, however the effective flux was typically 2 to 10 times less since the pion scattering trigger rate was adjusted to be less than or equal to the kaon scattering rate. The spectrometer solid angle was about 12 msr with a ±5% momentum acceptance.

The analysis phase of this experiment is almost complete except for an overall normalization factor which must be applied to the data due to a muon component in the incident beam. Typical spectra at two different angles are shown in figure 13. The peaks were fit with gaussians up to an excitation energy of about 10 MeV. The positions of the gaussians were chosen to correspond to actual states in ^{40}Ca (or ^{12}C). Differential cross sections were calculated using the fitted peak areas, measured beam fluxes (corrected for trigger efficiency) and a spectrometer acceptance as predicted by a Monte Carlo computer simulation program. The analysis procedure used for the pion data paralleled the analysis procedure used for kaon scattering data which is described in reference 1.

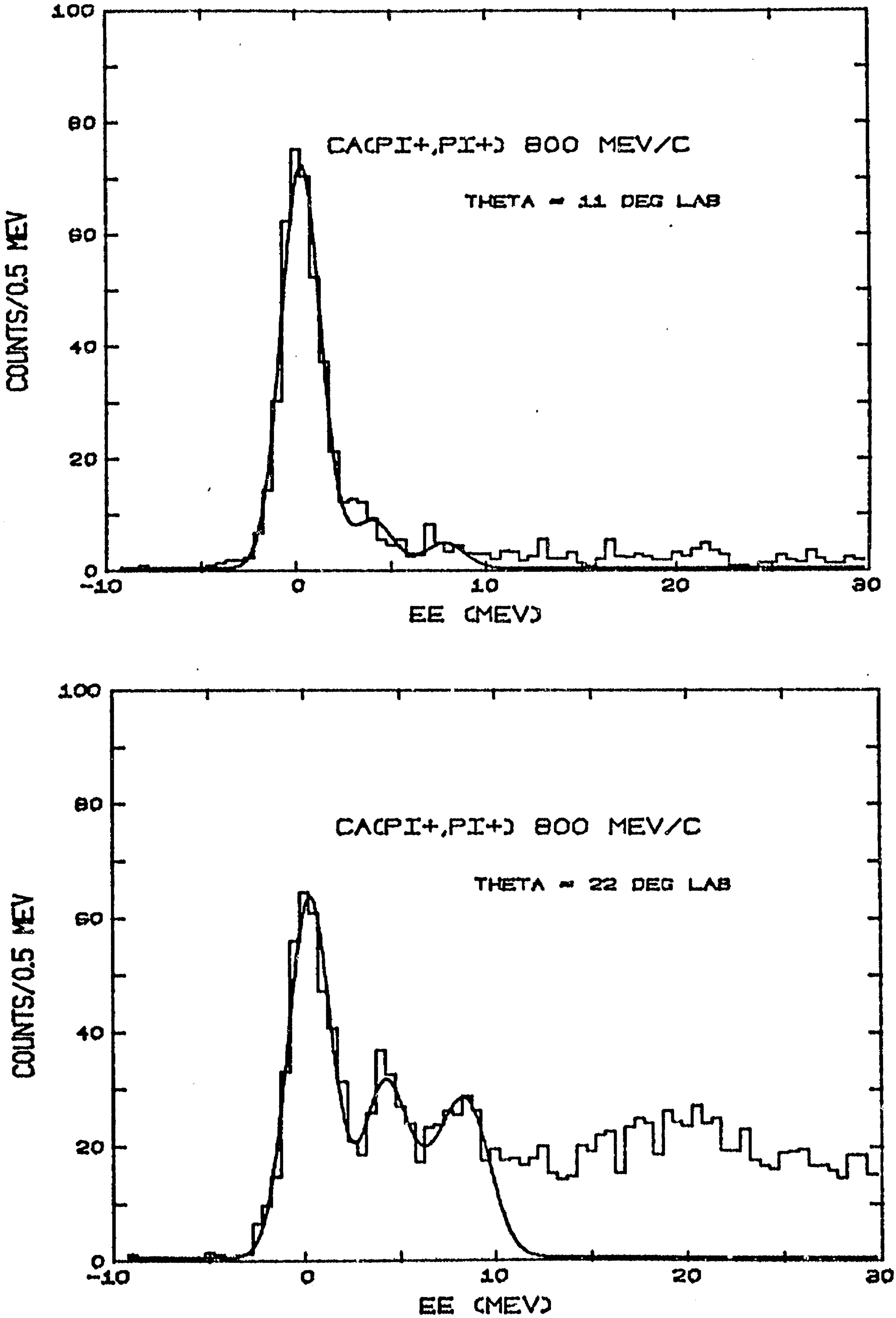
CA(PI+,PI+) 800 MEV/C
THETA = 11 DEG LAB
COUNTS/0.5 MEV
EE (MEV)
CA(PI+,PI+) 800 MEV/C
THETA = 22 DEG LAB
COUNTS/0.5 MEV
EE (MEV)

Fig. 13

The elastic differential cross section data is presented in figures 14 and 15 without a correction for the muon contamination in the incident beam. The dashed lines shown in the figures are momentum space calculations using the computer code PIPIT.[2] The basic amplitudes for the calculations were constructed from the CERN theoretical set including partial waves through $\ell=3$. Electron scattering ground state densities were used and a πN range of 0.25 fm. Variations in the πN range had little effect. The lack of agreement between the theory and the experimental data for the small angle regions suggest that the muon component of the incident beam may be substantial.

The 4.44 and 9.6 MeV states in ^{12}C were also analyzed. The differential cross sections for those states are shown in figures 16 and 17. Distorted wave calculations for these states are in progress at this time.

The overall normalization of this experiment will be based on pion scattering from protons taken with a CH_2 target over a limited angular range. Figure 18 shows both the π^- and π^+ scattering results along with other published experimental data (Bowler[3] and Brody[4]). The dashed lines are calculations based on the CERN theoretical phase shift set and the solid lines on a set generated by Cutkosky.[5] The Cutkosky set includes 80 partial waves and is based on fits to amalgamated data sets[6] which include incident pion momenta between 420 and 2000 MeV/c. Neither calculation includes Coulomb effects (although they are included in reference 5). The data of this experiment will be normalized to the Cutkosky results with Coulomb effects included. The overall normalization factor will be approximately 2 for both the π^+ and π^- differential cross sections. The differential cross sections for pion scattering on the carbon in the CH_2 target are shown in figure 15 as triangles and agreement is found with the natural carbon runs.

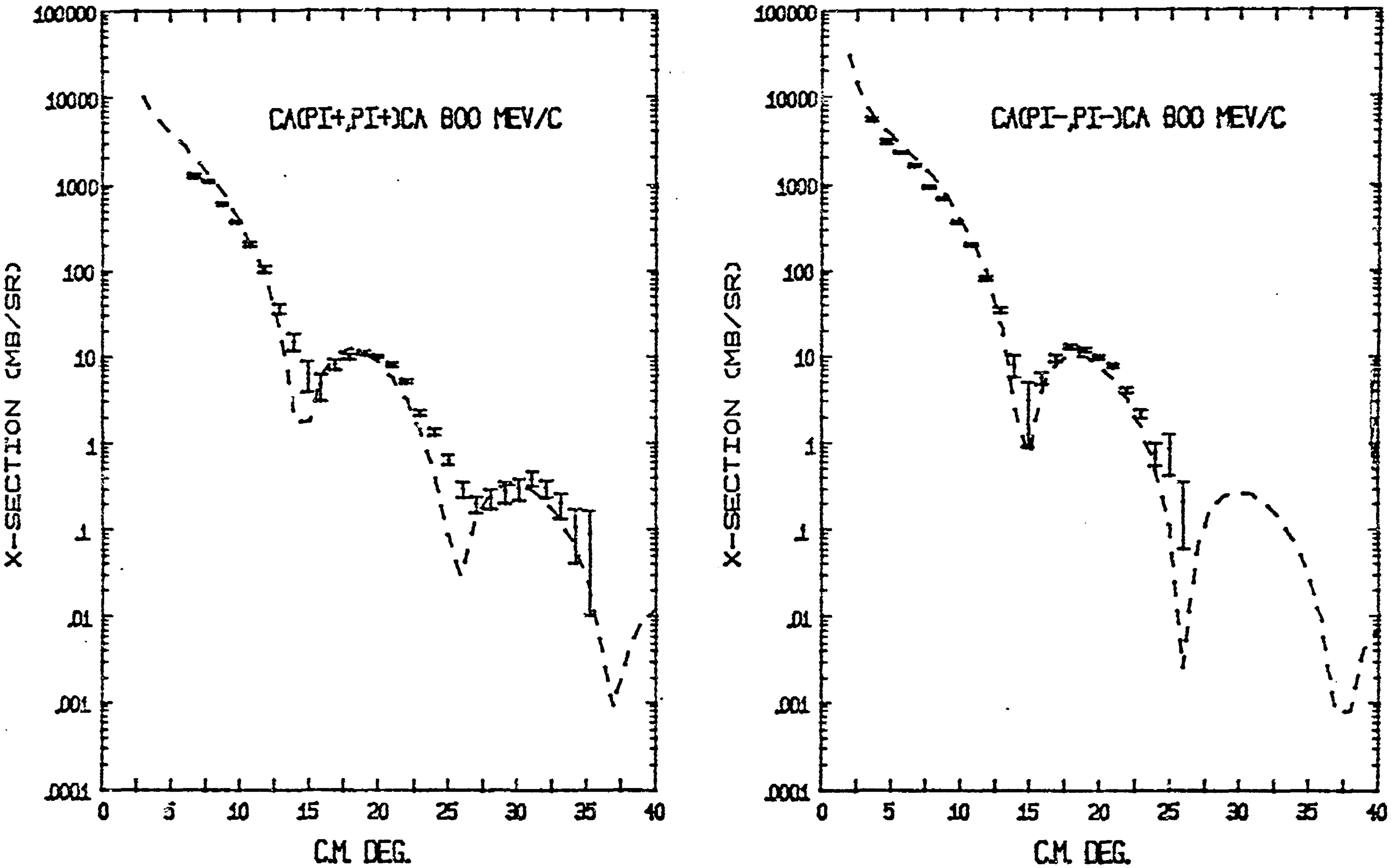
CA(PI+,PI+)CA 800 MEV/C
CA(PI-,PI-)CA 800 MEV/C
X-SECTION (MB/SR)
C.M. DEG.
100000
10000
1000
100
10
1
.1
.01
.001
.0001
0
5
10
15
20
25
30
35
40

Fig. 14

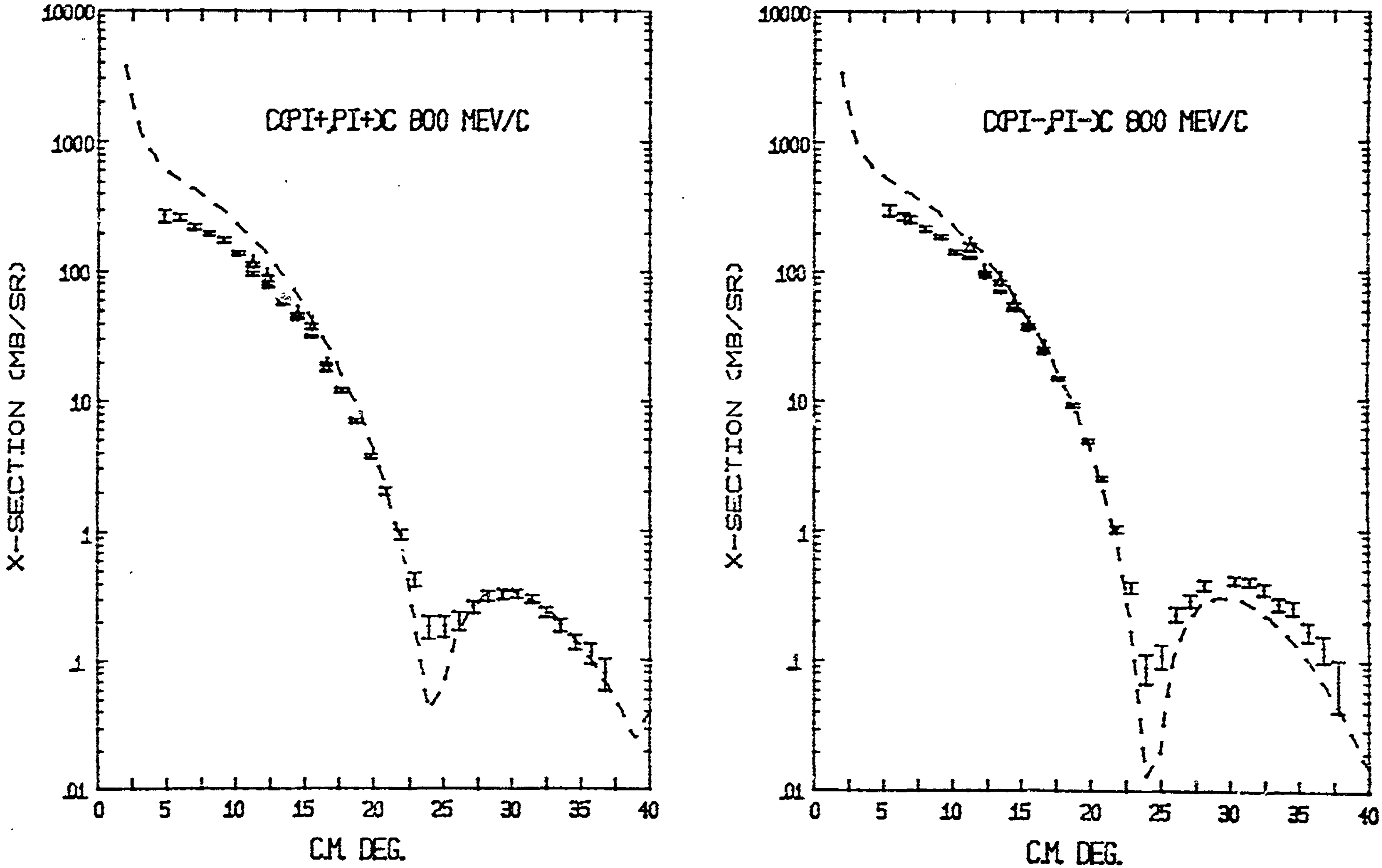
C(PI+,PI+)C 800 MEV/C
C(PI-,PI-)C 800 MEV/C
X-SECTION (MB/SR)
C.M. DEG.
10000
1000
100
10
1
.1
.01
0
5
10
15
20
25
30
35
40

Fig. 15

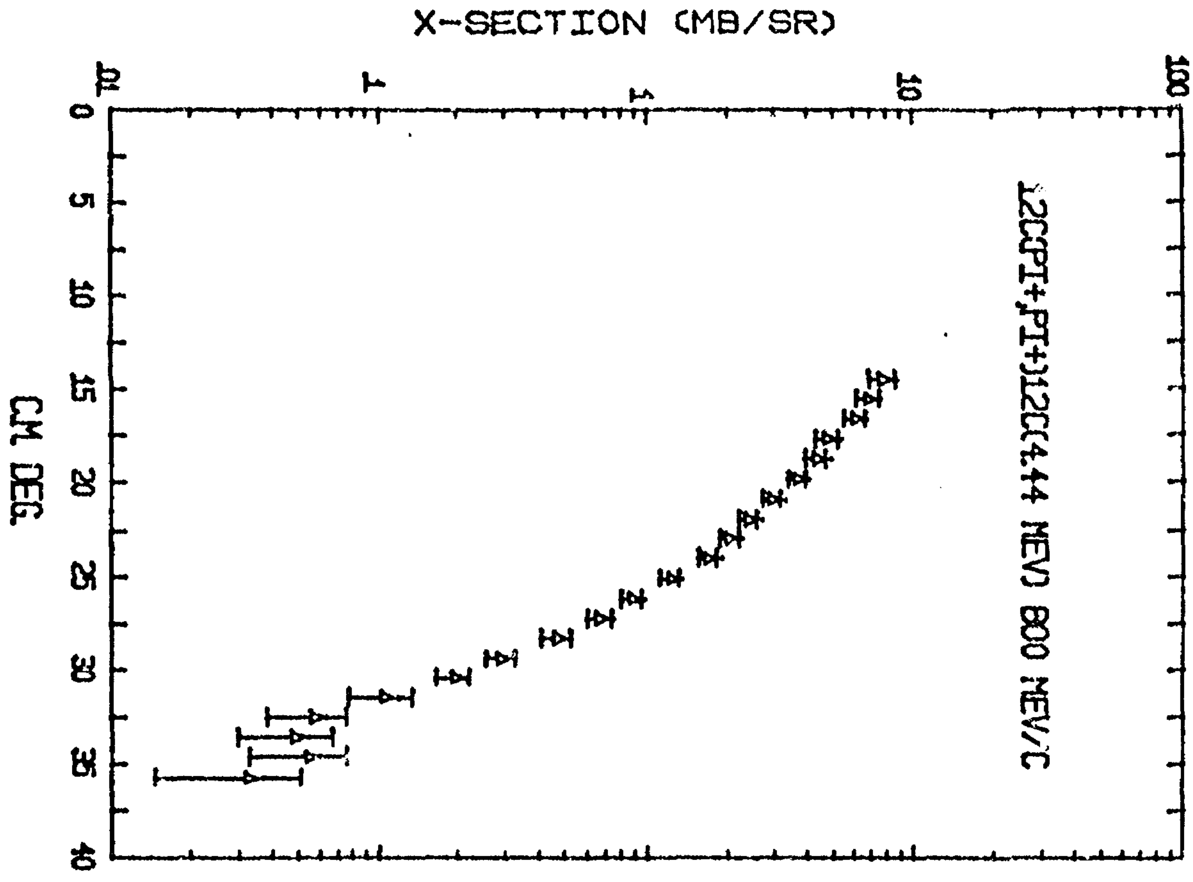
X-SECTION (MB/SR)
12C(PI+,PI+)12C(4.44 MEV) 800 MEV/C
C.M. DEG.

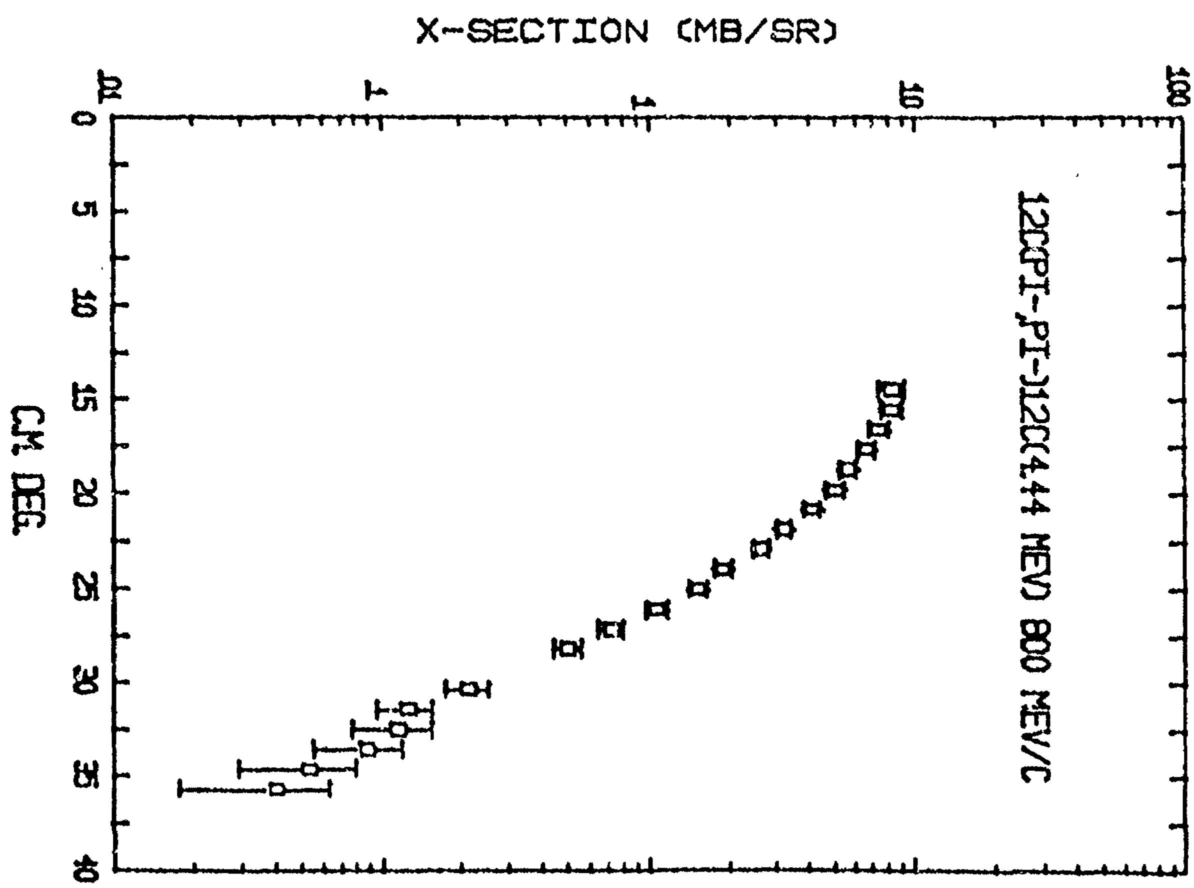
X-SECTION (MB/SR)
12C(PI-,PI-)12C(4.44 MEV) 800 MEV/C
C.M. DEG.

Fig. 16

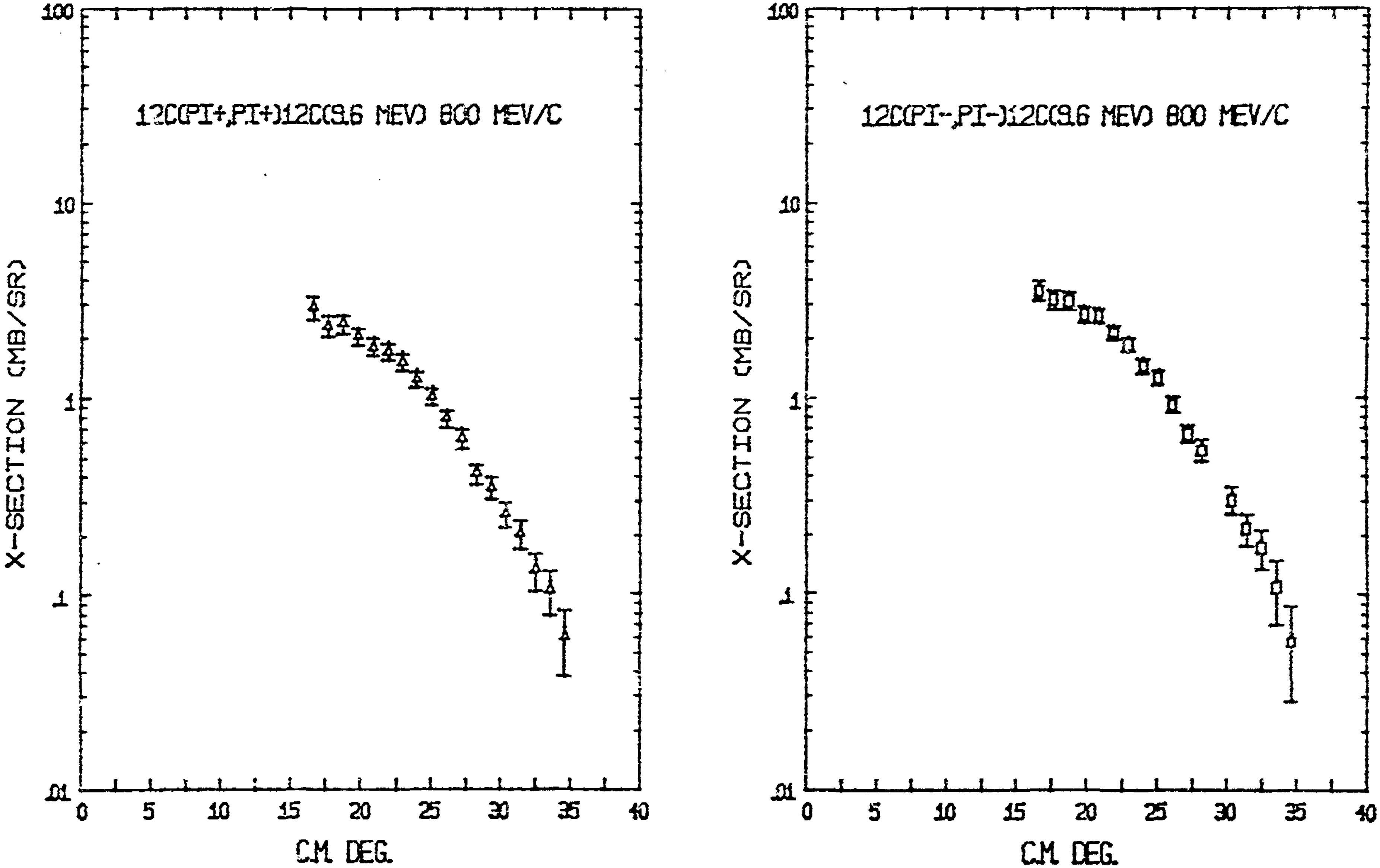
12C(PI+,PI+)12C(9.6 MEV) 800 MEV/C
12C(PI-,PI-)12C(9.6 MEV) 800 MEV/C
X-SECTION (MB/SR)
X-SECTION (MB/SR)
100
10
1
.1
.01
0
5
10
15
20
25
30
35
40
C.M. DEG.
C.M. DEG.

Fig. 17

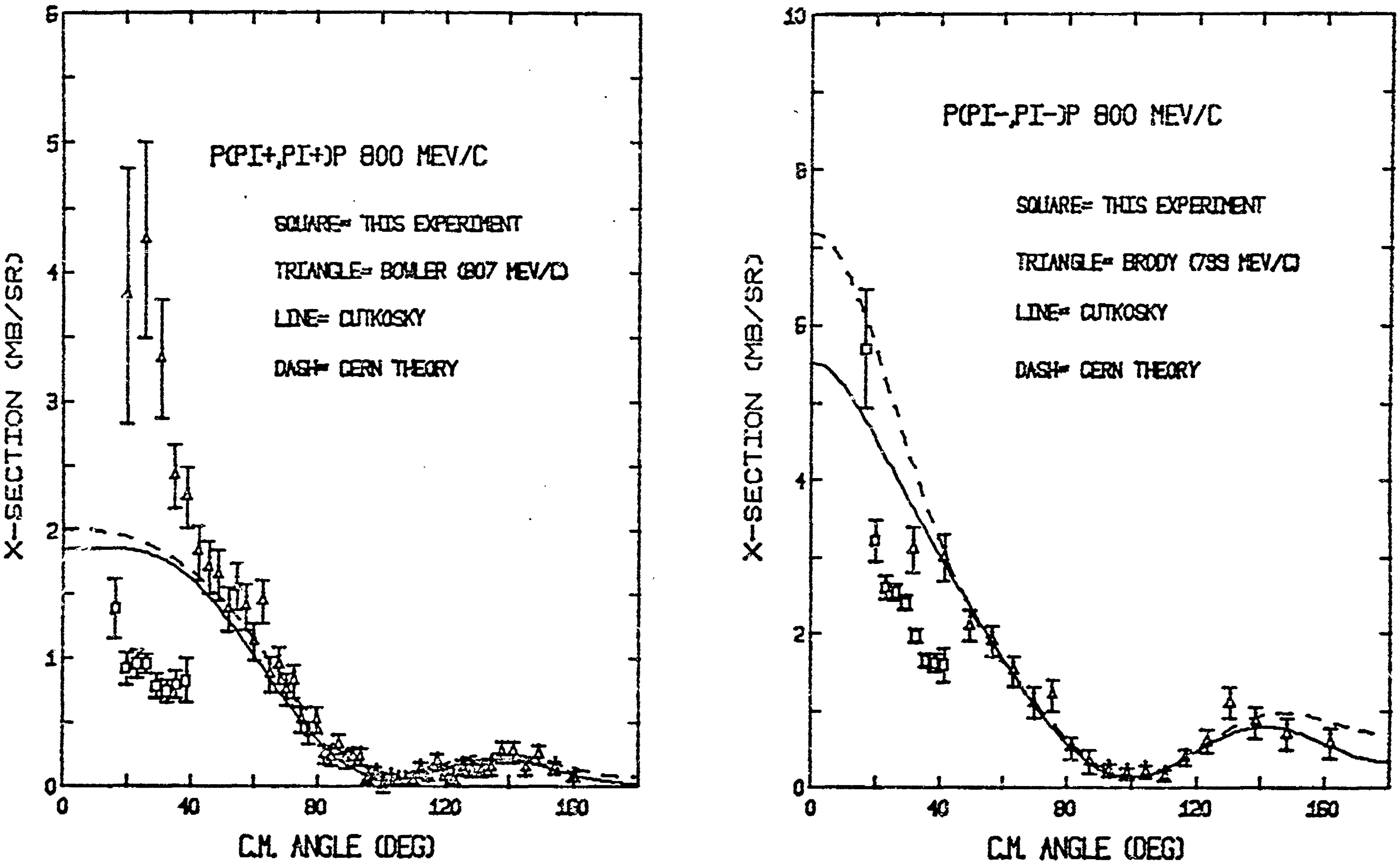
P(PI+,PI+)P 800 MEV/C
SQUARE= THIS EXPERIMENT
TRIANGLE= BOWLER (807 MEV/C)
LINE= CUTKOSKY
DASH= CERN THEORY
X-SECTION (MB/SR)
C.M. ANGLE (DEG)
P(PI-,PI-)P 800 MEV/C
SQUARE= THIS EXPERIMENT
TRIANGLE= BRODY (793 MEV/C)
LINE= CUTKOSKY
DASH= CERN THEORY
X-SECTION (MB/SR)
C.M. ANGLE (DEG)

Fig. 18

The time-of-flight resolution obtained during this experiment between the two trigger scintillators spaced 16.5 meters apart was about 1 nsec fwhm. The resolution was not adequate to clearly distinguish the presence of muons or electrons in the incident beam. At 800 MeV/c the pion-muon time-of-flight difference is about 350 psec. However, during the tuning phases of a recent experiment (May 1981) at the same beam line a time-of-flight measurement was made between the scintillator at the beginning of the kaon spectrometer and another small scintillator placed in the focal plane of the pion spectrometer (17.6 meters separation). We were able to obtain a time resolution of about 400 psec fwhm, which was adequate to clearly see a muon contribution to the pion time-of-flight peak. The beam line was set for negative 720 MeV/c particles with the beam separator tuned to accept kaons. Figure 19 shows the results of this test. The position of the muons and electrons with respect to the pion peak is indicated. Clearly the broadening of the "pion" peak with respect to the kaon peak is due to a substantial number of muons and a relatively small number of electrons. The relation number of muons and pions in the beam is dependent on the beam momentum and polarity; therefore, the pion/muon ratio that would be predicted by a fit to the time-of-flight spectrum in figure 19 could be used to obtain an absolute ratio at a beam momentum of 800 MeV/c. This figure does, however, tend to justify the large normalization factor needed to bring the present $p(\pi^{\pm},\pi^{\pm})p$ data in line with previous experiments.

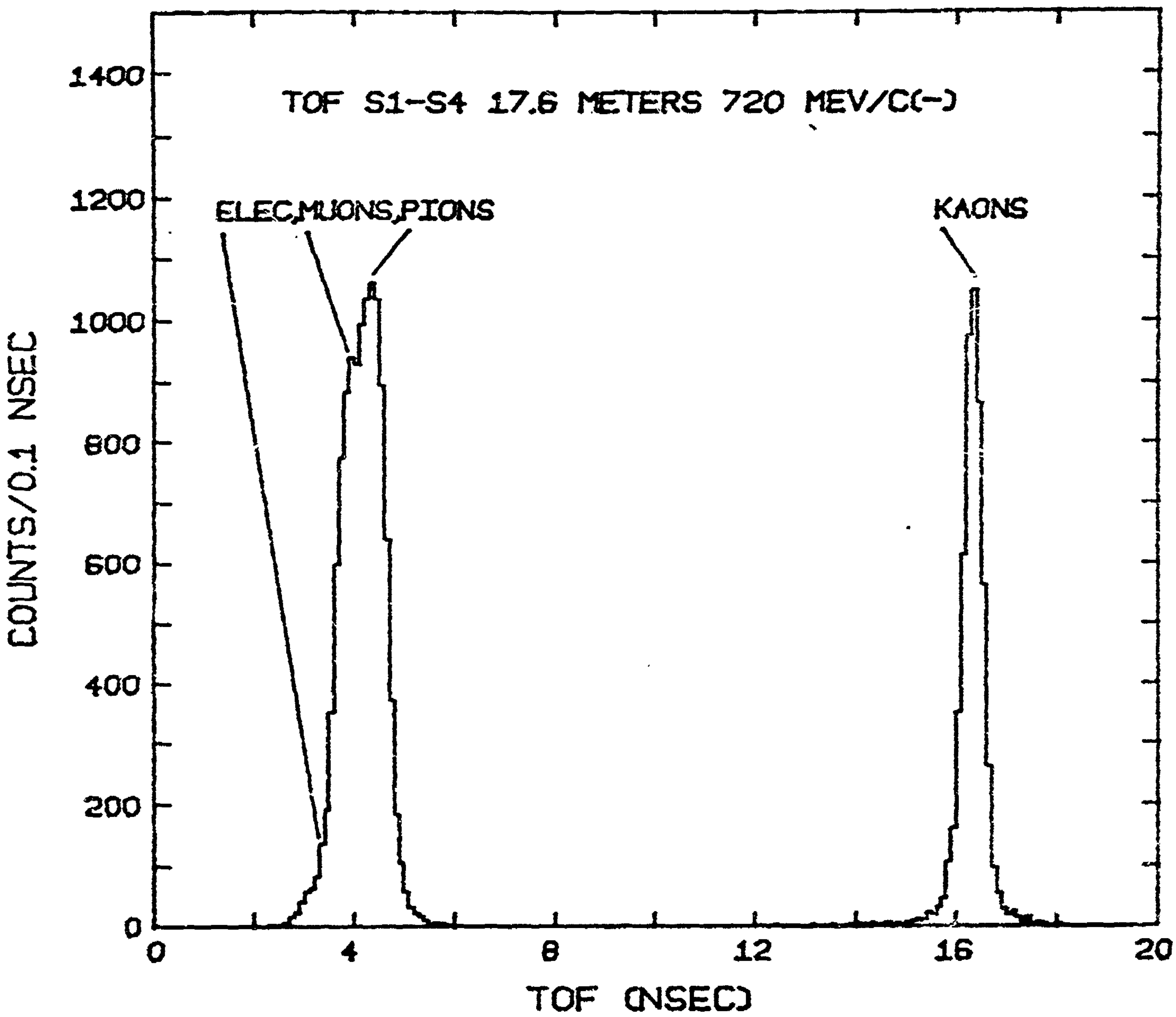
TOF S1-S4 17.6 METERS 720 MEV/C(-)
ELEC,MUONS,PIONS
KAONS
COUNTS/0.1 NSEC
TOF (NSEC)
0
200
400
600
800
1000
1200
1400
0
4
8
12
16
20

Fig. 19

References

1. D.R. Marlow, Ph.D. Thesis, Carnegie-Mellon University (1981).

2. R.A. Eisenstein and F. Tabakin, Comp. Phys. Commun. 12 (1976) 237.

3. M.G. Bowler et al., Nucl. Phys. B37 (1972) 133.

4. A.D. Broday et al., Phys. Rev. D3 (1971) 2619.

5. R.E. Cutkosky et al., Phys. Rev. D20 (1979) 2804.

6. R.L. Kelly and R.E. Cutkosky, Phy. Rev. D20 (1979) 2782.

III. A. 5 Measurement of the Magnetic Moment of the Negative Sigma Hyperon

In the hydrogen-like region the fine structure splitting of an atomic level is proportional to the magnetic moment of the particle in orbit. This has been used by Roberts[1] and Hu[2] to make a 1% measurement of the antiproton magnetic moment in good agreement with the magnitude of the proton moment. In atomic fine structure measurements of the Σ^- moment, Roberts et al.[3] obtain $\mu(\Sigma^-) = -1.48 \pm 0.37$ n m while Dugan et al.[4] obtain $-140 \pm {}^{0.41}_{0.28}$ n m which agree rather well. The simple quark model estimate with equal mass u,d and s quarks gives $\mu(\Sigma^-) = -0.88$ n m while a model in which the s quark is heavier gives $\mu(\Sigma^-) = -1.04$ n m[5]. In a recent paper Brown et al.[6] report a calculation in the chiral bag model in which they obtain $\mu(\Sigma^-) = -0.54$ n m. This problem is being further studied in an Σ^- atom experiment proposed at BNL[7] and a polarized Σ^- hyperon beam experiment at FNAL[8] and is clearly an important test of the quark model.

In AGS proposal #723 our aim is to measure the magnetic moment of the negative sigma hyperon with 0.05 nuclear magneton precision by observing the strength of the fine structure splittings of sigma exotic atom transitions. The institutions contributing to this effort are: Boston University, Carnegie-Mellon University, California Institute of Technology, College of William and Mary, and the University of Wyoming.

Construction of a target hodoscope at CMU (by Sutton and Colella) is now nearly complete. A pion trigger detector is under construction at Boston University while the William and Mary group are finishing the target construction. Execution of this experiment is now scheduled on BNL AGS beam LESB-I for early spring, 1982.

References

1. B. L. Roberts, Phys. Rev. D17 (1978) 358

2. E. Hu, Y. Asamo et al, Nucl. Phys. A254 (1975) 403

3. B. L. Roberts, C. R. Cox et al, Phys. Rev. D12 (1975) 1232

4. G. Dugan, Y. Asamo et al, Nucl. Phys. A254, (1975) 396

5. H. J. Lipkin, Phys. Lett. 89B (1980) 358

6. G. E. Brown, M. Rho, V. Vento, Phys. Lett. 97B (1980) 423

7. M. Eckhause, K. Giovanetti, R. Hartmann, D. W. Hertzog, J. R. Kane, J. Lindemuth, W. A. Orance, W. F. Vulcan, R. E. Welsh, R. G. Winter, B. L. Roberts, R. B. Sutton, N. J. Colella, R. J. Powers, and A. R. Kunselman, BNL Proposal #723

8. R. Rameika et al., (to be published); results reported by R. Handler, XXth Inter. Conf. on high energy physics, Madison, Wisconsin, 1980; T. Devlin, Bull, Am. Phys. Soc. 25 (1980) 572; O. Overseth, 4th Inter. Conf. on baryon physics, University of Toronto, July 14-16, 1980

III. A. 6 Weak Decay Modes of Lamda Hypernuclei

In order to augment our growing knowledge of hypernuclei we are preparing an experiment to study the weak decay (ie. particle decay.) of ^{12}C hypernucleus. This experiment will measure the hypernuclear lifetime (to ± 15%) as well as the energy distribution and partial rates for the charged particle decays making it the most complete and precise hypernuclear decay experiment to date. This project (BNL Exp. #759) was proposed and defended before the BNL-AGS program review committee in March, 1981. It was approved for 450 hours. We are now preparing the final detector designs and preparing for detector construction.

Experimental data up until recently have been obtained from bubble chambers and emulsion stacks. These experiments measured partial rates for A=1 to 12 and the mean lifetime for A=3 to 5. However these data are based on only a few events and are subject to large errors. (See figure 20.)

The most recent hypernuclear decay experiment was done by Nield et al. This experiment used an ^{16}O heavy ion beam on a polyethylene target. K^+ emission was used as the hypernuclear formation trigger, and the nuclear recoil track was reconstructed with spark chambers. These data however suffer from a large background and few good events (22 in all). (See figure 21.) Also this experiment is unable to measure any partial rates.

Theoretical calculations up until now have been of two types. One type due to Block and Dalitz ignores initial and final state interactions and is successful in predicting the lifetimes measured for light hypernuclei. The other type due to Adams is a nuclear matter calculation with initial and final state interactions included. This calculation predicts a lifetime to be much longer than the free lamda lifetime which contradicts the results of Nield et al.

The promise of high quality data from Exp. 759 has sparked new interest in this theoretical problem. In particular Holstein who has done extensive calculations on the related problem of nucleon nucleon parity violating forces has initiated a program to calculate hypernuclear decay rates.

Our objective in this experiment is to combine the hypernuclear formation trigger capability of the Moby Dick spectrometer at LESBI with a range spectrometer to detect the charged particles produced from the hypernuclear decay. The lifetime measurement will consist of a start signal from two scintillators in the beam on either side of the target, and a stop signal from the first two scintillators in the range spectrometer. These counters are state of the art timing scintillators which should achieve a timing resolution of 200 - 250 psec. FWHM.

The energy of the decay products will be measured in the range spectrometer which consists of two multi wire proportional chambers, two timing counters (also used for ΔE information) and up to 18 additional scintillators to measure the range of the particles. The range spectrometer design is presently being studied by means of Monte Carlo simulation. The simulated spectrometer has an energy resolution of $\pm$ 10% $\Delta E/E$, and can separate protons and pions at the 1% level using $E\Delta E$ and Range ΔE information.

LIFETIME AND BRANCHING RATIO FOR Λ HYPERNUCLEAR DECAY

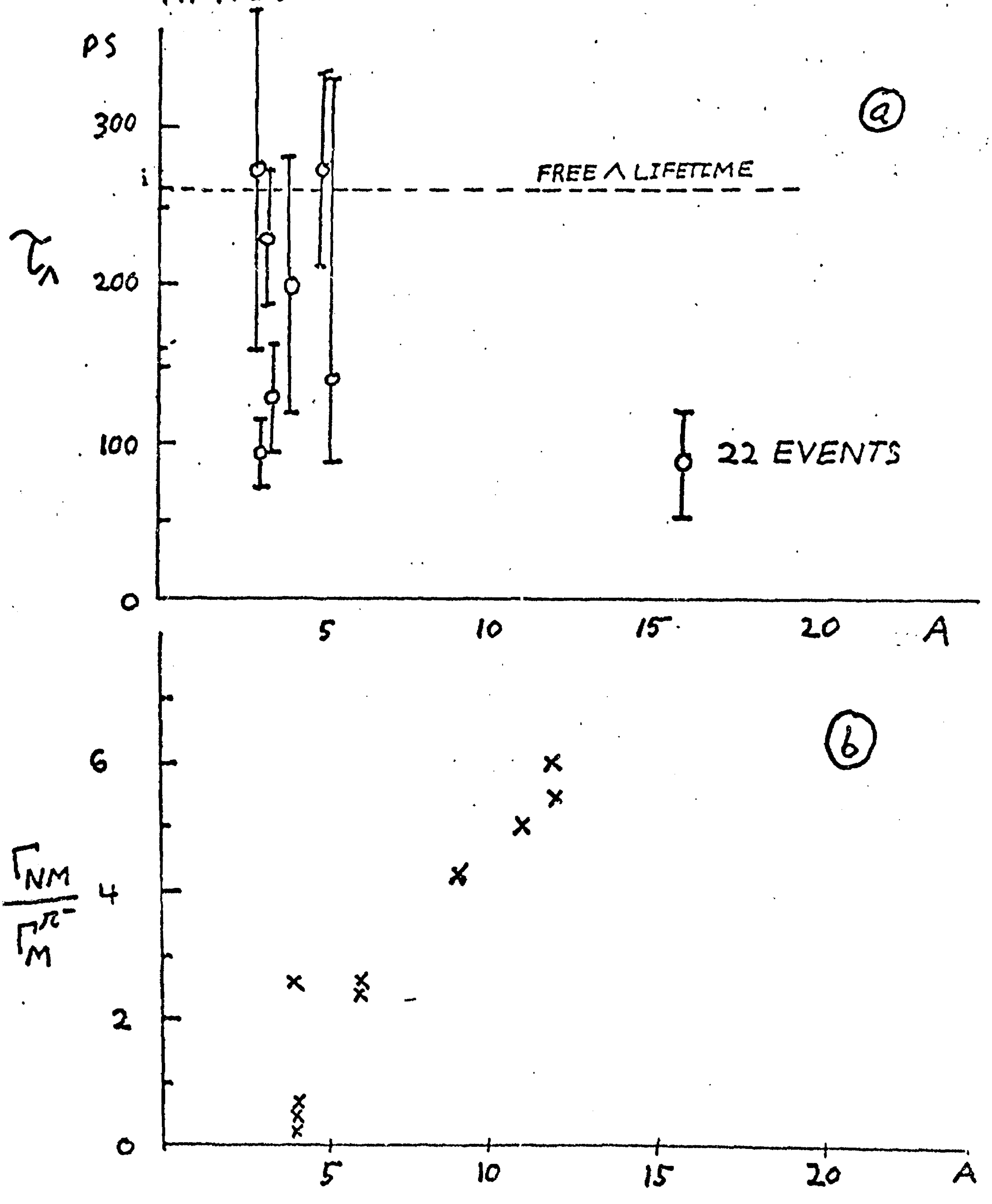

Figure 20 NUCLEAR MASS

RECOIL DISTANCE[13] DISTRIBUTION FOR $^{16}_{\Lambda}O$

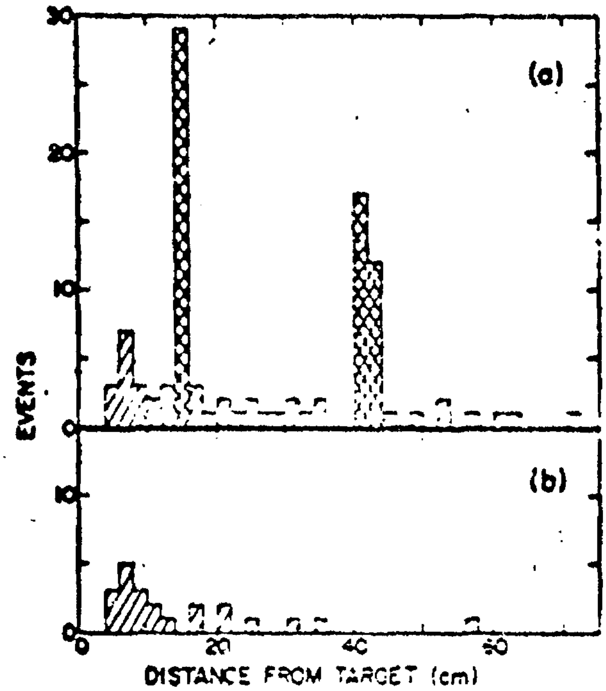

22 EVENTS

Vertex distance distribution. (a) The distribution for all events. The large peaks are due to nuclear interactions in the spark chamber plates. (b) The distribution for 2, 3, and 4 prong events left after interactions in the plates have been removed.

$$\lambda = 2.7^{+3.0}_{-2.3} \text{ cm}$$

$$\tau = 0.86^{+0.33}_{-0.26} \times 10^{-10} \text{ sec}$$

Figure 21

III. B Pion Annihilation

III. B. 1 The $(\pi^+,2p)$ Reaction - Experiment 315 at LAMPF

The purpose of experiment 315 is to study the reaction mechanism by which pions are absorbed in light nuclei. When a pion is absorbed at low energies it deposits a large amount of energy in a small region of a nucleus while carrying only a small amount of momentum with it. In contrast if a proton were to excite a nucleus by an amount of energy the order of the pion rest mass it would bring in a momentum close to 1 GeV/c. If the absorption of a pion involves primarily a single bound nucleon the nucleon must have a large momentum beforehand in order to have both energy and momentum conserved. Since a typical value of the Fermi momentum is $\sim$ 260 MeV/c higher momentum components of the nuclear wavefunction are not probable. Absorption of a pion involving two or more nucleons should be much more probable since the momentum can then be shared amongst those nucleons involved. A reaction involving two nucleons is attractive not only to study the reaction mechanism but also because it allows a study of two hole states.

In 1980 the targets ^{6}Li, ^{7}Li and ^{16}O were studied. ^{6,7}Li were studied at the following energies and angles: 40 MeV (82°,82°), 40 MeV (58.5°,107°), 75 MeV (80°,80°), and 75 MeV (57°,104°); for ^{16}O: 90 MeV (75°,105°). Improvements made during the previous year were the building of individual wire readout MWPC's and the addition of two silicon detectors. The analysis of last year's data shows that the wire chambers were very successful in handling high rates efficiently which allowed us to move much closer to the target increasing the solid angle by a factor of 10 and also increasing the angular spread of the coincidence events. Using the silicon detectors allowed the collection of many deuteron events corresponding to the (π^+,pd) reaction.

It is found that the cross section for (π^+,pd) is typically 20% as large as the $(\pi^+,2p)$ cross sections for $^{6,7}Li$. Figures 22 and 23 show the spectrum obtained from the two reactions $^6Li(\pi^+,2p)^4He$ and $^7Li(\pi^+,pd)^4He$. The resolution of the ^4He ground state from the $(\pi^+,2p)$ reaction is 1.8 MeV. The recoil momentum distributions of the ground states from the two reactions are shown in figures 24 and 25 and are very similar. Although the spectra are not corrected for phase space some recent calculations show that the distribution is shifted even more towards low values of recoil momentum. Since the residual nucleus experiences low recoil momenta it is very probable that it does not participate in the reaction very much and can be considered a spectator. ^6Li is frequently described as a deuteron orbiting in an L=0 state with respect to an alpha cluster. ^7Li is frequently described by a triton cluster in an L=1 orbit with respect to an alpha cluster (the spin of the triton combines with the L=1 to give the $3/2^-$ ground state of ^7Li). The ground state peak from $^6Li(\pi^+,2p)^4He$ is interpreted to be the absorption of the pion on the "quasideuteron". In the shell model interpretation these two nucleons are the two p-shell nucleons of ^6Li. The ground state of ^4He from the (π^+,pd) reaction could be from two sources, i.) absorption involving three nucleons or ii.) absorption involving only two nucleons with one of the nucleons picking up a neutron on the way out of the nucleus. In free space these two mechanisms are distinguished by the kinematics of the fast outgoing proton. In mechanism ii. the proton should have the kinematics of $\pi^+ + X \rightarrow p + d$: in ii. the proton should have the kinematics of $\pi^+ + d \rightarrow p + p$. The energy of the proton differs by 25 MeV for the two cases. Our data on Li shows only a few percent of the $^7Li(\pi^+,pd)^4He$ events have protons with energies corresponding to that of mechanism ii. Thus we are now investigating whether

Fig 22

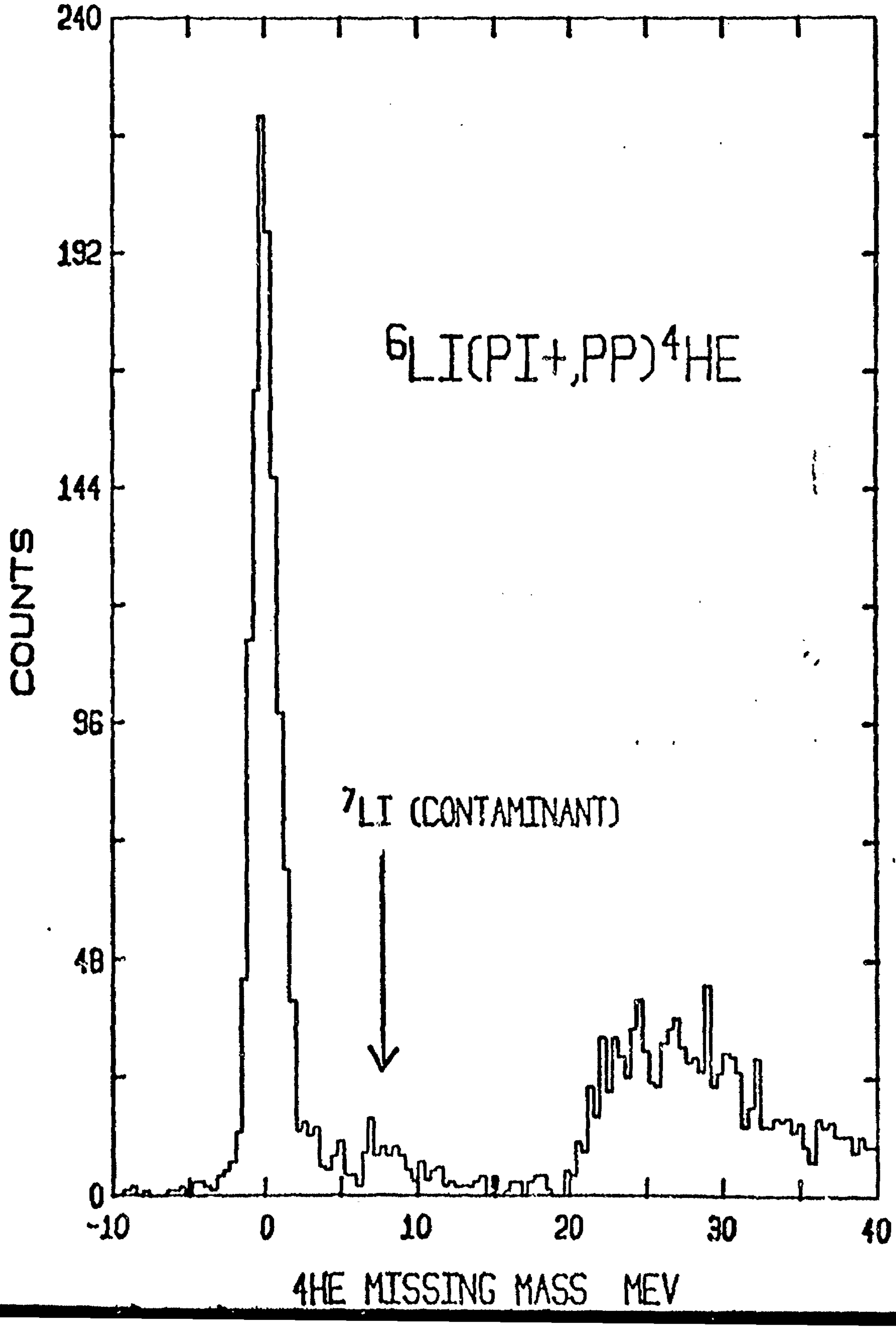

240
192
144
96
48
0
COUNTS
^{6}LI(PI+,PP)^{4}HE
^{7}LI (CONTAMINANT)
-10
0
10
20
30
40
4HE MISSING MASS MEV

Fig 23

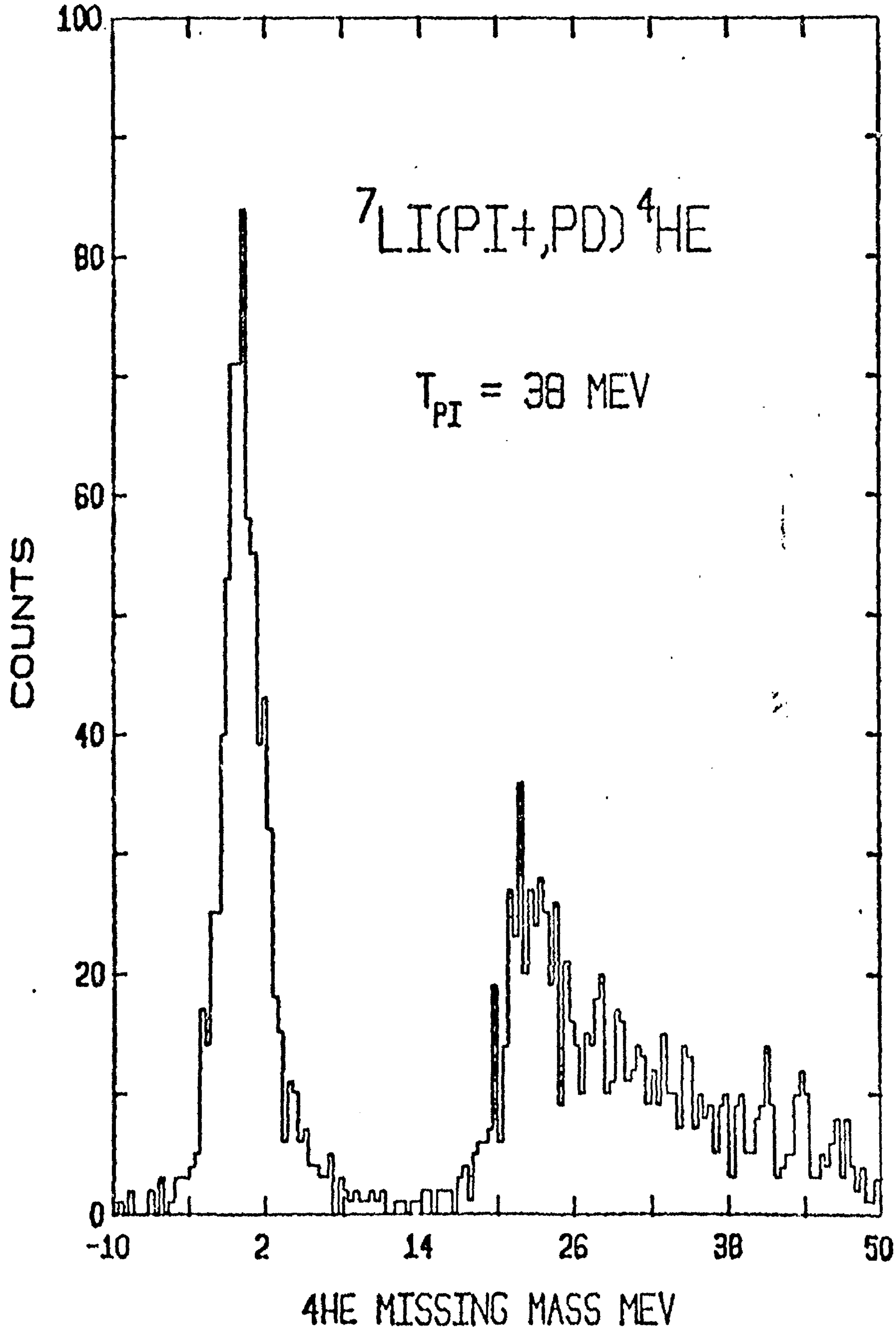

COUNTS
100
80
60
40
20
0
-10
2
14
26
38
50
4HE MISSING MASS MEV
7LI(PI+,PD)4HE
TPI = 38 MEV

Fig. 24

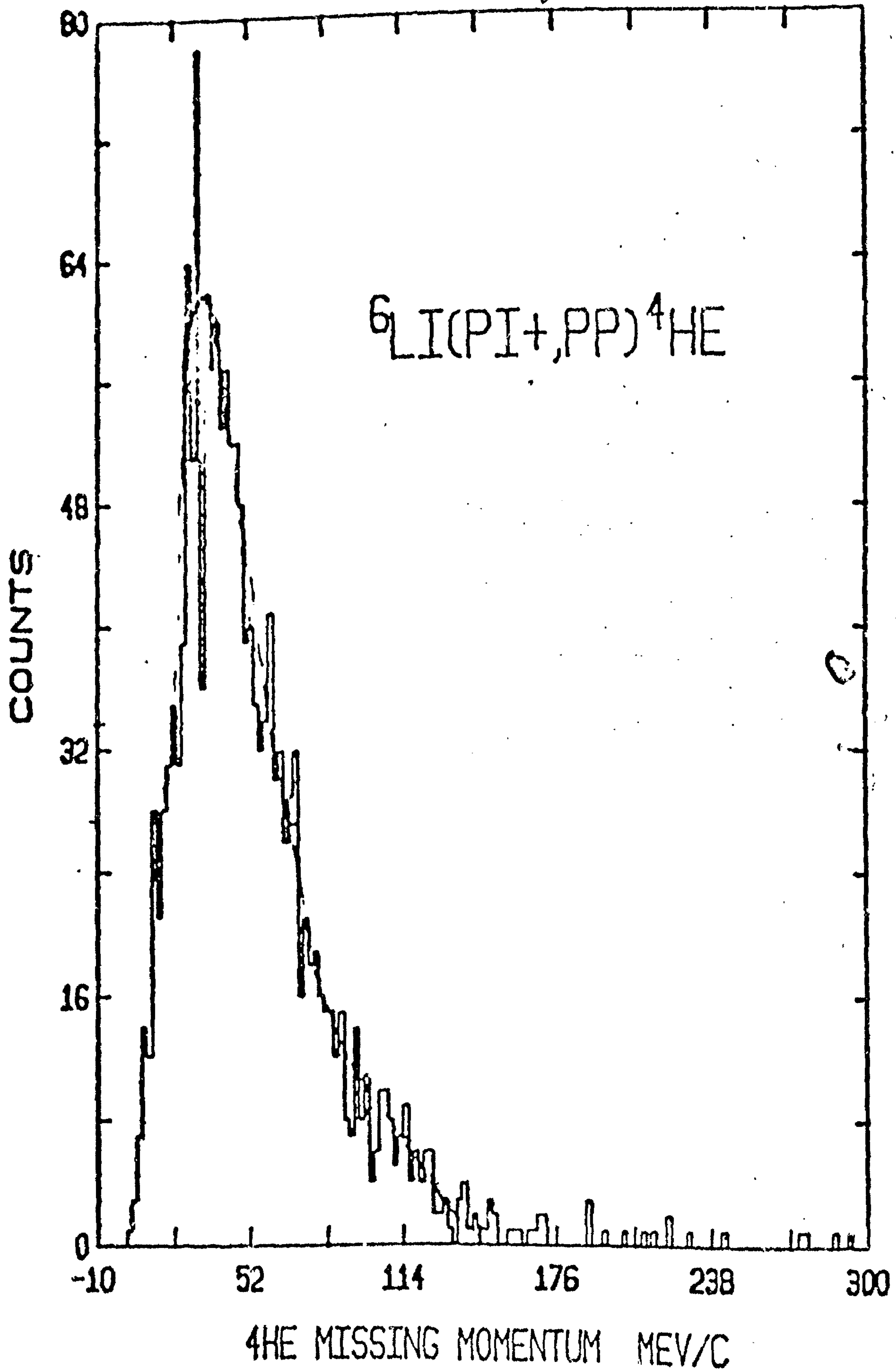

80
64
48
32
16
0
COUNTS
-10
52
114
176
238
300
4HE MISSING MOMENTUM MEV/C
6LI(PI+,PP)4HE

Fig. 25

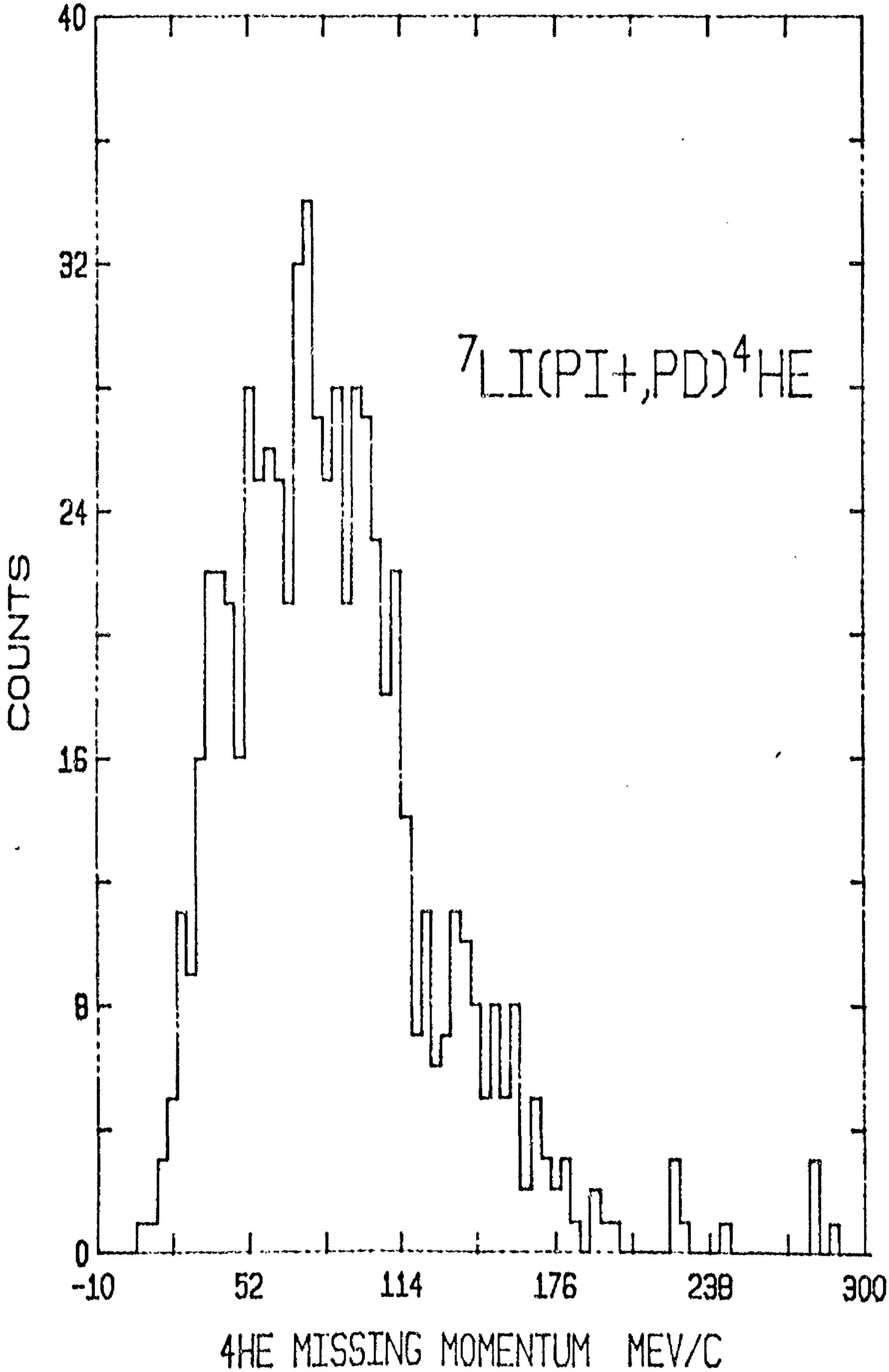

40
32
24
16
8
0
COUNTS
^{7}LI(PI+,PD)^{4}HE
-10
52
114
176
238
300
4HE MISSING MOMENTUM MEV/C

the ground state data can be interpreted as the absorption of the pion on the triton cluster (i.e. the three correlated nucleons) while the other four nucleons remain spectators. There is also a peak around 22 MeV whose recoil momentum distribution is shifted toward zero like an s-wave. An L=0 transition can only populate 2^- or 1^- states. There is a known 2^- state at 22.3 MeV. The enhancement of this state has not been seen in other types of reactions and therefore suggests pion absorption as a different, unique probe of nuclear structure.

Data was taken to observe the reaction $^{16}O(\pi^+,2p)^{14}N$ at T_π = 90 MeV and with the arms of our spectrometer set at 72° and 105°. This is 17° away from the kinematics of the two-body reaction (i.e. zero recoil momentum) of our 1979 run with ^{16}O (figure 26). A spectrum from the 1980 run is shown as figure 27 ; the enhancement of Λ=2 states such as the g.s., the 7.0 MeV state, and the 11.5 MeV state is seen to occur. (Λ is the total angular momentum of the pn pair with respect to the center of mass of the target nucleus.) The ground state is predicted to be nearly equal in strength to the first excited state (Λ=0) by c.f.p. calculations. Since coefficients of fractional parentage predictions contain only nuclear structure information and nothing about the reaction mechanism, the difference in strengths between the two states contains information about the reaction mechanism. According to the Mishinsky transformation the ground state transition is 50% L=2, ℓ=0 and 50% L=0, ℓ=2. (L is the angular momentum of the pn pair about the center of mass of the nucleus; ℓ is the angular momentum of one nucleon in the pair relative to the other.) The 1979 run was collected at angles corresponding to zero recoil. This configuration prefers L=0 to L=2 from the geometry. On the other hand we expect absorption involving two correlated nucleons to be close together. This implies a preference for ℓ=0, L=2. The recoil distribution for the g.s. contains the number of events with L=0 and L=2 (hence $\ell=0$, $\ell=2$). The unfolding of this information will give information about the mechanism. Unfortunately in 1980 there was not adequate time to collect the statistics necessary for such an analysis and a large amount of time will be spent on this during our next run.

We have been given an additional 550 hours of running time starting in late August, 1981. Extensive work has gone into the preparations of a new data acquisition program (see section IV.C) for use in our upcoming run. Also numerous refinements have been made to our spectrometer to facilitate the alignment and setting up of the apparatus this August.

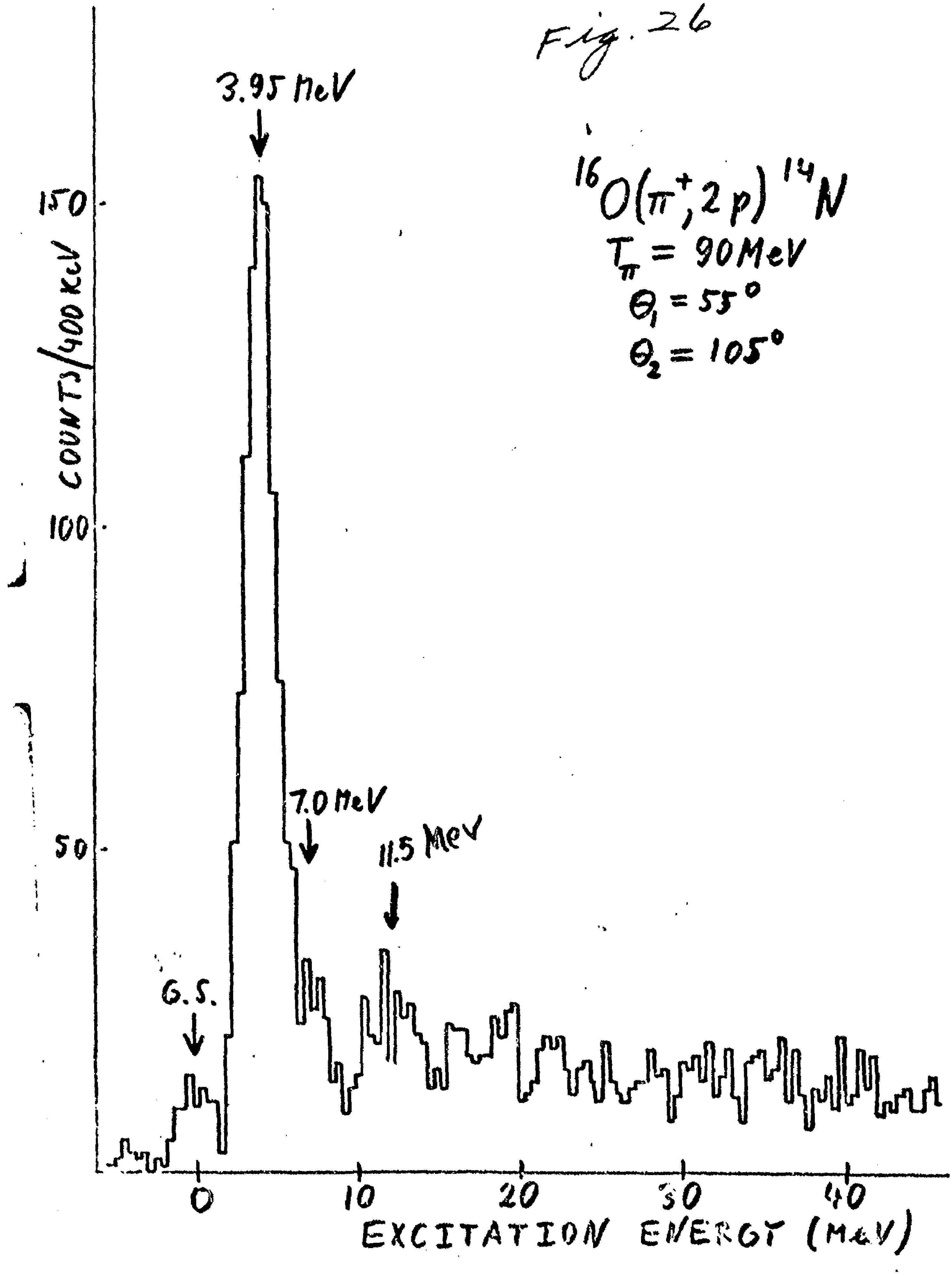
Fig. 26
3.95 MeV
$^{16}O(\pi^+,2p)^{14}N$
T_π = 90MeV
θ_1 = 55°
θ_2 = 105°
150
100
50
COUNTS/400 keV
7.0 MeV
11.5 MeV
G.S.
0
10
20
30
40
EXCITATION ENERGY (MeV)

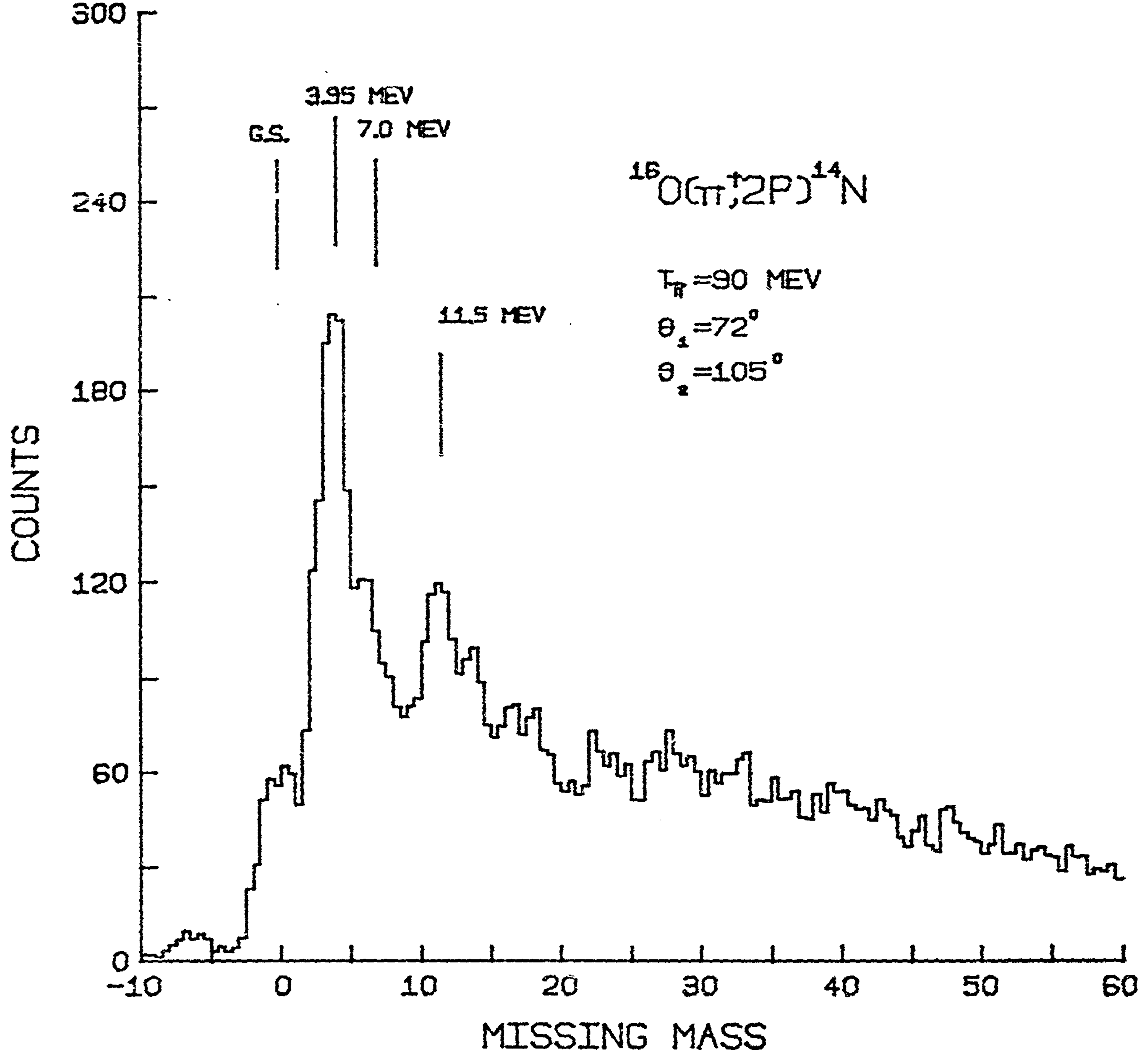

300
240
180
120
60
0
COUNTS
G.S.
3.95 MEV
7.0 MEV
11.5 MEV
16O(π+,2P)14N
Tπ=90 MEV
θ1=72°
θ2=105°
-10
0
10
20
30
40
50
60
MISSING MASS

Fig. 27

III. B. 2 The (π^+,p), (π^+,d), and (π^+,px) Reactions

During the last two years the study of pion annihilation has led to a close working relationship with the nuclear theory group. This work began with Wharton and Keister collecting and examining all available (p,π^+) and (π^+,p) data in the 1p shell (much of it from our group). They showed (Phys. Rev. C23, 1141, 1981) that a single neutron pickup distorted-wave calculation has serious problems in describing the systematic energy and A-dependence of the cross sections of ground state transitions in the 1p shell. They examined the data in terms of a two-nucleon absorption model and find that features of the two-nucleon model show good possibility of describing the systematics of the data.

As an outgrowth of this work Keister and Kisslinger have written a computer code which includes a coherent sum of both the one-nucleon and two-nucleon absorption processes. Furthermore the two-nucleon model is done more accurately, with less approximations, than all previously published two-nucleon model calculations. They are finding that many approximations made by other theorists have a large effect on the calculated (π^+,p) cross section, and that the (π^+,p) data is difficult to understand even with their most complete calculation.

This computer code is easily adaptable to other two-nucleon absorption processes and we are in the planning stage of applying it to our (π^+,d) and (π^+,pp) data. No serious attempt has previously been made to relate such diverse pion absorption reactions to the same theoretical model.

The (π^+,d) data is continuing to be collected during experiment #315 at LAMPF. One of our chief goals is to examine the spin dependence of the (π^+,d) reaction. Existing models of the (π^+,d) reaction predict that nucleon transitions with spin transfer S=1 are a factor of 100 weaker than the S=0 transitions. These models assume a single-step interaction in which a single nucleon absorbs the pion and picks up a second nucleon immediately thereafter. Shown in fig. 28 is a $^7Li(\pi^+,d)^5Li$ spectrum which suggests the population of the 16.7 MeV $3/2^+$ state. This state is the only narrow state known to exist in particle unstable ^5Li and must be populated by a S=1, L=1 transition. We are presently analyzing more data to confirm this S=1 transition. A confirmation of this transition will demonstrate a need for a revision of existing models of the (π^+,d) reaction mechanism.

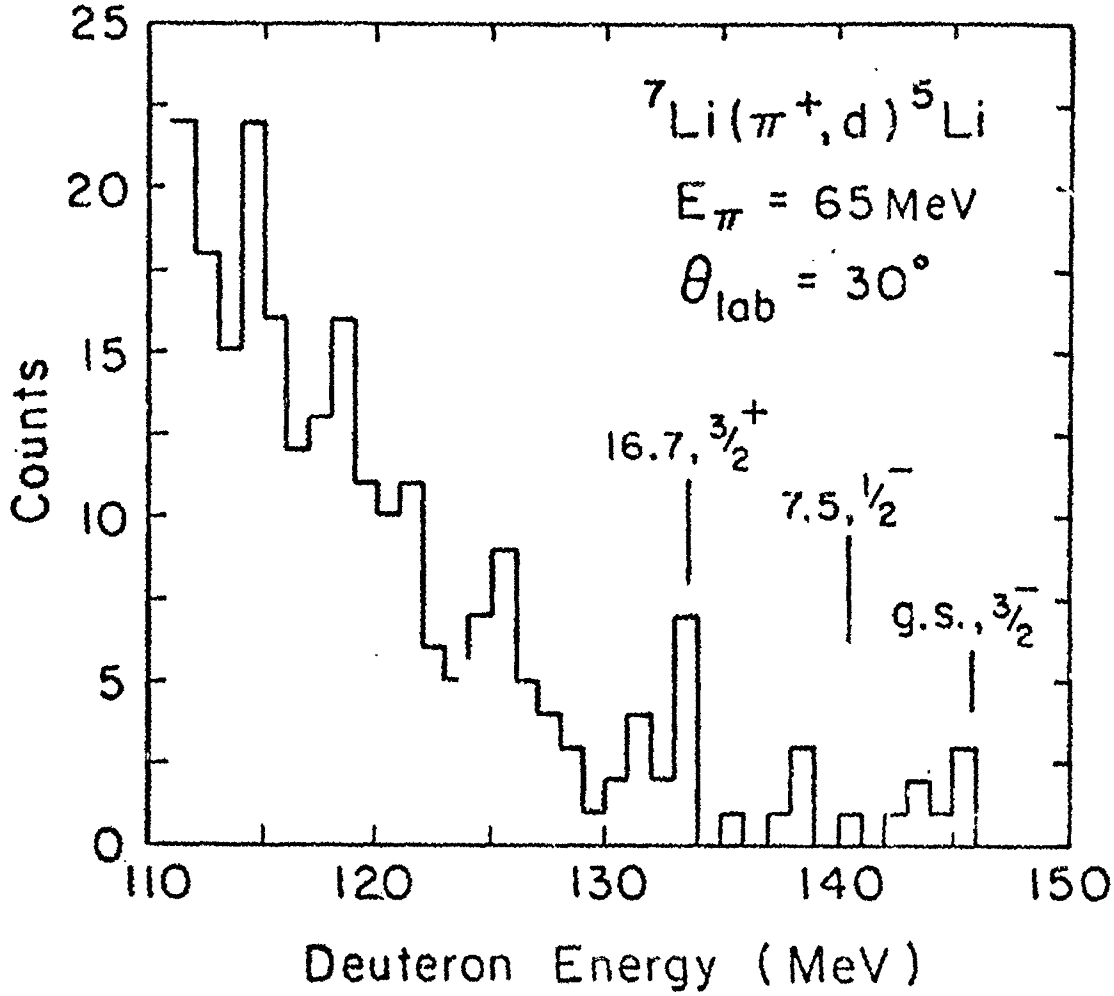

$^7Li(\pi^+,d)^5Li$
E_π = 65 MeV
θ_{lab} = 30°
16.7, 3/2+
7.5, 1/2−
g.s., 3/2−
Counts
25
20
15
10
5
0
110
120
130
140
150
Deuteron Energy (MeV)

Fig 28

III. B. 3 Feasability Study of Monopole Resonances with Pions

As an outgrowth of our collaboration with the University of Washington in LAMPF Exp #191 we have investigated the feasibility of using EPICS to see Giant Monopole Resonances.

The observation of the Giant Isoscalar Monopole excitation with inelastically scattered alpha particles has been reported.[1] It is difficult in alpha particle experiments to determine quantitative details of the monopole excitation due to the presence of a strong continuum and a relatively large, nearby quadrupole resonance. We are therefore attempting to observe the resonance with low energy pions. Since pions are 28 times lighter than alpha particles, it is possible that the excitation of the giant monopole resonance may be cleaner. In particular, with alpha particles of 120 MeV, the momentum transfer at 0° for 15 MeV excitation is about .35 F^{-1}, so excitation of multipoles of L less than 3 for heavy nuclei is not suppressed. With 67 MeV pions, however, the momentum transfer at 0° is less than 0.1 F^{-1}, while at 10° it is 0.15 F^{-1}, so one would expect L=1 excitations to become important (for lead) only beyond about 10°. Thus if it were possible to measure inelastic pion scattering cross sections at 10° and forward, one might expect to observe the giant monopole resonance relatively free from contributions of higher multipoles. Furthermore, excitation due to quasi-elastic scattering of pions is expected to be relatively low at forward angles. This trend has been observed in our studies of inelastic scattering at larger angles, and is expected because the basic pion-nucleon cross section is backward peaked, and because forward inelastic scattering is suppressed by Pauli blocking.

Distored wave Born approximation calculations from the University of Washington support the view we have just argued that the monopole might stand out at forward angles. (See Fig. 29.) The main competition to the isoscalar giant monopole is from the giant dipole resonance. DWBA calculations indicate that the dipole cross section will be less than that for the monopole for angles forward of 10 to 14° and substantially less at 0°. There is some ambiguity in the expected magnitude of the cross section, expecially for the dipole excitation, since the isovector part of the pion-nucleus potential is involved, and not much is known about the best parameterization for this part. These calculations use the free pion-nucleon parameters in a Kisslinger model for the isovector potential.

Together with a group at the University of Washington and Dr. J. Amann of LAMPF, we carried out some work on EPICS (Energetic Pion Channel and Spectrometer) in order to develop a technique for measuring pion inelastic scattering around 10°. The main problem that we addressed so far was the muon background. Since the pion decay length at 67 MeV is about 8 m, and since the maximum laboratory decay angle is about 15°, there is a very large muon background in the spectrometer at 10°. In a previous test, we determined

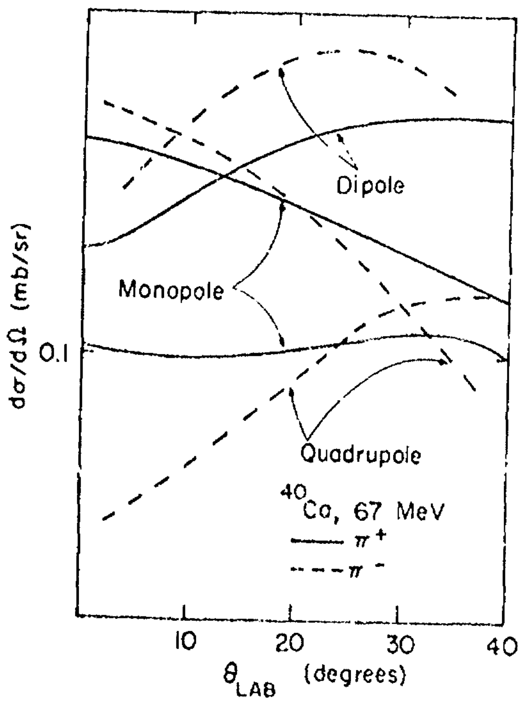

Fig. 29: Predicted differential cross sections for excitation of Giant Monopole and Giant Dipole resonances, using fitted parameters for all but the isovector excitation.

that the counters in the spectrometer could operate in this intense flux, but that the muon events would have to be vetoed in order to maintain a reasonable computer trigger rate. The muons at the focal plane of the spectrometer are fairly well localized by energy, so it is possible to differentiate between muons and pions by range, although it is necessary to use an absorber whose thickness varies with position along the focal plane. By installing and adjusting such an absorber, it was possible to veto from 95 to 98% of all muons, while losing only about 10% of the pions. The rate of non-vetoed muons was then comparable to the pion rate, and they could be identified by computing the mass associated with the measured time of flight from the spectrometer entrance and particle trajectory.

When the muons were satisfactorily eliminated, it became possible to study the pion spectra at forward angles. We found a large background resulting from degraded elastically scattered pions. It appears that about 0.2% of the flux of elastically scattered pions which enter the spectrometer is degraded by hitting flanges or walls of the vacuum system in the quadrupole triplet at the entrance to the spectrometer. Because of the focusing in the quadrupole, combined with multiple scattering in the timing scintillation counter immediately after the triplet, it is impossible to project the trajectories backward to the site of the scattering in the quadrupoles. Thus it will be necessary to use veto counters at the flanges to eliminate this background. Since the 10° elastic scattering cross section is around 20 barns/sr (for lead) whereas the giant monopole resonance cross section is expected to be only about 1 mb/sr, a reduction of this background by about two orders of magnitude will be required.

Although measurements at 10° are not possible with the present setup of EPICS, we were able to demonstrate the feasibility of measurements on C and Pb at 20°. We plan to continue these studies in the summer, in order to determine how large the dipole excitation really is at forward angles and to extend the range of our previous inelastic scattering studies on the LEP channel to the more forward angles already available at EPICS.

References:

1. D. H. Youngblood, Topical Conference on Giant Multipole Resonances, Oak Ridge, TN, F. E. Bertrand, Ed., Harwood Acad. Pub., 1980, p. 113.

III. C Nuclear Reaction Studies at IUCF

III. C. 1 Asymmetries in Positive Pion Production with Polarized Protons - IUCF Exp. #38

In the winter of 1979 one of our group (P. Pile) participated in the final phase of IUCF experiment #38 in collaboration with others from Indiana University. The IUCF DD̄ spectrometer[1)] was used to measure the asymmetry of the proton induced positive pion production from ^{16}O to the ground state and the 0.87 MeV states in ^{17}O. This data, along with asymmetry data previously obtained for ^{10}B, ^{12}C and ^{40}Ca, has been submitted (April 1981) for publication in Physical Review C. The title page (including the authors and abstract) of the submitted article is included as an enclosure to this report.

---

1) P.H. Pile and R.E. Pollock, Nucl. Inst. and Meth. 165 (1979) 209.

Positive Pion Production from the Bombardment of ^{10}B, ^{12}C, ^{16}O and ^{40}Ca with 147 to 159 MeV Polarized Protons

T.P. Sjoreen[†], P.H. Pile[††], R.E. Pollock, W.W. Jacobs, H.O. Meyer, R.D. Bent, M.C. Green, and F. Soga[†††]

Indiana University Cyclotron Facility, Bloomington, Indiana 47405

(Received

ABSTRACT

Differential cross sections and analyzing powers for the $(\vec{p},\pi^+)$ reaction have been measured with 147-to 159-MeV polarized protons. Transitions to the ground, 2.12- and 4.45-MeV states in ^{11}B, the ground, 3.09- and (3.68-3.85)-MeV doublet in ^{13}C, the ground and 0.87-MeV state in ^{17}O and the ground state in ^{41}Ca are studied. Pion center-of-mass energies range from 5 to 11 MeV. The results show distinct differences of the $(\vec{p},\pi^+)$ analyzing power for the various transitions.

[NUCLEAR REACTIONS ^{10}B, ^{12}C, ^{16}O, ^{40}Ca$(\vec{p},\pi^+)$, polarized protons, E_p=147-159 MeV; measured $\sigma(\theta)$, $A(\theta)$.]

III. C. 2 Quenching of the axial vector coupling constant

The ft value of Gamow Teller β decay is directly related to the στ matrix element of the transition through the axial vector coupling constant, g_A. If the free value of g_A is used, the measured ft value of the transition $^{14}O(\beta)^{14}N(3.95\ MeV)$ gives a Gamow Teller (GT) transition strength which is 40% lower than predicted by shell model calculations. We have derived a nearly model independent sum rule of the GT strength summed over all ^{14}N states. The $^{14}C(^{6}Li,^{6}He)^{14}N$ reaction was used to map out this GT strength and more than 40% was found to be missing. This lack of strength became even more dramatic when our neighbor, W. Daehnick, remeasured the $^{14}O(\beta)^{14}N(3.95\ MeV)$ ft value to much better accuracy. Just recently our collaborator, C. Goodman, remapped the Gamow Teller strength up to 30 MeV excitation energy in ^{14}N using the $^{14}C(p,n)^{14}N$ at $T_p = 160$ MeV. He finds that the relative distribution of strength agrees perfectly with shell model calculations. However only 60% of the strength is present, based upon the free value of g_A. All of this suggests a 40% quenching of g_A from its value for a free neutron. This quenching of g_A is undoubtedly related to the mesonic degrees of freedom inside nuclei. Many of ie models used to understand the quenching of g_A are also used in predictions of pion condensation and other features of pion nucleus interactions. Our continued interest in this subject is part of our total effort to understand the pion-nucleus interaction.

IV. Hardware and Software Development

IV.A Fast Timing Techniques with Scintillators

In preparation for BNL experiment 759 we have studied the timing properties of plastic scintillator detectors. In this study which is still in progress we have broken the counter down into four sections:

1) Scintillator Material.

2) Scintillator Geometry.

3) Light Guides.

4) Photomultiplier Tubes.

Each of these sections will be discussed in turn.

1) Scintillator Geometry

It is well known that small scintallators have better timing properties than large scintillators. Therefore our procedure was to examine scintillator samples of gradually increasing sizes in an attempt to determine the reason for the decreasing resolution with increasing size. A typical setup (figure 30) consists of a scintillator sample viewed on either side by a photomultiplier tube, and irradiated by a collimated Sr beta source.

The results of this section are shown in figure 31. We find that as the sample increases the pulse height, ph decreases and the resolution, Δt gets worse. The usual claim is that the timing resolution depends on the amount of light in a statistical manner that is $\Delta t = C(\frac{1}{\sqrt{ph}})$. Plotting pulse height vs. Δt (figure 31) one can see that the data fit a $\Delta t = C(\frac{1}{\sqrt{ph}})$ very well.

The functional dependence of Δt on ph is an important result. It allows us to make comparisons to counters presently in use in the Moby Dick spectrometer by measuring the light collection efficiency of these counters using a 90 Sr beta source. With this normalization we can achieve the desired resolution in the various counters in our experiment by adjusting the thickness of the counters to produce the desired amount of light.

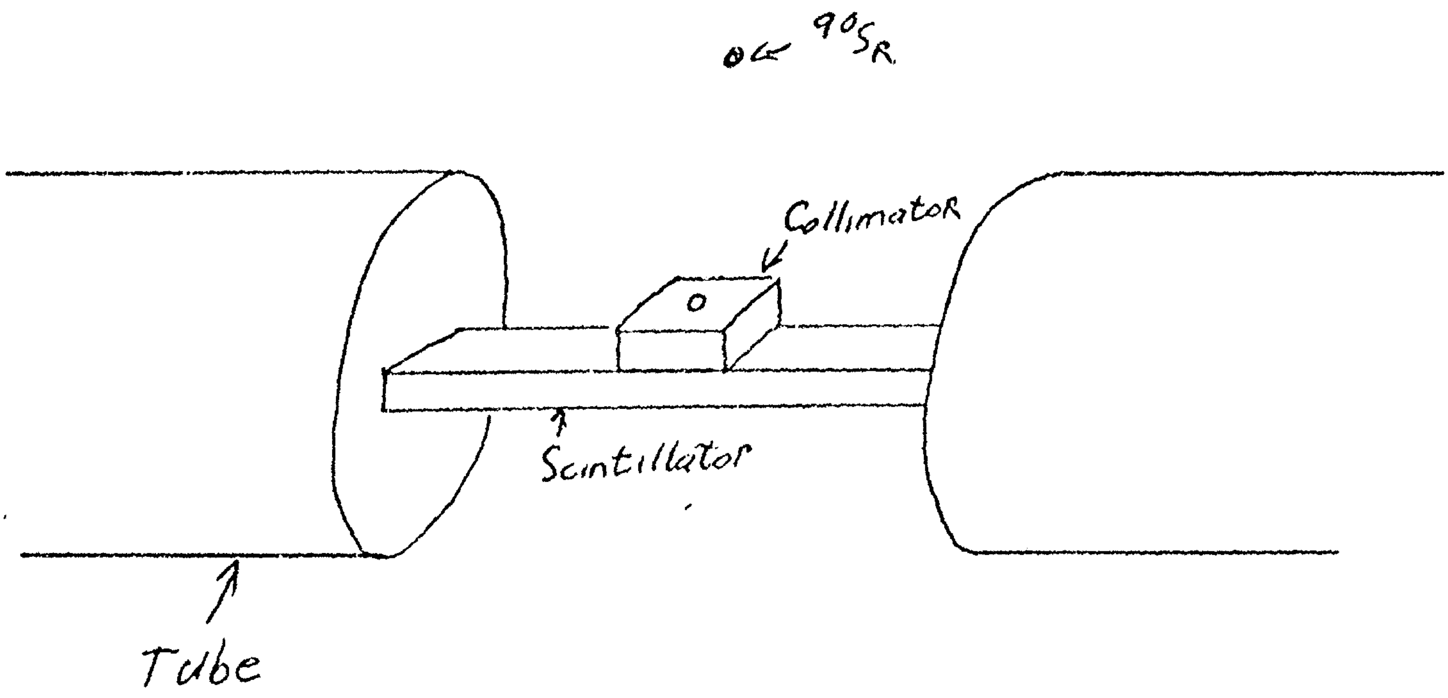

Typical Setup

Fig 30

Figure 2.

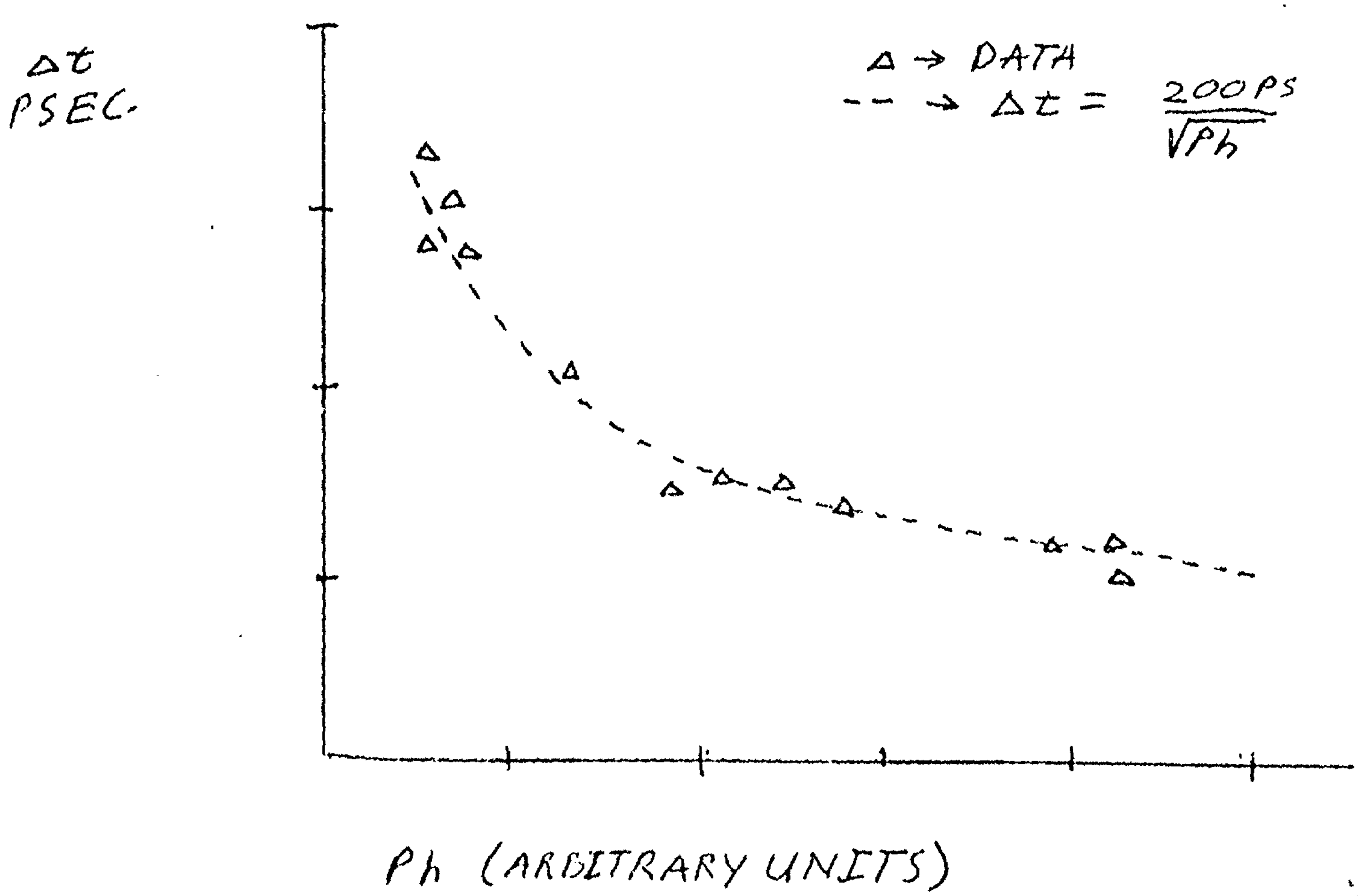

Fig. 31

2) Scintillator Material

Each scintillator material is characterized by parameters which describe the light pulse produced by the material when excited by some radiation. The usual parameters are: rise time t_r, mean fall time t, and light production dL/dX, and attenuation length, λ. One usually chooses a scintillator material with a fast rise time, a large light production and an attenuation length large with respect to the actual counter size.

Our preliminary results of tests comparing PILOT U, Ne102, and Ne111 show that timing resolution is independent of rise time at this level.

t_r(Ne111) = 350 psec

t_r(PILOT U) = 500 psec

t_r(NE102) = 800 psec

Our investigation is continuing.

3) Light Guides

A light guide is a section of plexiglass or other transparent material used to transmit light from a scintillator to a photomultiplier tube. Of the many different light guides one can use the most efficient (ref. 1) is the rectangular light guide. That is a light guide that has the same rectangular cross section as the scintillator fact throughout its length (figure 32). Since we are only interested in the most efficient light guides the rectangular type will be the only type discussed in this section.

Having chosen the efficient rectangular light guide the only problems left are coupling the light guide to the scintillator material and the photomultiplier tube. The latter of the two problems is easily soluble. The light guide is easily attached to the tube using optical grease. The only restriction is that the light guide can not be wider than the tube. This limits the width of the scintillator to 4cm in our case.

The problem of attaching the light guide to the scintillator is more difficult. The main difficulty is in matching the indices of refractions. The usual material used in constructing light guides is plexiglass. It has an index of refraction of 1.47 which is quite different from the scintillator's index of refraction, 1.58. This is in fact crucial. It causes the light entering the light guide to bend away from the normal of the surface, and therefore out of the angular range for total internal reflection.

To solve this problem of lost light at the interface one need only choose a material (such as quartz) which has an index of refraction slightly larger than that of the scintillator material. Another solution is to construct the light guide as shown in figure 4 with a slot for the scintillator to fit into. This geometry causes the light at large angle to enter through the sides therefore bending in the desired direction.

Light guides corresponding to the two methods described above are now under construction and will be tested in the near future.

4) The photomultiplier tubes which we have tested to date are:

RCA 8575

RCA 8850

HAMMATSU 1246

HAMMAMATSU R1294x

PHILLIPS XP2020

Of these the 8575 and the XP2020 give the best results. However the XP2020 tubes have somewhat better gain than the 8575 tubes. We shall investigate these two tubes in more detail in the future.

In order to investigate each of the above portions of our counters in more detail we have purchased a Techtronics 7912AD waveform digitizer this device will enable us to digitize in bins of 10 psec. The individual pulses from a photomultiplier tube. These pulses can then be read into our PDP 11/45

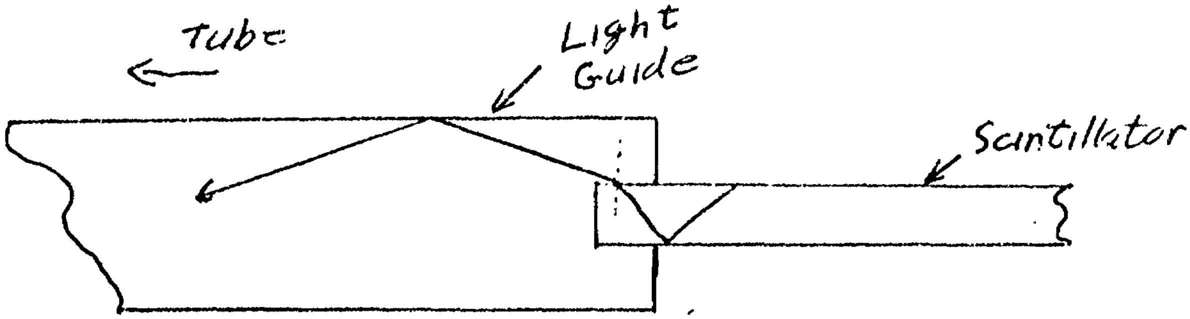

the Light entering through the sides bends towards the tube.

Fig 32

to be analyzed. This will allow us to measure quantities such as rise time fluctuations and determine their effect on timing. We hope that once we determine what properties of the pulses effect the timing we will be able to optimize the system for best timing.

Reference

1. D'Agustine et al., CERN preprint EP/80-228, Dec., 1980.

IV.B The New Kaon Beam Line and LESBI Modification Studies

During 1979 the Kaon Beam Line Working Group consisting of representatives from Carnegie-Mellon University, University of Houston, Massachusetts Institute of Technology, Brookhaven National Laboratory, Los Alamos Scientific Laboratory and Argonne National Laboratory was formed. The purpose of this group was to evaluate the possibility of building a new kaon beam line in the United States and to recommend a course of action.

With guidance from the Kaon Beam Line Working Group, H. Enge developed a beam line some of whose properties are listed below:

momentum	750 MeV/c
$\Delta\Omega$	6 msr
$\Delta P/P$	±5%
π/K ratio	1
$K^{-}/10^{12}$ protons	3×10^{5}
energy resolution	500 KeV

A schematic drawing of the beam line is shown in figure 33. The proposed design will allow for the possibility of extending the channel momentum to above 1.2 GeV/c by decreasing the bend angles of the dipoles. The decrease in bend angles is accomplished by physically moving D1 and D4 with respect to the rest of the channel. D1 through D4 are superconducting 5 tesla dipoles. The new beam line will provide about 100 times more kaons per second than are now available at the present target location and a reduction of about a factor of 10 in the number of unwanted particles in the kaon beam. The reduction in the number of unwanted particles will be achieved by a reimaging of the production target at the velocity slit before Q1 in figure33.

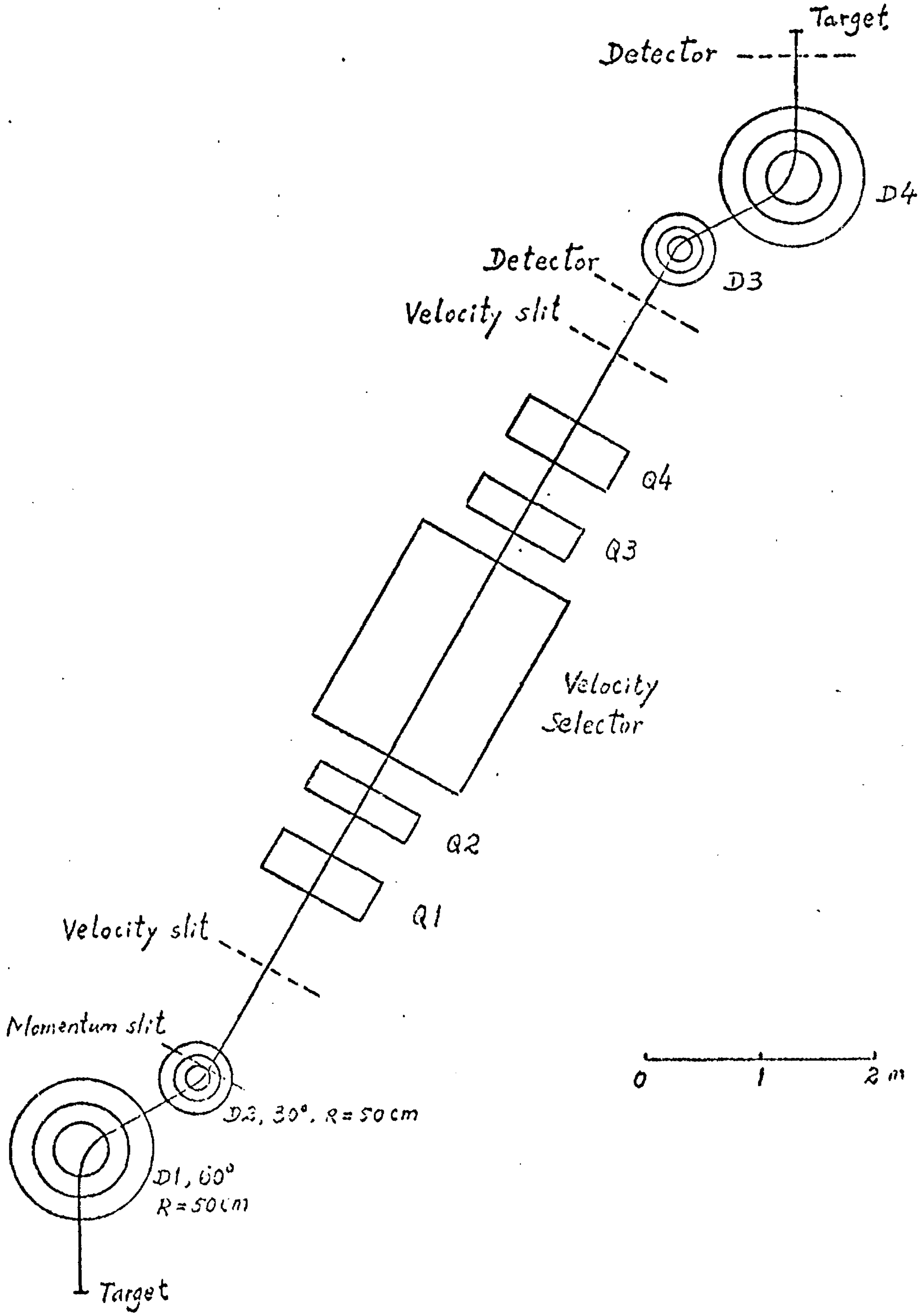
Target
Detector
D4
Detector
D3
Velocity slit
Q4
Q3
Velocity
Selector
Q2
Q1
Velocity slit
Momentum slit
D2, 30°, R=50cm
D1, 60°
R=50cm
Target
0
1
2 m

figure 33

A letter, prepared by working group members from Carnegie-Mellon and the University of Houston, describing the activities of the working group and the conclusions reached has been submitted (fall 1980) to the Brookhaven Laboratory Management. The essence of the letter states that if the new kaon beam line project is to become a reality, support of the project with detailed designs and construction personnel must be generated. This work is best done and most appropriately organized by BNL.

In view of the fact that a new kaon beam line may not be a reality until several years into the future, modifications to the present LESB-I beam line are anticipated to take place during the current year. The present LESB-I beam line and hypernuclear spectrometer are shown in figure 34. The kaon flux at the target location between P wire chambers P4 and P5 is about 5×10^3 $K^-/10^{12}$ protons and the flux between Q6 of LESB-I and Q1 of the kaon spectrometer is about 4×10^4 $K^-/10^{12}$ protons. The proposed design change will consist of moving the experimenter's target location to about the P2 location and either move the rotatable pion spectrometer forward to replace the kaon spectrometer or fix the kaon spectrometer at a small angle and eliminate the pion spectrometer. The kaon momentum will be measured by tracing the kaons through the Q5, D3 and Q6 elements of LESB-I. The principal difficulty with such a move involves making a scintillation counter, Cerenkov counter, and a wire chamber work efficiently in the high background environment encountered between the mass slit and Q5 in LESB-I.

We at Carnegie-Mellon have studied the properties of the kaon beam at the proposed new target location. The study has been carried out using the program TRANSPORT[1] and TURTLE.[2] TRANSPORT was used to determine the field strengths of the beam line elements after the LESB-I mass slit and TURTLE was used to simulate a beam of kaons originating from the production target.

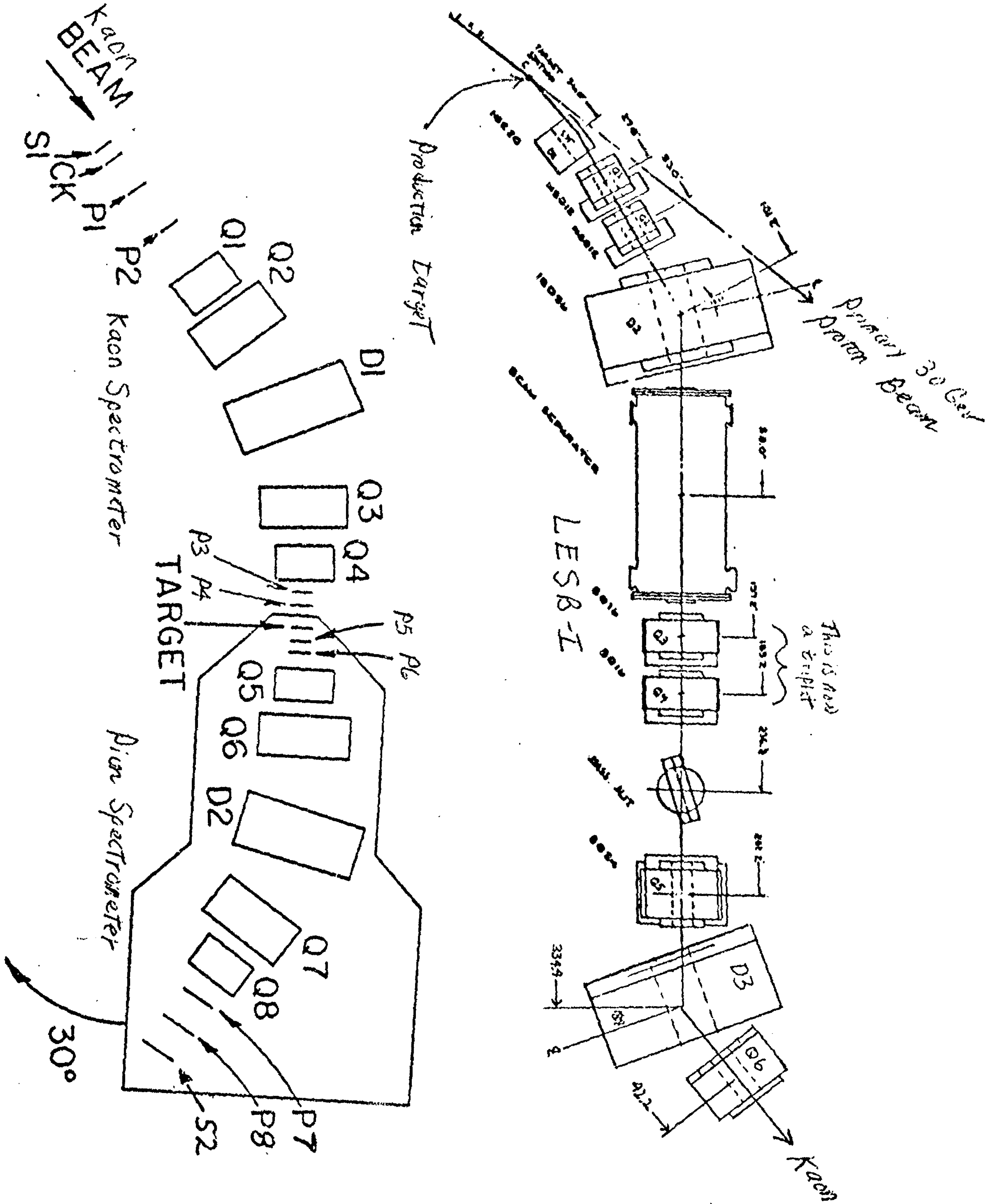

Kaon BEAM
S1 CK
P1
P2
Q1
Q2
D1
Q3
Q4
P3
P4
P5
P6
TARGET
Q5
Q6
D2
Q7
Q8
P7
P8
S2
30°
Kaon Spectrometer
Pion Spectrometer
Production Target
Primary 30 GeV Proton Beam
BEAM SEPARATOR
LESB-I
This is now a triplet
D3
Q6
Kaon beam

Figure 34

The following constraints were placed on the study:

1) The beam line elements and tune upstream of the mass slit remain unchanged.

2) The distance from the last element in the beam line to the target shall be no less than is now available at our present target location (0.88 meters).

3) The kaon flux shall not be reduced by any changes made to the beam line.

The TURTLE simulator assumes a kaon production target that is 6.4 cm x sin 10.5 deg wide and a proton beam 1.2 mm high. The transport coordinator theta (θ), phi (ϕ) and momentum range (δ) were chosen large enough to completely cover the entrance phase space of the LESB-I beam line. The program TURTLE then transports these particles through the beam line, taking into account the aperature constraints presented by the various elements. Figure 35 shows a comparison of the turtle simulator output with actual data at approximately the new target location. The TURTLE results shown in the figure are gated by those events that make it through the kaon spectrometer (as are the real beam events). The difference between the ϕ measured and predicted distributions is principally due to the 5 mr angular resolution in the actual measurement.

Figure 36 shows a schematic of a configuration that meets the criteria specified previously and allows one to adjust the x and y widths on the target to suit the experiment. The only change incorporated in figure 36 is the insertion of Q7 between Q6 and the target. The distance between Q6 and the entrance quadrupole Q1 (see figure 34) has remained unchanged. Without Q7 a small y dimension is not possible at the new target location. In fact,

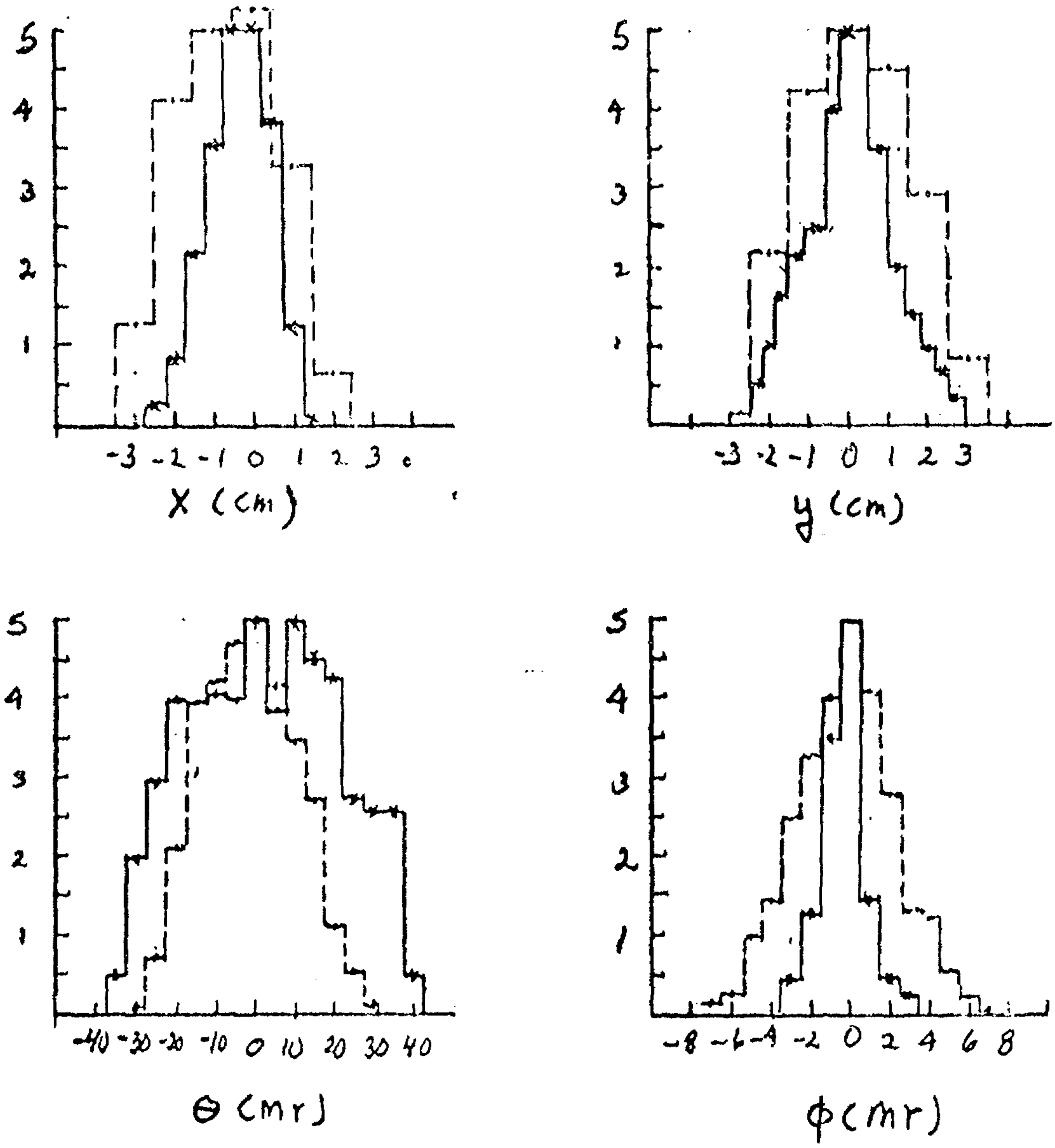

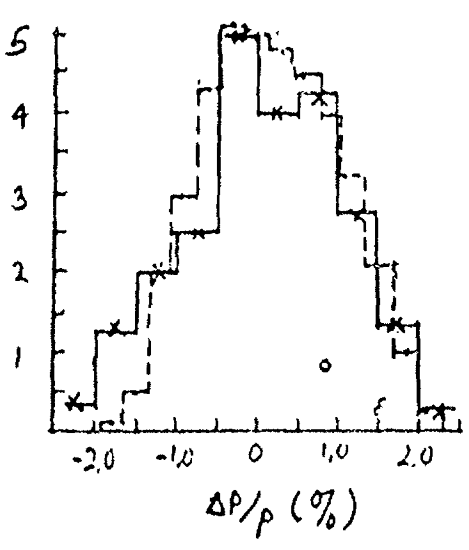

DASH = Actual data
SOLID = TURTLE Prediction

Phase Space at New Target
QDQ between mass Slit
and Target

Q5 = -4.029 kg
Q6 = +7.569 kg
2nd order calculation

Figure 35

Proposed Modification TO LESB-I

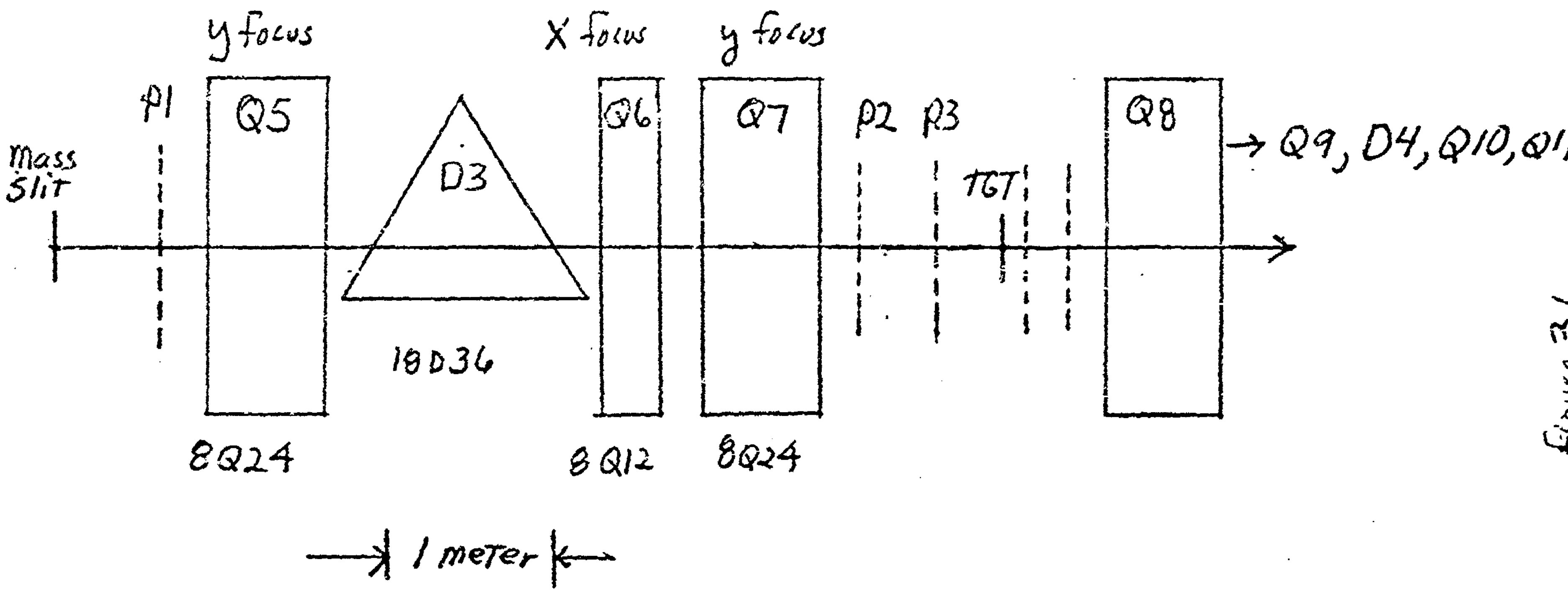

Figure 36

the phase space shown in figure 35 is a result of a Q5 D3 Q6 tune which minimizes the y dimension at the target consistent with an x waist at the target. The target can be moved closer to Q6 with a reduction in the y dimension, however the x magnification becomes so large (3 to 5 from the target area to P1) that the momentum resolution is seriously degraded. Even with a target closer to Q6 the y dimension is still over 3 cm. The phase space for a tune of the QDQQ configuration which minimizes the y extent of the beam while maintaining a 6 cm wide waist in the x coordinate is shown in figure 37. The beam envelope is shown in figure 38. The transport control deck for this tune is given in Table 1.

All other combinations of three quadrupoles and one dipole were tried (i.e. QQDQ, DQQQ, etc.) and were found unacceptable because of their low dispersion of about 0.5 cm/% from P3 to P1. The QQD and DQQ combinations proved undesirable because of grossly unequal x and y magnifications.

The momentum resolution obtainable with the QDQ or QDQQ combinations should be comparable. The tune giving the phase space shown in figure 35 gives a first order transport between P3 and P1 of

(1) $X = -2.26\ X_0 + 1.74\ \delta P$

while the QDQQ tune giving the phase space shown in figure 37 gives (this time between P2 and P1).

(2) $X = -1.91\ X_0 - .007\ \theta_0 + 1.63\ \delta P$

where X, θ, and δP have respective units cm, mr and %. With 1 mm chamber resolution and 8 mr (0.5 deg) θ_0 resolution the first order momentum resolution will be about 1.4×10^{-3} in either case (1.1 MeV/c at 800 MeV/c). Equations (1) and (2) should be compared with similar transport equations for the present kaon spectrometer, for example, between P3 and P1 in figure 34

$\bar{Q}DQ\bar{Q}$

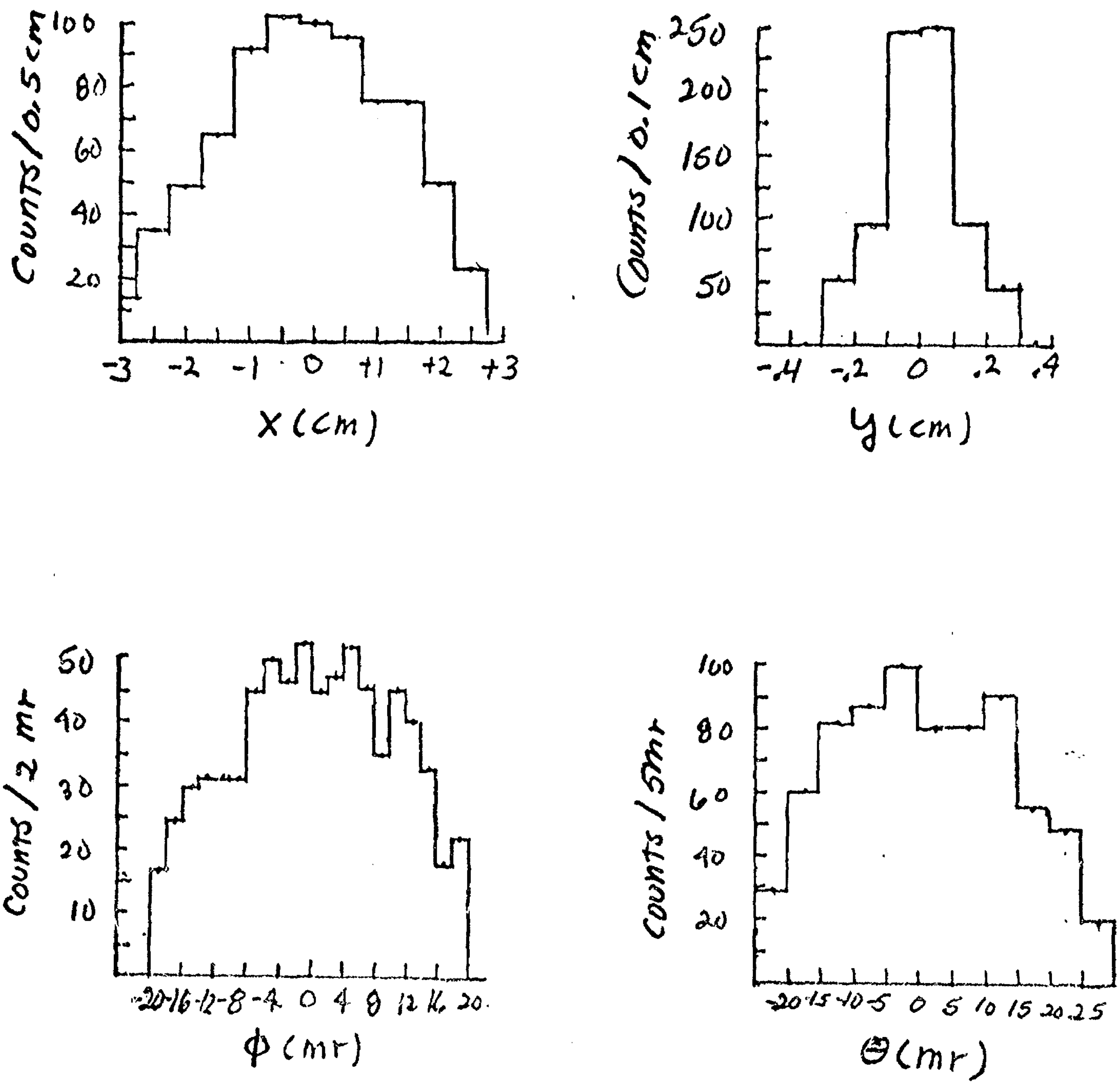

Q5 = −3.297 kg

Q6 = +11.470 kg

Q7 = −6.119 kg

2nd order calculations

figure 37

TABLE I

"SECOND ORDER   LESB-I Plus Q7 TRANSPORT   "

δP/p = ±2%

```
    1
    1.000000     "INPU"     0.50000     60.00000    0.06000    8.00000    0.0
*  17.           "SEC " ;
*  13.           "PRBE"     3.00000;
   16.00         "DGAP"     5.00000     2.54000;
   16.00         "K1  "     7.00000     0.45000;
   16.00         "K2  "     8.00000     2.80000;
    3.0          "TGD1"     0.60800;
    2.0          "D1R1"     5.75000;
    4.000        "D1PA"     0.61000     8.78039    0.00000;
    2.0          "D1R2"     5.75000;
    3.0          "D1Q1"     0.17690;
   16.00         "DGAP"     5.00000     7.62000;
    5.00         "Q1PA"     0.35600    10.91000   10.16000;
    3.0          "Q1Q2"     0.20310;
    5.00         "Q2PA"     0.45700    -4.50000   10.16000;
    3.0          "Q2D2"     0.60950;
    2.0          "D2R1"    14.70000;
    4.000        "D2PA"     1.11800    12.24762    0.00000;
    2.0          "D2R2"    14.70000;
    3.0          "SEDR"     1.66900;
    3.0          "SEDR"     1.58000;
    5.00         "Q3PA"     0.45700    -5.31000   10.16000;
    3.0          "Q3Q4"     0.22860;
    5.00         "Q4PA"     0.45700     6.95000   10.16000;
    3.0          "Q4LP"     0.42560;
    3.0          "LPMS"     0.61600;
    3.0          "MSW1"     0.63000;
    3.0          "W1Q5"     0.28500;
*   5.00         "Q5PA"     0.71100    -3.29691   10.16000;
    3.0          "Q5D3"     0.26960;
   20.0          "BROT"   180.00000;
    2.0          "D3R1"    18.40000;
    4.000        "D3PA"     1.11800    15.33035    0.00000;
    2.0          "D3R2"    18.40000;
   20.0          "BROT"  -180.00000;
    3.0          "D3Q6"     0.25090;
*   5.00         "Q6PA"     0.35600    11.46970   10.16000;
    3.0          "Q6Q0"     0.25000;
*   5.00         "Q0PA"     0.71100    -6.11934   10.16000;
    3.0          "Q6W2"     0.40000;
    3.0          "W2W3"     0.30000;
    3.0          "W3TG"     0.25000;
   13.                      1.00000;
   13.                      4.00000;
* -10.           "FIT1"     1.00000     1.00000    4.00000    0.00100;
* -10.           "FIT2"     3.00000     3.00000    0.00000    0.00100;
* -10.           "FIT5"     2.00000     1.00000    0.00000    0.00100;
    3.0          "TGW4"     0.15000;
   13.                      1.00000;
    3.0          "W4W5"     0.24000;
   13.                      1.00000;
    3.1          "W5Q7"     0.22100;

SENTINEL
```

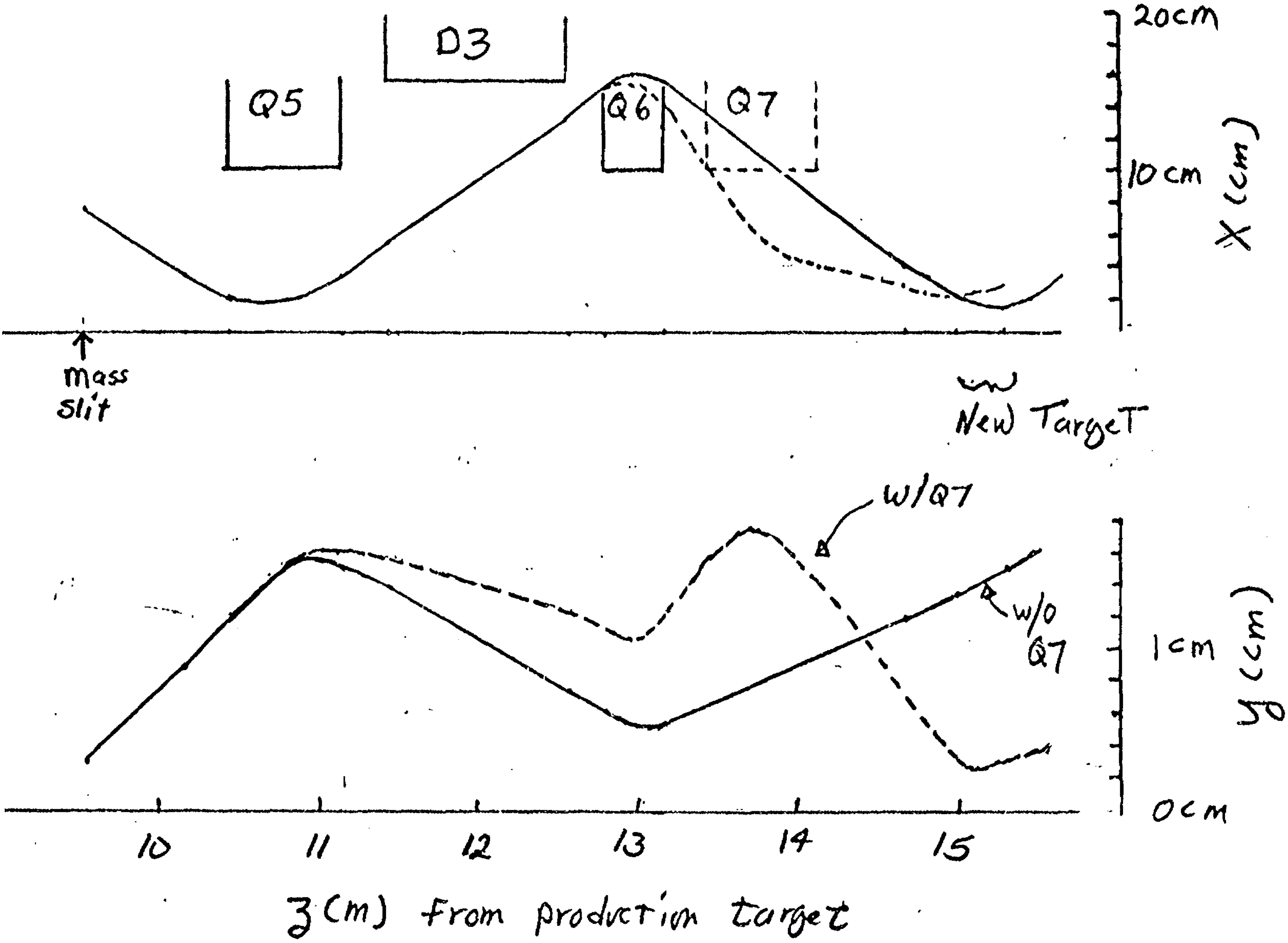

LESB-I Second Order Beam Envelope

Phase Space at Production Target

$x = \pm\ 0.6$ cm

$\theta = \pm\ 60$ mr

$y = \pm\ 0.06$ cm

$\phi = \pm\ 8$ mr

$\delta P/P = \pm\ 2\%$

Figure 38

we have

(3) $X = -1.82\ X_0 + .024\ \theta_0 + 3.51\ \delta P$

which gives a momentum resolution of about 8×10^{-4} (or 640 KeV at 800 MeV/c). The intrinsic resolution of the QDQQ spectrometer is therefore about a factor of two worse than the kaon spectrometer resolution.

The final design study of the LESB-I modifications is not complete. The design presented in this report is one solution which looks attractive at this time since it will give the experimenter a flexibility in choosing the beam size at the target and does not require major modifications to be made to the beam line.

References

1) K. L. Brown et al., CERN 73-16 (1973).

2) K. L. Brown et al., CERN 74-2 (1974).

IV.C DATA ACQUISITION WITH Q

During the past year we have converted the data acquisition software for our experiments at LAMPF to the Q system. This system is a set of programs written and supported by the MP-1 and MP-10 groups at LAMPF. These programs run under the RSX-11D operating system on the DEC PDP-11 series of computers. The system includes a Micro-programmed Branch Driver (MBD) which acquires data from the modules in a CAMAC system, stores and then transfers the data to the PDP-11. The PDP-11 then analyzes the data and can store it on magnetic tape.

There are three main advantages of the Q system over the current CMU data handling system. The first is that the Q system is easy to use. It has convenient editing features which permit the experimenter to easily change various parameters during data taking. This is particularly useful for debugging purposes. The display package includes a peak fitting routine which facilitates quick analysis when monitering an experiment. In addition Q has a special programming language to write the code used by the MBD to read and write data to the CAMAC system. This makes the data acquisition code much simpler and much easier to follow than in the current system. The second main advantage is that Q is supported by LAMPF and in fact is used in many experiments there. It is supplied with extensive documentation and has been tested through years of use. The third advantage is that the Q system is always being improved and within a year a completely updated version which will run under the newer RSX-11M operating system will be available. This new system will be compatible with the original Q system. Since it will run under RSX-11M it will be possible to use the new Q for data analysis on the CMU VAX computer.

Q is a multitasking system which does acquisition, analysis and display in different RSX-11 tasks. The MBS acquires data event by event until it has filled its own internal buffer. The data is then handed to the PDP-11 for processing. This processing includes a user written subroutine which does experiment specific analysis. From this subroutine the user can call on a testing package and a histogramming package so that cuts can be made to the data and spectra can be stored. During the data taking the user can call up the various spectra for display on a Tektronics 4010 graphics terminal. Scatter plots can also be displayed on the 4010 as a crude measure of correlations between different variables.

The Q system has been used in replay mode to analyze data from Exp 315 at LAMPF as a means of learning the system and to prepare the on line analysis for the extension of that experiment in September. We have found that in the replay environment Q has lived up to expectations. Work has begun on the actual data acquisition and so far the results have ben encouraging. We have been able to acquire, analyze, display and tape data using the program that will be used for our August 1981 experiment.

V. Professional Activities

Professor Barnes is presently serving on the Editorial Board, Physics Review C and as Senior Referee, Physical Review Letters.

In addition Professor Barnes is serving on the following committees:

1) American Physical Society, Division of Nuclear Physics; Publication Committee.

2) Argonne University Association; Advisory Committee.

3) National Science Foundation Review Committee of NSF Electron Accelerator Facilities.

4) Council for International Exchange of Scholars; Advisory Committee.

Professor Barnes completed his three-year appointment to the Nuclear Science Advisory Committee at the end of the calendar year, 1980.

Professor Eisenstein has served as Chairman of Los Alamos Meson Physics Facility Users group from January 80 - January 81, and organized the 14th Annual Meeting of LAMPF User's Group - October, 1980. He is a member of the following:

1) Committee for Physics, National Science Foundation, three-year term.

2) American Physical Society, Division of Nuclear Physics, Program Committee.

3) Program Advisory Committee, Bates Linear Accelerator, MIT

4) NSF Visiting Committee, Indiana Cyclotron Facility.

5) Los Alamos Meson Physics Facility Board of Directors - three-year term.

This past year Professor Wharton has served on the Technical Advisory Panel, Los Alamos Meson Physics Facility.

VI. Publications, Reports, Proposals, Talks

A. Publications

1. Eisenstein, R.A., "K^+ Elastic and Inelastic Scattering at 800 MeV/c - Experiment and Theory", Nukleonika Vol. 3 - 4/80, 535-544.

2. Wharton, W.R., B.D. Keister, "A Systematic Study of the (π^+,p) Reaction with Light Nuclei", Physical Review C23, March 1981, 1141.

3. Amann, J.F., P.D. Barnes, K.G.R. Doss, S.A. Dytman, R.A. Eisenstein, J.D. Sherman, W.R. Wharton, "Inelastic π^+ Scattering from ^{12}C and Si at Low Energies", Physical Review C23, Apr. 1981, 1635.

4. Barnes, P.D., "Λ and Σ Hypernuclear Physics", Proceedings of the Workshop on Nuclear and Particle Physics at Energies up to 31 GeV, Los Alamos Scientific Lab, Jan. 1981, LA-8775-C.

5. Eisenstein, R.A., "Meson-Nuclear Interactions at Medium Energies", Proceedings of the Workshop on Nuclear and Particle Physics at Energies up to 31 GeV, Los Alamos Scientific Lab, Jan. 1981, LA-8775-C.

6. Sjoreen, T.P., P.H. Pile, R.E. Pollock, W.W. Jacobs, H.O. Meyer, R.D. Bent, M.C. Green, F. Soga, "Positive Pion Production from the Bombardment of ^{10}B, ^{12}C, ^{16}O and ^{40}Ca with 147 to 159 MeV Polarized Protons". Submitted for Publication in Physical Review C.

7. Barnes, P.D., "Review of Exotic Atoms, Kaon-Nucleus Interactions and Hypernuclei". Submitted to Nuclear Physics A.

B. Reports

1. R.A. Eisenstein, TAP Report on Medium Term Objectives for LAMPF, a report prepared as a result of a study made by the Technical Advisory Panel at LAMPF, November 1980.

C. Invited Talks, Seminars, Etc.

1. Barnes, P.D., Invited Overview Talk, Workshop on Nuclear and Particle Physics at Energies up to 31 GeV, Los Alamos Scientific Lab, January 1981, "Λ and Σ Hypernuclear Physics".

2. Barnes, P.D., Invited Talk on "Exotic Atoms, Kaon-Nucleus interactions, and Hypernuclei", July 1981, IX International Conference on High Energy Physics and Nuclear Structure, Paris, France.
International Conference on High Energy Physics and Nuclear Structure, Paris, France.

3. Barnes, P.D., Colloquium, State University of New York at Stonybrook, March 1981, "Recent Progress in Hypernuclear Physics".

4. Barnes, P.D., Colloquium, University of Notre Dame, February 1981, "Recent Progress in Hypernuclear Physics".

5. Barnes, P.D., Colloquium, University of Pittsburgh, February 1981, "Recent Progress in Hypernuclear Physics".

6. Eisenstein, R.A., Seminar, University of Maryland, Dec. 1980, "Elastic and Inelastic Scattering of Pions, Kaons and Antiprotons".

7. Eisenstein, R.A., Invited Talk, Workshop on Nuclear and Particle Physics at Energies up to 31 GeV, Los Alamos Scientific Lab, January 1981, "Meson-Nuclear Interactions at Medium Energies".

8. Eisenstein, R.A., Invited Talk, 2nd TRIUMF Workshop on Kaon Factory Physics, August 1981, "Kaon-Nuclear Scattering and Reactions".

9. Wharton, W.R., Seminar, University of Maryland, April 1981, "Pion Absorption in Light Nuclei".

10. Wharton, W.R., Contributed Talk, APS Meeting, April 1981, "The $^{6,7}Li(\pi^+,pp)$ and (π^+,pd) Reactions at Low Energies".

11. Bassalleck, Bernd, Seminar, University of Minnesota, Feb. 23, 1981, "Present Status of Hypernuclear Physics".

12. Bassalleck, Bernd, Seminar, University of New Mexico, April 7, 1981, "What Do We Learn from Hypernuclei".

13. Bassalleck, Bernd, Colloquium, Arizona State University, April 24, 1981, "Some Aspects of Hypernuclear Physics".

14. Bassalleck, Bernd, Seminar, MIT, June 15, 1981, "Recent Experiments in Hypernuclear Physics".

15. Bassalleck, Bernd, Invited Talk, 2nd TRIUMF Workshop on Kaon Factory Physics, August 1981, "Experimental Hypernuclear Physics".

D. Conferences Attended

1. Workshop on Nuclear and Particle Physics at Energies up to 31 GeV, Los Alamos Scientific Lab, Jan. 1981 (P.D. Barnes, R.A. Eisenstein, Philip Pile).

2. Workshop on Hadronic Quark Structure and the NN Interaction: Impact on Nuclear Physics, MIT, January 1981 (P.D. Barnes)

3. APS Spring Meeting, Baltimore, April 1981 (W.R. Wharton, Richard Grace, Ronald Rieder).

4. Erice School (Sicily): "Quarks and the Nucleus", April 1981 (P.D. Barnes).

5. 9th International Conference on High Energy Physics and Nuclear Structure, Paris, July 1981 (P.D. Barnes, R.A. Eisenstein).

6. 2nd TRIUMF Workshop on Kaon Factory Physics, Vancouver, B.C., Canada, August 1981 (R.A. Eisenstein, B. Bassalleck).

7. APS Fall Meeting, Div. of Nuclear Physics, Minn. Minnesota, October, 1980 (P. Barnes, P. Pile, R. Eisenstein).

E. Abstracts Submitted

1. "The $^{6,7}Li(\pi^+,pp)$ and (π^+,pd) Reactions at Low Energies", W.R. Wharton, J.F. Amann, P.D. Barnes, B. Bassalleck, N.J. Colella, K.G.R. Doss, R.A. Eisenstein, R. Grace, D.R. Marlow, C. Maher, P.H. Pile, R.J. Rieder, F. Takeutchi, APS Spring Meeting, Baltimore, MD, April 1981.

2. "Preliminary Report on an Experiment to Observe Σ Hypernuclei in ℓp Shell Nuclei", E. Hungerford, S. Bart, R. Hackenburg, B. Mayes, L. Pinsky, K. Sekharan, R.E. Chrien, M. May, D. Maurizio, H. Piekarz, J. Piekarz, Y. Xu, S. Chen, P. Barnes, B. Bassalleck, R. Eisenstein, R. Grace, P. Pile, R. Rieder, W. Wharton, R. Stearns, ibid.

3. "Spin and Isospin Effects in Light Hypernuclei", S. Bart, L. Pinsky, R. Hackenburg, E. Hungerford, D. Marlow, F. Takeutchi, P. Pile, N. Colella, B. Bassalleck, R. Grace, W. Wharton, P. Barnes, M. Deutsch, J. Piekarz, R.L. Stearns, R. Cester, M. May, H. Peikarz, R.E. Chrien, Y. Xu, R. Sutter, H. Palevsky; ibid.

4. "Studies of Light Hypernuclei", M. May, S. Chen, R.E. Chrien, D. Maurizio, H. Palevsky, Y. Xu, R. Cester, M. Deutsch, J. Piekarz, S. Bart, E.V. Hungerford, R. Hackenberg, B. Mayes, L. Pinsky, H. Piekarz, R.L. Stearns, P. Barnes, B. Bassalleck, R. Eisenstein, R. Grace, P. Pile, R. Rieder, W. Wharton, IX International Conference on High Energy Physics and Nuclear Structure, Paris, France, July 1981.

5. "Observation of Σ-Hypernuclei: ${}^{6}_{\Sigma}H$ and ${}^{16}_{\Sigma}C$", R.E. Chrien, M. May, D. Maurizio, Y. Xu, S. Chen, E. Hungerford, S. Bart, R. Hackenberg, B. Mayes, L. Pinsky, K. Sekharan, H. Piekarz, J. Piekarz, P. Barnes, B. Bassalleck, R. Eisenstein, R. Grace, P. Pile, R. Rieder, W. Wharton, R. Stearns; ibid.

6. "The $(\pi^+,2p)$ and (π^+,pd) Reactions at Low Energies on Nuclei of the ℓp-Shell", W.R. Wharton, J.F. Amann, P.D. Barnes, B. Bassalleck, N.J. Colella, K.G.R. Doss, R.A. Eisenstein, R. Grace, D.R. Marlow, C. Maher, P.H. Pile, R.J. Rieder, F. Takeutchi; ibid.

7. "$\pi^{\pm}$-Scattering from Carbon and Calcium at 800 MeV/c", P.H. Pile, P.D. Barnes, N.J. Colella, S.A. Dytman, R.A. Eisenstein, D.R. Marlow, F. Takeutchi, W.R. Wharton, S. Bart, D. Hancock, R. Hackenburg, E. Hungerford, W. Mayes, L. Pinsky, T. Williams, R. Chrien, H. Palevsky, R. Sutter; ibid.

8. "$K^{\pm}$-Scattering from ^{12}C and ^{40}Ca at 800 MeV/c", D.R. Marlow, P.D. Barnes, N.J. Colella, S.A. Dytman, R.A. Eisenstein, P.H. Pile, F. Takeutchi, W.R. Wharton, S. Bart, D. Hancock, R. Hackenburg, E. Hungerford, W. Mayes, L. Pinsky, T. Williams, R. Chrien, H. Palevsky, R. Sutter; ibid.

9. "On Nuclear Density in Momentum Space", R.A. Eisenstein, F. Tabakin; ibid.

10. "$\pi^{\pm}$-Scattering from ^{12}C and ^{40}Ca at 800 MeV/c", P.H. Pile, P.D. Barnes, N.J. Colella, S.A. Dytman, R.A. Eisenstein. D.R. Marlow, F. Takeutchi, W.R. Wharton, S. Bart, D. Hancock, R. Hackenburg, E. Hungerford, W. Mayes, L. Pinsky, T. Williams, R. Chrien, H. Palevsky, R. Sutter, APS Fall Meeting, Division of Nuclear Physics, Minneapolis, Minn., October 1980.

11. "$K^{\pm}$-Scattering from ^{12}C and ^{40}Ca at 800 MeV/c", D.R. Marlow, P.D. Barnes, N.J. Colella, S.A. Dytman, R.A. Eisenstein, F. Takeutchi, W.R. Wharton, S. Bart, D, Hancock, R. Hackenburg, E. Hungerford, W. Mayes, L. Pinsky, T. Williams, R. Chrien, H. Palevsky, R. Sutter; ibid.

2 OF 2

DOE/ER

03244-TI

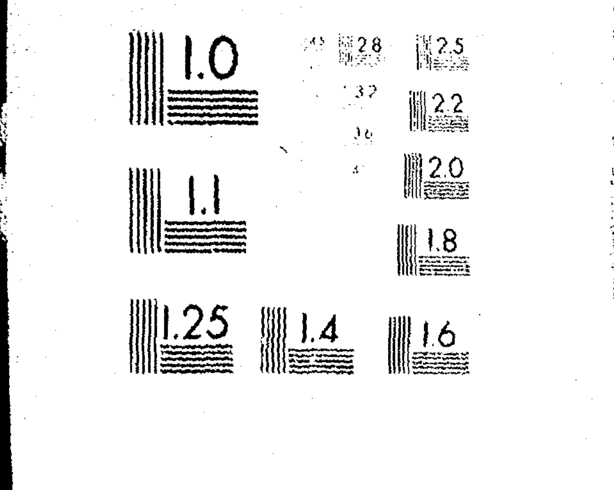

F. Thesis

1. Marlow, Daniel R., "Elastic and Inelastic Scattering of 800 MeV/c $K^{\pm}$ Mesons from ^{12}C and ^{40}Ca", a dissertation submitted in partial fulfillment of the requirements for the degree of Doctor of Philosophy in the Department of Physics, Carnegie-Mellon University.

G. Proposals Submitted

AGS - Brookhaven National Labs:

2. "The Weak Decay Modes of Hypernuclei", Experiment 759, P.D. Barnes, Spokesman, (approved for 450 hours).

END

DATE FILMED

09/08/81